REGULATION OF DEVELOPMENT AND METABOLIC HOMEOSTASIS BY HEPATOCYTE NUCLEAR FACTOR 4

by

William Ellert Barry

A dissertation submitted to the faculty of
The University of Utah
in partial fulfillment of the requirements for the degree of

Doctor of Philosophy

Department of Human Genetics

The University of Utah

December 2016

The University of Utah Graduate School

STATEMENT OF DISSERTATION APPROVAL

The dissertation of **William Ellert Barry**

has been approved by the following supervisory committee members:

Carl Senrich Thummel	, Chair	**8/29/2016** Date Approved
Charles L. Murtaugh	, Member	**8/29/2016** Date Approved
Jared P. Rutter	, Member	**8/29/2016** Date Approved
Claudio Javier Villanueva	, Member	**8/29/2016** Date Approved
Shige Sakonju	, Member	Date Approved

and by **Lynn B. Jorde**, Chair/Dean of

the Department/College/School of **Human Genetics**

and by David B. Kieda, Dean of The Graduate School.

ABSTRACT

The maintenance of metabolic homeostasis presents a major challenge to animal biology. Dysregulation of this process is central to the etiology of diabetes and obesity, which have placed an ever-increasing burden on global human health. Nuclear receptors are a family of ligand-regulated transcription factors that play important roles in preventing metabolic dysfunction by coordinating downstream transcriptional programs to support physiological homeostasis. This dissertation is focused on one of these nuclear receptors, Hepatocyte Nuclear Factor 4A (*HNF4A*), which acts as a critical regulator of systemic glucose homeostasis. Mutations in *HNF4A* were established 20 years ago as the monogenic cause of an inherited form of diabetes called Maturity-Onset Diabetes of the Young 1 (MODY1). The mechanistic link between HNF4A dysfunction and diabetes onset, however, remains unclear. In this dissertation, I present work that provides new insights into the mechanisms by which HNF4 supports physiological homeostasis and prevents diabetes.

The fruit fly *Drosophila* melanogaster provides an ideal system for studies of metabolism and physiology that can guide our understanding of these pathways in mammals. We developed and optimized methods for studies of metabolism in *Drosophila* to further advance its utility in these efforts. Using these techniques, I investigated potentially conserved roles for *Drosophila* HNF4 (dHNF4) in supporting development and metabolic homeostasis. Through this work, I discovered that *dHNF4* mutants

recapitulate hallmark features of MODY1, including hyperglycemia and impaired glucose-stimulated insulin secretion (GSIS). dHNF4 functions in the adult insulin producing cells and the fat body to support GSIS and peripheral glucose clearance during adulthood. These functions are linked to a role for dHNF4 in promoting mitochondrial activity in the mature animal through up-regulation of both nuclear and mitochondrial-encoded genes involved in oxidative phosphorylation (OXPHOS).

By extending my analysis to mammals through a collaborative effort with several labs, we uncovered evidence suggesting that the role for HNF4 in supporting mitochondrial function has been conserved through evolution. Taken together, my work has identified HNF4 as an important regulator of mitochondrial activity, and suggests that this function has been conserved through evolution to support normal development, physiology, and metabolic homeostasis.

TABLE OF CONTENTS

LIST OF FIGURES

ACKNOWLEDGEMENTS

Selecting a graduate advisor is arguably the most important decision a student makes during their graduate career. I had the good fortune of having Carl Thummel as my advisor, who could not have been more supportive in my development as a scientist. Carl's sincere investment in the success of his students is astounding. He cultivates a positive and supportive lab environment that has been a true pleasure to work in over the past several years. I am also greatly indebted to my former undergraduate research advisor at the University of Iowa, Pam Geyer. I joined Pam's lab as a completely naïve undergraduate with no clear career trajectory. Pam challenged me with substantial research responsibilities and helped me develop strong fundamentals in biochemistry, molecular biology, and genetics. She deserves major credit for my love of science and research.

I would also like to thank the members of my advisory committee: Charlie Murtaugh, Jared Rutter, Shige Sakonju, Claudio Villanueva, and previously, Don McClain. These individuals have provided valuable training by advancing my scientific thought process through challenging discussions and critical feedback. I greatly respect and value each of their scientific perspectives and have enjoyed my interactions with them on a personal level. I have also had the pleasure of participating as a trainee on the developmental biology training grant, which allowed me to interact with a number of bright scientists and wonderful people. Joe Yost, Rich Dorsky, and Kristen Kwan worked

so hard on top of their busy schedules to make the training grant a valuable experience for the trainees and I truly appreciate their effort and support.

During my time in the Thummel lab, I have been lucky to work with many people that I admire and personally care for. These individuals helped me to grow as a person and as a scientist. I would like to thank Dan Bricker and Jyoti Misra for entertaining me during my early years in the lab, both with their friendship and through lengthy scientific discussions. I also thank Jason Tennessen who contributed to the early phase of my project, and Janelle Evans, Patty Lisieski, Mike Horner, Geanette Lam, Stefanie Marxreiter, Sophia Praggastis, Becky Palu, Roo Wisidagama, Tom Gallagher, Kate Beebe, and Wendou Yu for helpful discussions and for making the Thummel lab a fun place to work.

Lastly, I would like to thank my friends and family who have provided endless support and encouragement. The friends that I have made during my time in graduate school are some of the most wonderful and selfless people I have ever met, and their friendship is priceless to me. My family's love and support has also been limitless, I could not have made it through graduate school without them. On top of their unmatched support, my parents, John and Suzanne Barry, and my brothers, Grant and John, have helped prepare me my whole life for being a scientist through our endless intellectual debates about anything and everything. Finally, and most importantly, I thank my wife Abby. Her love and friendship gives my life purpose and there are not enough words to express my thanks for her.

CHAPTER 1

INTRODUCTION

Animal biology fundamentally relies on the ability of organisms to maintain metabolic homeostasis. As physiological and environmental conditions vary, these complex networks of biochemical reactions must be properly coordinated to meet cellular and organismal needs. The regulation of systemic nutrient supply is central to this process. In many metazoans, simple carbohydrates such as glucose are maintained at abundant levels in circulation to provide a dependable source of fuel for vital organs. Systemic glucose homeostasis must therefore be tightly regulated to support normal physiology. Hypoglycemia, for example, can result in acute neuronal dysfunction, stroke, and even death. Persistent excess of serum glucose is also detrimental, leading to chronic defects in tissue integrity and organ function. As a result, diabetes mellitus represents a major cause of adult blindness, lower-limb amputation, end-stage renal failure, heart attack, stroke, and death (Centers for Disease Control and Prevention, 2014). The alarming rise in the prevalence of diabetes has therefore placed a major burden on global healthcare, prompting increased efforts to better understand metabolic systems and how they become disrupted in the diseased state.

HNF4A in development, metabolism, and disease

Nuclear receptors are a family of ligand regulated transcription factors that play critical roles in the regulation of development and metabolic homeostasis. More than 10% of all drugs approved by the US Food and Drug Administration act on nuclear receptors, highlighting their utility in providing treatment options and insight into human diseases (Overington et al., 2006). Hepatocyte Nuclear Factor 4A (HNF4A) represents one of the most ancient members of this family, with identifiable homologs present in all animals examined to date (Sladek, 2011). Mutations in *HNF4A* have also been implicated in several human diseases including diabetes, hemophilia, hepatocellular carcinoma, kidney dysfunction, and disorders of the intestinal tract. As a result, significant efforts have been made to better understand the complex functions of HNF4A in development, physiology, and disease.

The Hnf4a nuclear receptor was first discovered through its association with regulatory elements for expression of several hepatocyte-specific genes in rodents (Costa et al., 1989; Sladek et al., 1990). Extensive studies have since proven Hnf4a to be a critical player in the transcriptional control of various developmental and metabolic processes, both in hepatocytes and elsewhere. In mice, complete loss of Hnf4a causes early embryonic lethality due to defects in gastrulation, revealing an essential requirement in mammalian development (Chen et al., 1994). Accordingly, tissue-specific approaches have been employed to investigate its regulatory activities during later stages of development and in adulthood.

Loss-of-function studies in the mouse liver have established Hnf4a as a master regulator of hepatic identity. Consistent with this, liver-specific deletion leads to

dedifferentiation and over proliferation of hepatocytes, along with steatosis, reduced glycogen storage, and early lethality (Bonzo et al., 2012; Hayhurst et al., 2001; Walesky et al., 2013a; Walesky et al., 2013b). As part of this differentiation, hepatocytes require extensive and specific metabolic programming to support liver function. Hnf4a contributes to this by regulating the expression of select metabolic genes involved in lipid metabolism and transport, gluconeogenesis, glycolysis, drug detoxification, and bile acid synthesis.

Although the liver represents the region of highest *Hnf4a* expression, it is also found in the intestine and proximal tubules of the kidney, and at lower levels in the pancreas. Loss of *Hnf4a* in the fetal colon causes defects in epithelial differentiation and crypt formation, along with an increased inflammatory response (Ahn et al., 2008; Chahar et al., 2014; Garrison et al., 2006). Consistent with these findings, mutations in human *HNF4A* are linked to intestinal disorders such as ulcerative colitis and pediatric Crohn's disease (Babeu and Boudreau, 2014). While functional studies of Hnf4a in the kidney have been limited, *ex vivo* organ culture of rat kidney with an Hnf4a antagonist (BI6015) suggests a role in differentiation of the proximal tubules and expression of drug metabolizing enzymes (Martovetsky et al., 2013). In line with these findings, patients with mutations in *HNF4A* have been reported to display defects in kidney function, manifested in the form of Fanconi syndrome (Hamilton et al., 2014).

Finally, the most well-established link between HNF4A dysfunction and human disease is the monogenic form of diabetes called Maturity Onset Diabetes of the Young 1 (MODY1). Although MODY1 is considered to be a disorder caused solely by defects in β-cell function, deletion of *Hnf4a* in this cell type does not produce overt diabetes in mice

(Gupta et al., 2005; Miura et al., 2006). Nonetheless, these mice do display defects in glucose tolerance and glucose-stimulated insulin secretion (GSIS). The mechanisms by which Hnf4a regulates this process, however, remain unresolved.

Maturity onset diabetes of the young (MODY)

The genetic and environmental insults leading to diabetes onset are often complex and unclear. Monogenic forms of diabetes, however, display clear patterns of heritability mapped to causative mutations in single genes. To date, mutations in thirteen genes have been identified that lead to autosomal dominant inheritance of diabetes, classified as Maturity Onset Diabetes of the Young (MODY1-13). MODY patients typically present with hyperglycemia and reduced glucose-stimulated insulin secretion (GSIS) by young adulthood, while lacking signs of β-cell autoimmunity and obesity (Fajans and Bell, 2011).

The monogenic nature of this disease has highlighted MODY genes as critical regulators of systemic glucose homeostasis. Indeed several of these loci encode well-known factors for insulin secretion and glucose uptake, including Insulin (*INS*, MODY10) and the glycolytic enzyme, Glucokinase (*GCK*, MODY2). Although *GCK* mutations are amongst the most common cause of monogenic diabetes, MODY2 patients display a relatively mild disease phenotype without the need for treatment (Fajans and Bell, 2011). In contrast, mutations in the transcription factors *HNF4A* (MODY1), *HNF1A* (MODY3), and *HNF1B* (MODY5) represent the most common forms of MODY that require clinical intervention due to their more severe and progressive disease complications. Despite this, the precise functions of these transcription factors in preventing diabetes onset remain unclear.

The genetic basis for the first form of MODY was mapped to mutations in the *HNF4A* locus twenty years ago (Yamagata et al., 1996). *HNF4A*, like many other MODY-related genes, is expressed in several organs that are important for systemic glucose homeostasis, including the liver, pancreas, kidney, and intestine. The development of MODY, however, is solely attributed to β-cell dysfunction. Accordingly, efforts to model MODY1 in mice have focused on tissue-specific deletion in pancreatic β-cells. Using this approach, two separate groups reported glucose intolerance and aberrant GSIS in adult mice, however overt diabetes was not observed (Gupta et al., 2005; Miura et al., 2006). Several discrepancies were also noted between these studies, including conflicting reports on the basal levels of circulating glucose and insulin. Furthermore, no consensus was reached as to the molecular function of Hnf4a in the β-cell to support GSIS. As a result, we still have a limited understanding of where and how HNF4A functions to prevent hyperglycemia.

Drosophila as a model system for genetic studies of diabetes

For more than a century, genetic studies using the fruit fly, *Drosophila melanogaster,* have provided important insights into conserved aspects of animal development and cell biology. More recently, investigations of metabolic homeostasis in flies have also demonstrated a high degree of conservation with mechanisms regulating systemic metabolism in mammals (Alfa and Kim, 2016; Alfa et al., 2015; Diop and Bodmer, 2015; Owusu-Ansah and Perrimon, 2014; Padmanabha and Baker, 2014; Teleman et al., 2012). This includes pathways for intermediary metabolism, along with hormonal signaling mechanisms to support metabolic homeostasis between feeding and fasting cycles.

The insulin-signaling pathway represents a highly conserved hormonal response to the fed state, helping to control the balance of circulating and stored nutrients. In humans, defects in insulin signaling are central to the pathogenesis of diabetes, characterized by chronic hyperglycemia. Flies display a similar reliance on insulin signaling for regulation of circulating sugars and prevention of diabetes-like phenotypes. In *Drosophila,* the insulin-producing cells (IPCs) are made up of a cluster of neuroendocrine cells in the brain that express three *Drosophila* insulin-like peptides (DILP2, 3, and 5). Functionally analogous to mammalian β-cells, the IPCs respond to nutrient signals for release of DILPs into circulation. Unlike mammals, however, which encode separate receptors for insulin and insulin-like growth factor (IGF) signaling, DILPs act through a single insulin receptor (InR) to promote growth during larval development and to maintain metabolic homeostasis throughout the life of the animal. As a result, ablation of the IPCs leads to reduced body size and hallmarks of diabetes, including elevated levels of circulating carbohydrates (Haselton et al., 2010; Rulifson et al., 2002). Consistent with the highly conserved nature of this pathway, DILPs are capable of lowering blood glucose in rats, and mammalian insulin can also activate the *Drosophila* InR to decrease circulating sugar levels (Haselton and Fridell, 2011; Sajid et al., 2011).

Counter to the functions of insulin, the peptide hormone glucagon is secreted from mammalian pancreatic α-cells in response to low serum glucose to prevent hypoglycemia during fasting. The *Drosophila* adipokinetic hormone (AKH) is similarly secreted from the corpora cardiac (CC) in response to fasting, and disruption of this pathway leads to reduced circulating carbohydrates, establishing AKH as a functional

homolog of mammalian glucagon (Isabel et al., 2005; Kim and Rulifson, 2004; Lee and Park, 2004). Taken together, the CC and IPCs represent physiological equivalents of the mammalian endocrine pancreas.

Despite the extensive conservation of intermediary metabolism and mechanisms regulating physiological homeostasis between flies and mammals, some discrepancies are worth noting. In mammals, elevations in circulating glucose act as the primary stimulus for insulin release from β-cells. *Drosophila* larvae, in contrast, do not respond to either glucose or sucrose for DILP release from the IPCs (Geminard et al., 2009) (Figure 1.1). Rather, dietary amino acids are sensed by the fat body, an organ functionally equivalent to mammalian liver and white adipose tissue, to remotely trigger DILP release (Geminard et al., 2009). Furthermore, free glucose is largely absent from the larval circulating fluid (Figure 1.1). Instead, the glucose disaccharide trehalose represents the primary circulating sugar (Tennessen et al., 2014). Although a recent report has demonstrated that trehalose is capable of stimulating secretion of a single DILP (DILP3) from the IPCs, the proposed pathway does not follow canonical mechanisms for glucose sensing in mammals (Kim and Neufeld, 2015).

More recent studies in adult *Drosophila*, however, have revealed notable differences with larval DILP secretion and glucose homeostasis. Electrophysiological measurements and calcium imaging of isolated IPCs from adult flies have demonstrated responsiveness to free glucose, suggesting that IPCs in the adult may employ similar pathways to mammalian GSIS (Kreneisz et al., 2010). Consistent with this, these cells also express the sulfonylurea receptor (Sur) and are responsive to the anti-diabetic sulfonylurea drug Glibenclamide, unlike larval IPCs (Fridell et al., 2009; Kreneisz et al.,

2010) (Figure 1.1). Subsequent studies have further confirmed the presence of GSIS in adult *Drosophila in vivo* using a recently developed sandwich ELISA assay for DILP2 secretion (Park et al., 2014). In line with these developmental changes in IPC physiology, my studies have uncovered differences in the basal levels of circulating glucose between larvae and adults, which are discussed further in Chapters 2 and 3. Taken together, these findings suggest that insulin secretion and glucose homeostasis are differentially regulated during *Drosophila* development, with the adult stage representing a more accurate context for studies relating to diabetes in humans (Figure 1.1).

Studies of *Drosophila HNF4* (*dHNF4*)

In addition to studies of diabetes, fruit flies provide an ideal context for investigating physiological functions of nuclear receptors. In contrast to mice, which encode 48 nuclear receptor genes, the *Drosophila* genome contains 18, with many representing an entire subclass in mammals (King-Jones and Thummel, 2005). The predominant lack of paraologous nuclear receptor genes in flies prevents issues of genetic redundancy when performing loss-of-function studies. In line with this, *D. melanogaster* express a single highly conserved member of the HNF4 family, *dHNF4*. In mammals, two paralogs of *HNF4* are present, *HNF4A* and *HNF4G*, with *Drosophila HNF4* most closely related to *HNF4A,* showing eighty-nine percent amino acid identity at the DNA-binding domain and sixty-one percent at the ligand-binding domain.

Previous studies of *dHNF4* revealed an essential requirement for *Drosophila* development, where null mutants die during the transition to adulthood (Palanker et al., 2009). During larval development, *dHNF4* mutants display starvation sensitivity and defects in lipid catabolism. These defects are linked to a critical role for dHNF4 in

promoting expression of genes involved in lipid mobilization and mitochondrial oxidation of fatty acids (Palanker et al., 2009). As a result, *dHNF4* mutants display elevated levels of stored triacylglycerol (TAG) and reduced levels of the stored carbohydrate glycogen, similar to loss of *Hnf4a* in the mouse liver (Walesky et al., 2013b). Analysis of the tissue distribution of dHNF4 in larvae has also demonstrated an analogous expression pattern to that of mammalian HNF4A, with dHNF4 protein and/or transcript detectable in the larval fat body (liver/white adipose tissue), oenocytes (hepatocyte-like cells), intestine, and malpighian tubules (kidney-like organ) (Palanker et al., 2006; Palanker et al., 2009; Wilk et al., 2013). Taken together, these studies highlight the potential overlap in physiological functions for *Drosophila* and mammalian HNF4.

Coordination of metabolism with development

Studies of insect physiology nearly two centuries ago provided early findings that development and metabolism are tightly coordinated (Newport, 1836). This included observations of differential rates of respiration throughout the life cycle, showing a U- or J-shaped curve between larval, pupal and adult stages. Although the mitochondrion was not discovered until over fifty years later, extensive work has since demonstrated that the differential activity of this organelle is a principal feature of developmental metabolism.

The mitochondrion acts a central hub for cellular metabolism, with pathways for carbohydrate, lipid, and amino acid metabolism all converging on this organelle. The bulk of ATP production also occurs within mitochondria through oxidative phosphorylation (OXPHOS). OXPHOS is facilitated by the electron transport chain (ETC), which resides within the inner mitochondrial membrane and establishes the proton gradient that drives the ATP synthase machinery.

While differentiated cells tend toward higher rates of OXPHOS, growing and proliferative cells have a greater demand for biosynthesis and predominantly employ aerobic glycolysis (Figure 1.2). Proliferating cells still depend on mitochondrial function for their survival, however, due to a reliance on mitochondria for aspartate biosynthesis (Birsoy et al., 2015; Sullivan et al., 2015). Nonetheless, the differential regulation of mitochondrial respiration and glycolytic flux is a broadly observed strategy to accommodate differential metabolic needs during cellular development (Figure 1.2).

Although the importance of coordinating metabolism with development has gained more attention in recent years, the mechanisms by which this occurs remain largely uncharacterized. Early studies of this phenomenon, however, have highlighted nuclear receptors as major players in this process. This is evident in the mammalian heart, where the nuclear receptors PPARα and ERRγ support a postnatal metabolic switch towards increased oxidative metabolism. Studies in *Drosophila* have also highlighted the importance of nuclear receptors in developmental metabolism. *Drosophila* ERR, for example, acts as a master transcriptional regulator at the embryo-to-larva transition to induce a metabolic switch towards aerobic glycolysis. This metabolic program is critical to support the robust growth phase of larval development. *Drosophila* neuroblasts have also been characterized to undergo a metabolic switch during development, transitioning from aerobic glycolysis to increased OXPHOS upon differentiation. This metabolic shift is critical for proper neuronal development and is mediated by the nuclear receptor EcR. Although studies of such phenomenon have been limited, fruit flies have proved to be a valuable system for uncovering the mechanisms by which metabolism is coordinated with developmental progression. Growing evidence has also demonstrated that a failure

to achieve this coordination can have major consequences for animal health.

Dissertation summary

In this dissertation, I present my work investigating the functions of the nuclear receptor HNF4 in animal physiology and development. In Chapter 2, I present a collaborative effort detailing methods for studies of metabolism in *Drosophila*, including assays for metabolite quantitation, dietary manipulations, and developmental differences in assay utility and circulating glucose abundance.

In Chapter 3, I discuss the role of dHNF4 to regulate metabolic homeostasis during development to prevent adult-onset diabetes. Here I report my discovery that *dHNF4* mutants provide an animal model of MODY1. These findings were initiated by my observation that *dHNF4* mutants are sensitive to dietary sugar levels, such that rearing on a low sugar diet suppresses *dHNF4* mutant lethality at eclosion and supports adult survival. At the transition to adulthood, *dHNF4* mutants develop hallmark features of MODY1, including impaired GSIS, glucose intolerance, and hyperglycemia. This is due in part to a critical role for dHNF4 to maintain mitochondrial function for glucose uptake by the fat body and GSIS from adult IPCs. dHNF4 supports these functions through the regulation of both nuclear and mitochondrial-encoded genes involved in the TCA cycle and ETC. As a result, *dHNF4* mutants display a range of mitochondrial defects including fragmented morphology, reduced membrane potential, and impaired TCA cycle metabolism. During the pupal-to-adult transition, dHNF4 transcript levels increase along with both nuclear and mitochondrial target genes involved in OXPHOS. These findings reveal a developmental switch in metabolism whereby dHNF4 promotes increased mitochondrial function and GSIS in adulthood to support systemic glucose

homeostasis and the energetic needs of the mature animal.

Lastly, in Chapter 4, I further examine the role for dHNF4 in regulating mitochondrial activity and the potential conservation of these functions in mammals through collaborative efforts. In contrast to *dHNF4* mutant adults, which display fragmented mitochondrial morphology and impaired activity of ETC complexes I and IV, mutant larvae display normal morphology and ETC function. Interestingly, this defect in complex I activity is linked to a direct role for dHNF4 to promote expression of a nuclear-encoded acyl-CoA enzyme, *CG7461*, in addition to supporting mtDNA gene expression. *CG7461* is the *Drosophila* homolog of mammalian *ACAD9*, which functions in both fatty acid oxidation and complex I activity. In fact, mutations in *ACAD9* are a common cause of complex I deficiency in humans (Nouws et al., 2014). Consistent with this, knockdown of *CG7461* impairs complex I activity to a similar level as disruption of a known complex I assembly factor, CIA30. Analysis of publically available ChIP-seq data for Hnf4a genomic localization in mouse hepatocytes showed significant enrichment at the *ACAD9* promoter. Additionally, loss of Hnf4a in the adult liver results in reduced *ACAD9* expression under metabolic stress, in the form of cold exposure. Hnf4a was also found associated with a number of other important mitochondrial genes including genes involved in mtDNA gene expression, such as *Tfam* and *Polrmt*, as well as *Pink1,* a critical gene involved in mitochondrial quality control. Consistent with this, *Hnf4a* mutant livers show significantly reduced expression of mtDNA-encoded genes. Although immunostaining for Hnf4a in hepatocytes failed to show appreciable mitochondrial subcellular localization, these data suggest that the role for HNF4 to support mitochondrial function has been conserved through evolution.

In addition to the mouse liver, we also examined HNF4A subcellular localization in the human pancreas. Surprisingly, HNF4A shows distinct mitochondrial localization in pancreatic islets and no observable nuclear staining. Although intriguing, the absence of nuclear signal and lack of available mutant tissue to validate the specificity of this staining makes it difficult to assess the significance of this finding. Nonetheless, a direct role for HNF4 within mitochondria is consistent with my findings in *Drosophila* and raises the possibility that this represents a conserved, albeit tissue-restricted, function of HNF4.

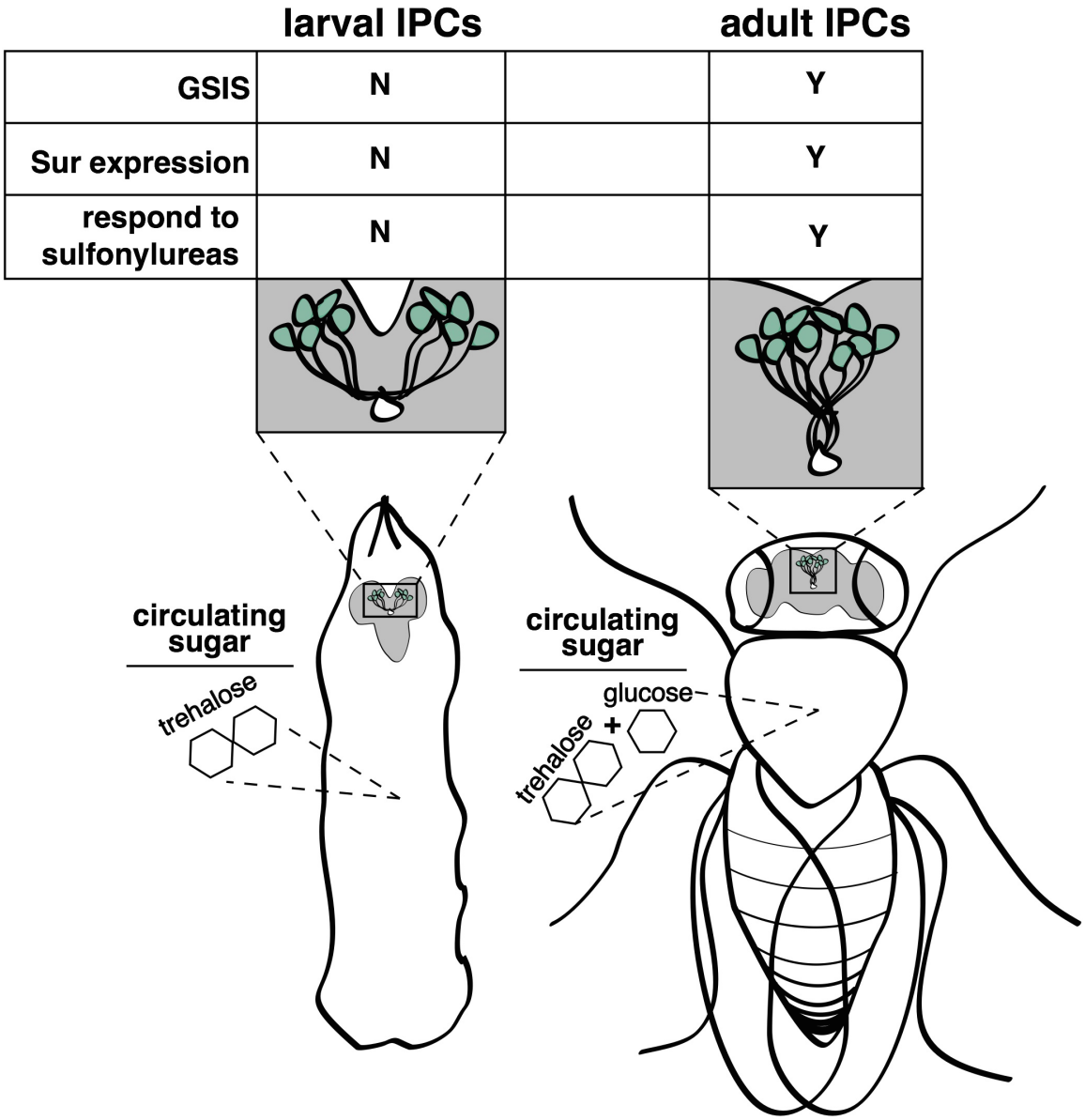

Figure 1.1. *Drosophila* display developmental differences in glucose homeostasis and insulin secretion

Left panel- Larval insulin-producing cells (IPCs) are unresponsive to glucose for secretion of DILPs. Trehalose, a glucose disaccharide, represents the predominant circulating sugar in larvae, while glucose is almost undetectable. Right panel- Adult IPCs are responsive to glucose for DILP secretion and express the sulfonylurea receptor (Sur). Consistent with this, adult IPCs, also depolarize in response to the sulfonylurea, Glibenclamide. Adult flies also display abundant levels of circulating free glucose, in addition to trehalose. The brain is shaded gray and insulin-producing cells are marked in green.

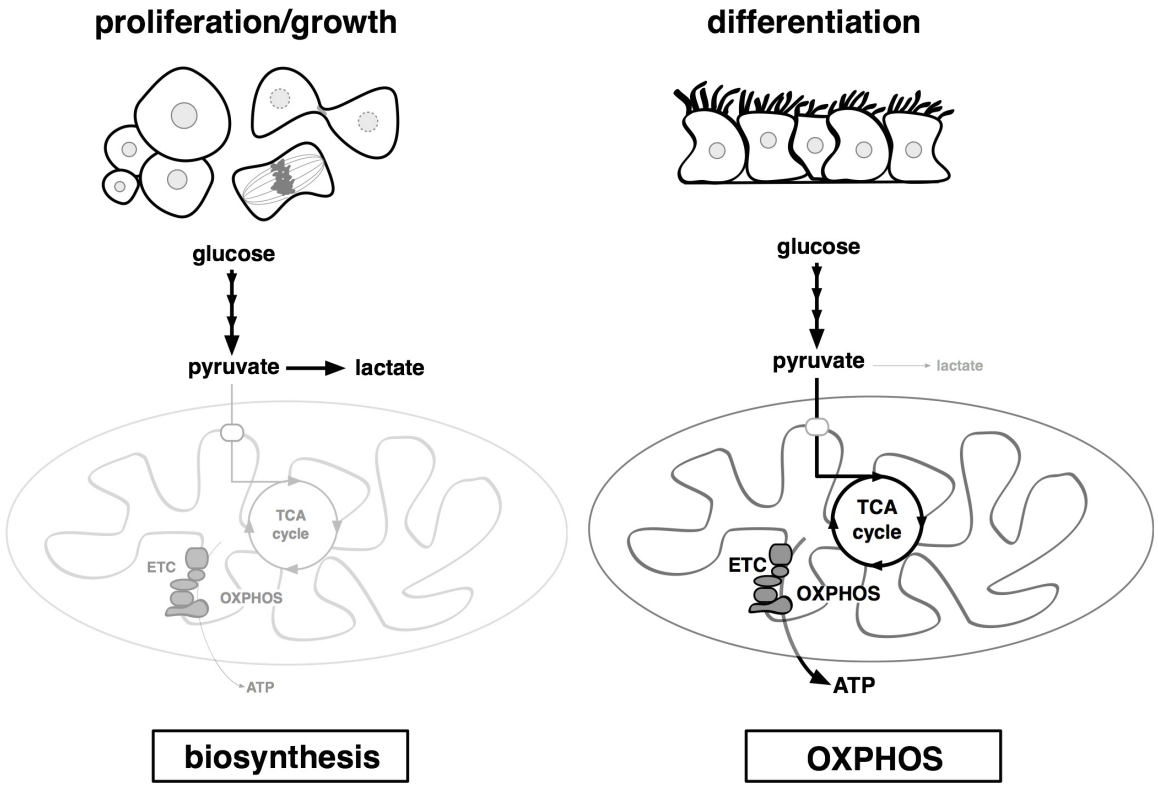

Figure 1.2. General differences in mitochondrial metabolism during cellular development

Left panel – Proliferative and/or rapidly growing cells require high levels of biosynthesis and exhibit elevated rates of glycolysis and low OXPHOS, even in the presence of oxygen. This metabolic program is referred to as aerobic glycolysis, where pyruvate is predominantly converted to lactate rather than entering the TCA cycle within the mitochondrial matrix. Right panel – Differentiated cells generally display higher levels of mitochondrial respiration, with the bulk of pyruvate oxidized through the TCA cycle within the mitochondrial matrix. This generates high-energy electron donors in the form of NADH and FADH2 to fuel the electron transport chain (ETC) for ATP production.

References

Centers for Disease Control and Prevention. (2014) National diabetes statistcs report: estimates of diabetes and its burden in the United States. Atlanta, GA: US Dept. of Health and Human Services.

Ahn, S.H., Shah, Y.M., Inoue, J., Morimura, K., Kim, I., Yim, S., Lambert, G., Kurotani, R., Nagashima, K., Gonzalez, F.J., et al. (2008). Hepatocyte nuclear factor 4alpha in the intestinal epithelial cells protects against inflammatory bowel disease. Inflamm. Bowel Dis. *14*, 908-920.

Alfa, R.W., and Kim, S.K. (2016). Using *Drosophila* to discover mechanisms underlying type 2 diabetes. Dis. Model. Mech. *9*, 365-376.

Alfa, R.W., Park, S., Skelly, K.R., Poffenberger, G., Jain, N., Gu, X., Kockel, L., Wang, J., Liu, Y., Powers, A.C., et al. (2015). Suppression of insulin production and secretion by a decretin hormone. Cell Metab. *21*, 323-333.

Babeu, J.P., and Boudreau, F. (2014). Hepatocyte nuclear factor 4-alpha involvement in liver and intestinal inflammatory networks. World J. Gastroenterol. *20*, 22-30.

Birsoy, K., Wang, T., Chen, W.W., Freinkman, E., Abu-Remaileh, M., and Sabatini, D.M. (2015). An essential role of the mitochondrial electron transport chain in cell proliferation is to enable aspartate synthesis. Cell *162*, 540-551.

Bonzo, J.A., Ferry, C.H., Matsubara, T., Kim, J.H., and Gonzalez, F.J. (2012). Suppression of hepatocyte proliferation by hepatocyte nuclear factor 4alpha in adult mice. J. Biol. Chem. *287*, 7345-7356.

Chahar, S., Gandhi, V., Yu, S., Desai, K., Cowper-Sal-lari, R., Kim, Y., Perekatt, A.O., Kumar, N., Thackray, J.K., Musolf, A., et al. (2014). Chromatin profiling reveals regulatory network shifts and a protective role for hepatocyte nuclear factor 4alpha during colitis. Mol. Cell Biol. *34*, 3291-3304.

Chen, W.S., Manova, K., Weinstein, D.C., Duncan, S.A., Plump, A.S., Prezioso, V.R., Bachvarova, R.F., and Darnell, J.E., Jr. (1994). Disruption of the HNF-4 gene, expressed in visceral endoderm, leads to cell death in embryonic ectoderm and impaired gastrulation of mouse embryos. Genes Dev. *8*, 2466-2477.

Costa, R.H., Grayson, D.R., and Darnell, J.E., Jr. (1989). Multiple hepatocyte-enriched nuclear factors function in the regulation of transthyretin and alpha 1-antitrypsin genes. Mol. Cell Biol. *9*, 1415-1425.

Diop, S.B., and Bodmer, R. (2015). Gaining Insights into diabetic cardiomyopathy from *Drosophila*. Trends Endocrin. Met. *26*, 618-627.

Fajans, S.S., and Bell, G.I. (2011). MODY: history, genetics, pathophysiology, and clinical decision making. Diabetes Care *34*, 1878-1884.

Fridell, Y.W., Hoh, M., Kreneisz, O., Hosier, S., Chang, C., Scantling, D., Mulkey, D.K., and Helfand, S.L. (2009). Increased uncoupling protein (UCP) activity in *Drosophila* insulin-producing neurons attenuates insulin signaling and extends lifespan. Aging *1*, 699-713.

Garrison, W.D., Battle, M.A., Yang, C., Kaestner, K.H., Sladek, F.M., and Duncan, S.A. (2006). Hepatocyte nuclear factor 4alpha is essential for embryonic development of the mouse colon. Gastroenterology *130*, 1207-1220.

Geminard, C., Rulifson, E.J., and Leopold, P. (2009). Remote control of insulin secretion by fat cells in *Drosophila*. Cell Metab. *10*, 199-207.

Gupta, R.K., Vatamaniuk, M.Z., Lee, C.S., Flaschen, R.C., Fulmer, J.T., Matschinsky, F.M., Duncan, S.A., and Kaestner, K.H. (2005). The MODY1 gene HNF-4alpha regulates selected genes involved in insulin secretion. J. Clin. Invest. *115*, 1006-1015.

Hamilton, A.J., Bingham, C., McDonald, T.J., Cook, P.R., Caswell, R.C., Weedon, M.N., Oram, R.A., Shields, B.M., Shepherd, M., Inward, C.D., et al. (2014). The HNF4A R76W mutation causes atypical dominant Fanconi syndrome in addition to a beta cell phenotype. J. Med. Gen. *51*, 165-169.

Haselton, A., Sharmin, E., Schrader, J., Sah, M., Poon, P., and Fridell, Y.W. (2010). Partial ablation of adult *Drosophila* insulin-producing neurons modulates glucose homeostasis and extends life span without insulin resistance. Cell Cycle *9*, 3063-3071.

Haselton, A.T., and Fridell, Y.W. (2011). Insulin injection and hemolymph extraction to measure insulin sensitivity in adult *Drosophila melanogaster*. J. Vis. Exp. *52*, doi: 10.3791/2722.

Hayhurst, G.P., Lee, Y.H., Lambert, G., Ward, J.M., and Gonzalez, F.J. (2001). Hepatocyte nuclear factor 4alpha (nuclear receptor 2A1) is essential for maintenance of hepatic gene expression and lipid homeostasis. Mol. Cell Biol. *21*, 1393-1403.

Isabel, G., Martin, J.R., Chidami, S., Veenstra, J.A., and Rosay, P. (2005). AKH-producing neuroendocrine cell ablation decreases trehalose and induces behavioral changes in *Drosophila*. Am. J. Physiol. Regul. Itegr. Comp. Physiol. *288*, R531-538.

Kim, J., and Neufeld, T.P. (2015). Dietary sugar promotes systemic TOR activation in *Drosophila* through AKH-dependent selective secretion of dilp3. Nat. Commun. *6*, 6846.

Kim, S.K., and Rulifson, E.J. (2004). Conserved mechanisms of glucose sensing and regulation by *Drosophila* corpora cardiaca cells. Nature *431*, 316-320.

King-Jones, K., and Thummel, C.S. (2005). Nuclear receptors - a perspective from *Drosophila*. Nat. Rev. Genet. *6*, 311-323.

Kreneisz, O., Chen, X., Fridell, Y.W., and Mulkey, D.K. (2010). Glucose increases activity and Ca2+ in insulin-producing cells of adult *Drosophila*. Neuroreport *21*, 1116-1120.

Lee, G., and Park, J.H. (2004). Hemolymph sugar homeostasis and starvation-induced hyperactivity affected by genetic manipulations of the adipokinetic hormone-encoding gene in *Drosophila melanogaster*. Genetics *167*, 311-323.

Martovetsky, G., Tee, J.B., and Nigam, S.K. (2013). Hepatocyte nuclear factors 4alpha and 1alpha regulate kidney developmental expression of drug-metabolizing enzymes and drug transporters. Mol. Pharmacol. *84*, 808-823.

Miura, A., Yamagata, K., Kakei, M., Hatakeyama, H., Takahashi, N., Fukui, K., Nammo, T., Yoneda, K., Inoue, Y., Sladek, F.M., et al. (2006). Hepatocyte nuclear factor-4alpha is essential for glucose-stimulated insulin secretion by pancreatic beta-cells. J. Biol. Chem. *281*, 5246-5257.

Newport, G. (1836). On the respiration of insects. Philos. Trans. R. Soc. Lond. *126*, 529-566.

Nouws, J., Te Brinke, H., Nijtmans, L.G., and Houten, S.M. (2014). ACAD9, a complex I assembly factor with a moonlighting function in fatty acid oxidation deficiencies. Hum. Mol. Gen. *23*, 1311-1319.

Overington, J.P., Al-Lazikani, B., and Hopkins, A.L. (2006). How many drug targets are there? Nat. Rev. Drug Discov. *5*, 993-996.

Owusu-Ansah, E., and Perrimon, N. (2014). Modeling metabolic homeostasis and nutrient sensing in *Drosophila*: implications for aging and metabolic diseases. Dis. Model. Mech. *7*, 343-350.

Padmanabha, D., and Baker, K.D. (2014). *Drosophila* gains traction as a repurposed tool to investigate metabolism. Trends Endocrin. Met. *25*, 518-527.

Palanker, L., Necakov, A.S., Sampson, H.M., Ni, R., Hu, C., Thummel, C.S., and Krause, H.M. (2006). Dynamic regulation of *Drosophila* nuclear receptor activity in vivo. Development *133*, 3549-3562.

Palanker, L., Tennessen, J.M., Lam, G., and Thummel, C.S. (2009). *Drosophila* HNF4 regulates lipid mobilization and beta-oxidation. Cell Metab. *9*, 228-239.

Park, S., Alfa, R.W., Topper, S.M., Kim, G.E., Kockel, L., and Kim, S.K. (2014). A genetic strategy to measure circulating *Drosophila* insulin reveals genes regulating

insulin production and secretion. PLoS Genet. *10*, e1004555.

Rulifson, E.J., Kim, S.K., and Nusse, R. (2002). Ablation of insulin-producing neurons in flies: growth and diabetic phenotypes. Science *296*, 1118-1120.

Sajid, W., Kulahin, N., Schluckebier, G., Ribel, U., Henderson, H.R., Tatar, M., Hansen, B.F., Svendsen, A.M., Kiselyov, V.V., Norgaard, P., et al. (2011). Structural and biological properties of the *Drosophila* insulin-like peptide 5 show evolutionary conservation. J. Biol. Chem. *286*, 661-673.

Sladek, F.M. (2011). What are nuclear receptor ligands? Mol. Cell. Endocrinol. *334*, 3-13.

Sladek, F.M., Zhong, W.M., Lai, E., and Darnell, J.E., Jr. (1990). Liver-enriched transcription factor HNF-4 is a novel member of the steroid hormone receptor superfamily. Genes Dev. *4*, 2353-2365.

Sullivan, L.B., Gui, D.Y., Hosios, A.M., Bush, L.N., Freinkman, E., and Vander Heiden, M.G. (2015). Supporting aspartate biosynthesis is an essential function of respiration in proliferating cells. Cell *162*, 552-563.

Teleman, A.A., Ratzenbock, I., and Oldham, S. (2012). *Drosophila*: a model for understanding obesity and diabetic complications. Exp. Clin. Endocrinol. Diabetes *120*, 184-185.

Tennessen, J.M., Barry, W.E., Cox, J., and Thummel, C.S. (2014). Methods for studying metabolism in *Drosophila*. Methods *68*, 105-115.

Walesky, C., Edwards, G., Borude, P., Gunewardena, S., O'Neil, M., Yoo, B., and Apte, U. (2013a). Hepatocyte nuclear factor 4 alpha deletion promotes diethylnitrosamine-induced hepatocellular carcinoma in rodents. Hepatology *57*, 2480-2490.

Walesky, C., Gunewardena, S., Terwilliger, E.F., Edwards, G., Borude, P., and Apte, U. (2013b). Hepatocyte-specific deletion of hepatocyte nuclear factor-4alpha in adult mice results in increased hepatocyte proliferation. Am. J. Physiol. Gastrointest. Liver Physiol. *304*, G26-37.

Wilk, R., Hu, J., and Krause, H.M. (2013). Spatial profiling of nuclear receptor transcription patterns over the course of *Drosophila* development. G3 *3*, 1177-1189.

Yamagata, K., Furuta, H., Oda, N., Kaisaki, P.J., Menzel, S., Cox, N.J., Fajans, S.S., Signorini, S., Stoffel, M., and Bell, G.I. (1996). Mutations in the hepatocyte nuclear factor-4alpha gene in maturity-onset diabetes of the young (MODY1). Nature *384*, 458-460.

CHAPTER 2

METHODS FOR STUDYING METABOLISM IN *DROSOPHILA*

Originally published as – Tennessen, J.M, Barry, W.E., Cox, J., Thummel, C.S. (2014) Methods for studying metabolism in *Drosophila*. *68*, 105-115.

Methods 68 (2014) 105–115

Contents lists available at ScienceDirect

Methods

journal homepage: www.elsevier.com/locate/ymeth

Methods for studying metabolism in *Drosophila*

Jason M. Tennessen [a,1], William E. Barry [a], James Cox [b], Carl S. Thummel [a,*]

[a] Department of Human Genetics, University of Utah School of Medicine, Salt Lake City, UT 84112-5330, USA
[b] Department of Biochemistry and the Metabolomics Core Research Facility, University of Utah School of Medicine, Salt Lake City, UT 84112, USA

ARTICLE INFO

Article history:
Received 12 February 2014
Revised 21 February 2014
Accepted 25 February 2014
Available online 12 March 2014

Keywords:
Drosophila
Metabolism
Metabolomics
Physiology

ABSTRACT

Recent research using *Drosophila melanogaster* has seen a resurgence in studies of metabolism and physiology. This review focuses on major methods used to conduct this work. These include protocols for dietary interventions, measurements of triglycerides, cholesterol, glucose, trehalose, and glycogen, stains for lipid detection, and the use of gas chromatography-mass spectrometry (GC-MS) to detect major polar metabolites. It is our hope that this will provide a useful framework for both new and current researchers in the field.

1. Introduction

Metabolism and physiology provided a major focus for *Drosophila* research in the middle of the last century [1]. This work included fundamental studies of biochemical genetics, starting with classic work on eye pigment biosynthesis and the one gene-one enzyme hypothesis [2], as well as detailed characterization of basic energy physiology [e.g. Ref. [3–5]]. Although the advent of recombinant DNA technology shifted the *Drosophila* field toward studies of developmental biology, recent efforts have refocused on metabolism, with a particular emphasis on the mechanisms that maintain energy homeostasis and the use of *Drosophila* as a model for studies of diabetes and obesity [6–10]. In this review, we highlight methods that have been developed to conduct current genetic studies of metabolism in *Drosophila*, with a focus on energy homeostasis and physiology. We begin with an overall discussion of the challenges facing researchers in the field, given the contributions of both environmental and genetic factors to metabolic control. We then move on to review protocols for dietary intervention in *Drosophila*, followed by widely used assays to quantify basic metabolites in the animal. We end with protocols for metabolomic profiling by gas chromatography–mass spectrometry (GC-MS). Our goal is not to be comprehensive in our coverage of metabolic protocols, since that is beyond the scope of one article, but rather to focus on some major methods currently being used, with the hope that this will provide a useful framework for both new and current researchers in the field.

2. Experimental design

The profound interplay between environment and genetics requires that metabolic studies be undertaken with careful attention to genetic background, diet, stock maintenance, and statistical analysis of data. Particular concern should be directed toward the selection of control strains and the establishment of an appropriately matched genetic background for the mutant being studied. Outcrossing mutants to the control strain provides a good way to achieve this goal, as does confirming results with more than one control line. Matching the genetic background becomes more difficult, however, when GAL4 drivers and UAS transgenes are included in the genotype, although a uniform *white* mutant background and controls with the driver and/or responder alone can be included. Tissue-specific RNAi provides an invaluable and widely used tool for functional studies of metabolism. In addition to the standard concerns with off-target effects, however, RNAi can have nonspecific effects on physiology [e.g. Ref. [11]]. Finally, some care should be taken when using commercial kits for quantifying specific metabolites. Although these kits may be widely used in mammalian research, most have not been validated in *Drosophila*. As discussed below for quantifying simple metabolites such as glucose, glycogen, and triglycerides, protocols need to be adapted to the system. A good way to achieve this for a new assay is to use known mutants in the pathway being studied, and score for the predicted changes in metabolite levels. Alternatively, methods such as GC-MS can be used to confirm the changes in metabolite levels de-

* Corresponding author.
E-mail address: carl.thummel@genetics.utah.edu (C.S. Thummel).
[1] Present address: Department of Biology, Indiana University, 1001 East Third Street, Bloomington, IN 47405, USA.

http://dx.doi.org/10.1016/j.ymeth.2014.02.034
1046-2023/

tected by an enzymatic kit. In general, the more labile the metabolite (such as ATP), the more care that is needed for its quantification.

3. Starvation and dietary paradigms

The metabolic state of an animal is intimately linked with its diet. Accordingly, dietary conditions must be carefully controlled when performing metabolic studies. Often this will require the lab making special batches of media to maintain both breeding and experimental stocks. This point becomes particularly important when considering the recent evidence that parental diet can influence the metabolic state of offspring, as has been well documented in mammals [12,13]. While carefully controlled dietary conditions are essential, dietary manipulation also provides one of the most useful approaches for studies of metabolism and animal physiology. For example, enrichment or restriction of particular nutrients can often evoke robust metabolic phenotypes in mutants that may otherwise appear normal under ideal dietary conditions [14–17].

Starvation provides an important dietary stress that tests the animal's ability to mobilize stored nutrients for survival. This can be achieved by transferring larvae or flies to either water or PBS. Although moist filter paper is employed for larvae, studies of adult starvation should use 1% agar as a substrate, as it provides a more uniform moist environment for long-term studies (>12 h).

Alteration of dietary sugar levels is a useful method for investigating potential defects in carbohydrate homeostasis. This can be easily achieved by using an 8% yeast and 1% agar medium to serve as the dietary foundation for manipulating sugar concentrations. A range from 3–15% dietary sugar (ratio of 2:1 glucose to sucrose, by weight) represents the low-to-high spectrum found within a relatively normal diet for *Drosophila* (Table 1). In our studies, altering the sugar concentration of this media has proven to be an effective tool for both enhancing and suppressing diabetic phenotypes. For example, several *Drosophila* mutants that are sensitive to dietary sugar can maintain euglycemia on a 3% sugar diet but display increasingly severe hyperglycemia as dietary sugar is increased (W. Barry, D. Bricker, and R. Somer, unpublished results).

Very high sugar diets have been developed for studies of type 2 diabetes in *Drosophila*. These diets consist of either 1% agar, 3.4% yeast, 8.3% cornmeal, and 30% sucrose [15] or 1% agar, 8% yeast, 2% yeast extract, 2% peptone, and 34.2% sucrose [18] (Table 1). These diets lead to hallmarks of type 2 diabetes in wild-type *Drosophila*, including hyperglycemia, insulin resistance, obesity, and cardiac dysfunction [15,18,19]. High lipid diets have also been developed for studies of diet-induced obesity in *Drosophila*. These can be achieved by supplementation of standard growth media with either soy lipids [20] or coconut oil [21,22], which has been most widely used for this purpose.

Although the above media allow the researcher to crudely manipulate the overall levels of carbohydrates and lipids in the diet, precise addition or removal of dietary components is often desirable. Fortunately, two labs have recently developed chemically defined diets that support *Drosophila* development and growth (although at a reduced rate), and are well suited for the study of adult physiology and aging [23,24]. The advent of these defined diets provides a level of control not possible in past work, and should greatly facilitate nutritional and metabolic studies in *Drosophila*.

3.1. Measuring feeding rate

It is often important to assess whether changes in feeding rate contribute to an observed metabolic phenotype. The use of dietary dyes can provide a crude yet simple method to visually assess food consumption [25]. This approach is particularly useful when analyzing responses to an acute feeding bout, by ensuring that only animals that have consumed the food are analyzed. Dietary dyes are not well suited for quantitative analysis, however, and cannot be used to accurately assess feeding rate over extended periods of time. In contrast, adding radioactive material to the food provides a more quantitative measurement of consumption based on ingested radiation after a fixed period of time [26]. This can be achieved for individual flies by adding 10^8 counts/min/ml (final volume) α-^{32}P dCTP (or any other nucleotide) to the diet and permitting the animals to feed for 2 h. Lower levels of radiation can be used if multiple flies are measured. Labeled animals are transferred to unlabeled food for several hours to allow them to clear radioactivity that is nonspecifically bound to the cuticle. They are then subjected to Cerenkov counting in a scintillation counter to quantify food uptake [27,28]. Scintillation fluid can be used if the animals are sacrificed and lower levels of radiation are employed in the diet.

The Capillary Feeder (CAFE) assay has been developed as a means to directly quantify food consumption by making use of a capillary feeder containing a liquid medium [29]. While this technique allows for direct and precise analysis of ingested food quantities, some researchers have raised concerns that the diet and its method of delivery might not represent a natural feeding scenario [29,30]. This led to an alternate technique that measures the number of times an animal extends its proboscis to feed in a fixed time period [30]. A more detailed description of these techniques can be found in a recent review on *Drosophila* feeding behavior [31].

4. Methods to measure basic metabolites: lipids

Under normal feeding conditions, dietary triglycerides (TAG) and cholesterol esters are broken down into free fatty acids, monoacylglycerols, and free sterols in the intestine. These digested lipids can then be absorbed by the intestinal cells, where TAG is resynthesized and packaged together with cholesterol, cholesterol esters, and carrier proteins to form lipoprotein particles that are trafficked throughout the body. These lipids can be either utilized by cells or deposited in storage tissues. Most lipids reside in the fat body, although some are also present in the gut and oenocytes of both larvae and adults. Two different types of assays can be used to detect lipids – either specific assays to quantify TAG or sterols from whole animals or dissected tissues, or lipophilic dyes to visualize neutral lipids within cells. Taken together, these provide a valuable indication of the lipid distribution within the animal.

4.1. Colorimetric quantification of triglycerides

Overall quantification of TAG is often a first step in a metabolic study, along with measurements of basic carbohydrates and protein. An accurate, although insensitive means of measuring TAG is to use Bligh and Dyer lipid extraction followed by thin layer chromatography (TLC) [32,33]. This allows fractionation and detection of total fatty acids, diacylglycerol (the major circulating form of lipid in insects), and TAG. The most widely used assay for detecting triglycerides, however, is a coupled colorimetric assay that detects free glycerol levels after cleaving TAG with lipoprotein lipase [32,34,35]. Although a few studies have suggested that this approach does not provide an accurate assessment of stored fat in insects [36,37], both TLC and the colorimetric assay produce similar results [32]. It is, however, worth noting that the colorimetric assay releases glycerol from mono- and diacylglycerides [38] in addition to TAG and, therefore, conclusions regarding any

Table 1
Caloric content of *Drosophila* diets.

Semi-defined (Bloomington)	g/liter	Carbs (g)	Protein (g)	Fat (g)	Total kcal
Agar	10	8.9	0	0.1	
Yeast	80	30.8	38.6	3.12	
Yeast extract	20	7.7	8.6	1.72	
Peptone	20	0.1	14.6	0	
Sucrose	30	30	0	0	
Glucose	60	60	0	0	
Total grams		137.5	61.8	4.94	
Total kcal		550	247.2	42.29	839.5
Percent total kcal		65.5	29.4	5.04	
9% Sugar diet (normal)					
Agar	10	8.9	0	0.1	
Yeast	80	30.8	38.6	3.12	
Sucrose	30	30	0	0	
Glucose	60	60	0	0	
Total grams		129.7	38.6	3.22	
Total kcal		518.8	154.4	27.56	700.8
Percent total kcal		74.0	22.0	3.93	
3% Sugar diet (low sugar)					
Agar	10	8.9	0	0.1	
Yeast	80	30.8	38.6	3.12	
Sucrose	10	10	0	0	
Glucose	20	20	0	0	
Total grams		69.7	38.6	3.22	
Total kcal		278.8	154.4	27.56	460.8
Percent total kcal		60.5	33.5	5.98	
15% Sugar diet (high sugar)					
Agar	10	8.9	0	0.1	
Yeast	80	30.8	38.6	3.12	
Sucrose	50	50	0	0	
Glucose	100	100	0	0	
Total grams		189.7	38.6	3.22	
Total kcal		758.8	154.4	27.56	940.8
Percent total kcal		80.7	16.4	2.93	
Diabetic diet					
Agar	10	8.9	0	0.1	
Yeast	80	30.8	38.6	3.12	
Yeast extract	20	7.7	8.6	1.72	
Peptone	20	0.1	14.6	0	
Sucrose	342	342	0	0	
Total grams		389.5	61.8	4.94	
Total kcal		1558	247.2	42.29	1847.5
Percent total kcal		84.3	13.4	2.29	

Diabetic diet from Musselman et al. [18].

particular form of glycerolipid should be validated by TLC. The presence of eye pigment in adult samples could also interfere with accurate absorbance measurements at certain wavelengths; however, assay kits designed to measure absorbance at 540 nm do not detect eye pigment [32].

4.2. Protocol: coupled colorimetric assay for triglycerides

(1) Collect samples (25 mid-second instar larvae; 5 adult flies).
(2) Rinse several times with 1 ml cold PBS to remove all traces of food that might be attached to the outside of the animal. Larvae can be washed in a 1.5 ml microfuge tube, but adults should be rinsed in a 9-well glass plate. Transfer adult flies to a 1.5 ml microfuge tube. Carefully remove all liquid. For larvae, centrifuge at 3000×*g* and remove all remnants of PBS. Snap freeze animals in liquid nitrogen for later homogenization or add 100 μl of cold PBS + 0.05% Tween 20 (PBST).
(3) Rapidly homogenize animals in PBST with a pellet pestle (Kontes; 749521-1500) on ice. A motor can be used to facilitate homogenization (Kontes; 749540-–0000). Frozen samples should be kept on dry ice until addition of PBST. If samples are not kept cold, stored glycerolipids will be enzymatically degraded into free glycerol by endogenous enzymes and skew the final analysis.
(4) Remove 10 μl of homogenized sample to measure protein content with a Bradford assay. Keep samples on ice and do not heat-treat. Protein samples can be frozen and stored at −80 °C for later analysis.
(5) Heat supernatant for 10 min at 70 °C. Do not centrifuge the heat-treated lysate because lipids are partially insoluble in PBST. At this time, the heat-inactivated sample can be frozen and stored at −80 °C, if desired.
(6) Prepare standards: Dilute 40 μl of the glycerol standard solution (Sigma 2.5 mg/ml triolein equivalent glycerol standard; G7793) with 60 μl PBST (100 μl final volume) to generate a 1.0 mg/ml triolein equivalent standard. Do two 2-fold serial dilutions into PBST (50 μl 1 mg/ml + 50 μl PBST for 0.5 mg/ml standard, etc.) to generate 0.125, 0.25 and 0.5 mg/ml standards. Glycerol stock solutions can be stored at −20 °C or 4 °C.
(7) Add 20 μl of the glycerol standards, fly samples, and a PBST blank to each of two 1.5 ml microfuge tubes. Add 20 μl of PBST to one tube (this sample will be used to measure free glycerol). Add 20 μl of triglyceride reagent (Sigma; T2449) to the other tube (the TAG in this sample will be digested by lipase to free the glycerol backbone). Incubate tubes at 37 °C for 30–60 min.
(8) Centrifuge for 3 min at full speed. Transfer 30 μl of each sample to a clear-bottom 96-well plate.

(9) Add 100 μl of free glycerol reagent (Sigma; F6428) to each sample with a multichannel pipette and mix well. Seal the wells with parafilm to prevent evaporation and incubate the plate for 5 min at 37 °C. Centrifuge the plate in an appropriate swing-bucket rotor to clear condensate from the sides of the wells and to remove any air bubbles present in the samples. Use a plate reader to measure absorbance at 540 nm.
(10) Determine the TAG concentration for each sample by subtracting the absorbance for the free glycerol in the untreated samples from the total glycerol concentration in samples that have been incubated with triglyceride reagent. The TAG content in each sample is calculated based on the triolein-equivalent standard curve. This assay is linear from 0–1.0 mg/ml TAG.

As with any metabolic measurement, TAG levels must be considered in the larger context of animal growth and physiology. Mutations that delay developmental progression and alter adult body size could produce proportional changes in TAG in that do not reflect metabolic defects. Similarly, wild-type adult flies do not feed for a prolonged period after eclosion, and need to be aged several days to achieve maturity [39]. Thus to prevent inaccurate results, all samples should be developmentally staged and normalized to an internal parameter such as soluble protein (although the effects of a mutation on protein levels may require another method, such as body weight, for normalization). A simple method for measuring protein concentration is to remove 10 μl of homogenized sample prior to heat treatment, dilute between 1:10 and 1:20 in cold PBS, and use 10 μl of the dilution to conduct a Bradford assay [40]. If protein concentration is not measured immediately, samples should be stored at −80 °C.

4.3. Cholesterol quantification

Cholesterol is an essential component of cell membranes and also the precursor for steroid hormone biosynthesis. In addition to free cholesterol, cholesterol esterified to long chain fatty acids is present in circulating lipoprotein particles as well as stored in lipid droplets. A fluorometric assay has been widely used to quantify free cholesterol in *Drosophila* larvae and adults [14,41–44]. In addition, by sonicating the extracts to emulsify lipids and including cholesterol esterase in the reaction, cholesterol esters can be digested into free cholesterol, which can then be quantified by the fluorometric assay and compared to the background level of free cholesterol present in the sample. We use the Amplex Red Cholesterol assay (Invitrogen; A12216) to detect either free cholesterol or esterified cholesterol, as described below. This kit uses cholesterol oxidase to convert free cholesterol into cholest-4-en-3-one and hydrogen peroxide. The hydrogen peroxide then reacts with 10-acetyl-3,7-dihydroxyphenoxazine in the presence of horseradish peroxidase to generate resorufin, which can be detected by its fluorescence at ~590 nm. It should be noted that this assay will detect all sterols, including the abundant sterols in *Drosophila* (ergosterol and dehydrocholesterol), all of which are defined by a hydroxyl group at the 3-position of the A-ring [33].

4.4. Protocol: fluorescent assay for free cholesterol

This assay does not involve sonicating the samples and thus measures primarily free sterols. Sonication is needed to release and emulsify the cholesterol esters stored in lipid droplets. Although cholesterol esterase is included in this assay, it makes little difference in the final result.

(1) Follow the Amplex Red Cholesterol Assay Kit (Invitrogen; A12216) instructions to prepare aliquots of the 20 mM Amplex Red reagent in DMSO, 200 U/ml HRP in 1× reaction buffer, 200 U/ml cholesterol oxidase in 1× reaction buffer, and 200 U/ml cholesterol esterase in 1× reaction buffer. These can be stored at −20 °C for later use.
(2) Collect samples in 1.5 ml microfuge tubes (75 embryos, 30 first instar larvae, 5 adult male flies). Rinse several times with cold PBS to remove all traces of food that might be attached to the outside of the animal. Embryos should be dechorionated following standard procedures and subsequently transferred to a 1.5 ml microfuge tube. Larvae can be washed in a 1.5 ml microfuge tube, but adults should be rinsed in a 9-well glass plate. Transfer adult flies to a 1.5 ml microfuge tube. Carefully remove all liquid. For larvae, centrifuge at 3000×*g* and remove all remnants of PBS.
(3) Homogenize animals in 100 μl of 1× reaction buffer with a pellet pestle (Kontes; 749521–1500) on ice. A motor can be used to facilitate homogenization (Kontes; 749540–0000).
(4) Centrifuge homogenate for 5 min at 2300×*g* at room temperature. Transfer the supernatant to a fresh 1.5 ml microfuge tube, including the upper "fatty" layer and mix gently. Remove 10 μl of homogenized sample to measure protein content with a Bradford assay. Keep samples on ice and do not heat-treat. Protein samples can be frozen and stored at −80 °C for later analysis.
(5) Prepare cholesterol standards in 1× reaction buffer using the 2 mg/ml cholesterol reference standard provided in the kit. We prepare a dilution series, ending up with at least 50 μl each of 0, 2, 4, 6, 8 μg/ml cholesterol.
(6) Add 50 μl of the cholesterol standards and a 1× reaction buffer blank to the first row of a black 96 well plate (Optiplate-96 Perkin Elmer; 6005270). In the next row, add 50 μl of each sample into individual wells.
(7) Prepare the reaction mix using stored aliquots:
15 μl 20 mM Amplex Red reagent in DMSO
10 μl 200 U/ml HRP in 1× reaction buffer
10 μl 200 U/ml cholesterol oxidase in 1× reaction buffer
1 μl 200 U/ml cholesterol esterase in 1× reaction buffer
+1494 μl 1× reaction buffer
(8) Add 90 μl of reaction mix to each well with a multichannel pipette. Be sure to keep in the dark and incubate at least 30 min at 37 °C.
(9) Measure immediately using a fluorescence plate reader with excitation at 530 nm and emission at 590 nm. Each data point resulting from the assay should represent an average of at least three collections of animals, and the assay should be repeated at least three times.

4.5. Protocol: fluorescent assay for cholesterol esters

This assay uses sonication of the animal homogenates to release and emulsify the cholesterol esters stored in lipid droplets. Each sample is then divided into two tubes, one of which is treated with cholesterol esterase. The amount of cholesterol esters is determined by subtracting the background level of free cholesterol in the untreated sample from the total amount of esterified and free cholesterol present in the sample treated with cholesterol esterase.

(1) Follow the Amplex Red Cholesterol Assay Kit (Invitrogen; A12216) instructions to prepare aliquots of the 20 mM Amplex Red reagent in DMSO, 200 U/ml HRP in 1× reaction buffer, and 200 U/ml cholesterol oxidase in 1× reaction buffer. These can be stored at −20 °C for later use.

(2) Collect samples in 1.5 ml microfuge tubes (30 adult male flies). Rinse animals several times with cold PBS to remove all traces of food. Carefully remove all liquid and homogenize animals in 250 μl of cold PBS + 0.05% Tween 20 (PBST) with a pellet pestle (Kontes; 749521-1500) on ice. A motor can be used to facilitate homogenization (Kontes; 749540-0000). Remove 10 μl of homogenized sample to measure protein content with a Bradford assay. Protein samples can be frozen and stored at −80 °C for later analysis.
(3) Add 650 μl of cold PBST to each sample and sonicate on ice using a tip sonicator, three times for 30 sec each, at a medium setting to prevent foaming.
(4) Split each sample into two 1.5 ml microfuge tubes and add 10 μl of 200 U/ml cholesterol esterase (either Sigma C1403 or C3766) to one set of tubes.
(5) Incubate both sets of tubes overnight (>16 h) at 37 °C with occasional vortexing.
(6) Extract all tubes with 900 μl 2:1 chloroform:methanol by shaking the tubes several times vigorously over a period of about 3 min. Centrifuge to separate the phases, remove the lower organic phase, and transfer to a fresh 1.5 ml microfuge tube. Use a centrifugal vacuum concentrator to remove all of the organic solvent, leaving an oily lipid residue (approx. 30 min).
(7) Solubilize lipids in 500 μl PBST by vortexing and sonicating as above.
(8) Prepare free cholesterol standards in 1× reaction buffer using the 2 mg/ml cholesterol reference standard provided in the kit. We prepare a dilution series, ending up with at least 50 μl each of 0, 2, 4, 6, 8 μg/ml cholesterol.
(9) Add 50 μl of the cholesterol standards and a 1× reaction buffer blank to the first row of a black 96 well plate (Optiplate-96 Perkin Elmer; 6005270). In the next rows, add a 1:1 dilution of each sample with 1× reaction buffer (25 μl of each sample + 25 μl 1× reaction buffer) to each well.
(10) Prepare the reaction mix using stored aliquots:
15 μl 20 mM Amplex Red reagent in DMSO
10 μl 200 U/ml HRP in 1× reaction buffer
10 μl 200 U/ml cholesterol oxidase in 1× reaction buffer
+1495 μl 1× reaction buffer
(11) Add 90 μl of reaction mix to each well with a multichannel pipette. Be sure to keep in the dark and incubate for at least 30 min at 37 °C.
(12) Measure immediately using a fluorescence plate reader with excitation at 530 nm and emission at 590 nm.
(13) Determine the amount of cholesterol esters by subtracting the measurements performed on samples that were not treated with cholesterol esterase from those that were treated with the enzyme. Each data point resulting from the assay should represent an average of at least three collections of animals, and the assay should be repeated at least three times.

4.6. Stains

While quantitative assays provide a means of measuring total stored TAG or cholesterol, staining of these neutral lipids in the intestine, fat body, and oenocytes provide a valuable cell based assay. This is especially powerful when combined with clonal analysis of mutant cells [45–47]. If relative quantification between samples is the goal, however, all samples should be prepared simultaneously and analyzed to ensure that the final results are not influenced by variations in temperature, dye concentration, incubation time, or microscope settings. Ideally, experimental and control slides should be randomized and scored blindly to eliminate confirmation bias. Many dyes are available for lipid detection, with Oil Red O, Sudan Black, and Nile Red being the most commonly used.

4. 6.1. Oil Red O

The dye Oil Red O provides a reliable means to visually assess neutral lipids in fixed tissues [48–51]. Animals are dissected and fixed using 4% formaldehyde in PBS for 30 min, washed twice in PBS and twice in 100% propylene glycol. Fixed tissues are then stained in a solution of 0.5% Oil Red O (Sigma; O0625) dissolved in propylene glycol, which has been filtered through Whatman #1 filter paper and preheated to 60 °C. Allow samples to incubate for 1 h at 60 °C, then wash twice with 85% propylene glycol and twice with PBS at room temperature. Stained samples are mounted on microscope slides using glycerol. The use of this dye in *Drosophila* is well documented and provides a sensitive means to assay neutral lipids in the oenocytes and intestine. The density of TAG in the fat body, however, results in an Oil Red O stain that is too intense for identifying modest defects in fat storage.

4.6.2. Sudan Black

Similar to Oil Red O, the dye Sudan Black allows for an accurate assessment of neutral lipid stores in fixed tissues [49,52]. Tissues that have been fixed with 4% formaldehyde are rinsed twice with PBS, once with 50% ethanol, and then stained for 2 min at room temperature with prefiltered 0.5% Sudan Black (Sigma; 199664) dissolved in 75% ethanol. Once staining is completed, samples are sequentially rinsed with 50% ethanol, 25% ethanol, and PBS before mounting on a microscope slide with glycerol. In general, Sudan Black results in less intense tissue stains than Oil Red O and thus is better suited for visualizing the high levels of TAG in the fat body.

4.6.3. Nile Red

Unlike Oil Red O and Sudan Black, Nile Red can be used to visualize neutral lipids in unfixed tissues [53]. Animals should be quickly dissected in a solution of 0.00002% Nile Red (Sigma; 19123) and 75% glycerol, and visualized using confocal microscopy. Although relatively straightforward, the use of Nile Red is somewhat limited and can be employed improperly [54–56]. While this dye allows for the qualitative assessment of lipid droplet size and shape, it should not be used to quantitatively measure fat reserves.

5. Methods to measure basic metabolites: carbohydrates

Proper regulation of carbohydrate homeostasis is critical for maintaining normal physiology. The two primary forms of circulating carbohydrates in *Drosophila* are glucose and trehalose (a disaccharide of glucose). While trehalose is abundant in larval hemolymph, circulating glucose and trehalose can be readily detected in the adult fly (Fig. 1). These sugars serve a variety of purposes, including providing an essential energy source through glycolysis, substrates for biosynthetic reactions in growing animals, and energy storage in the form of glycogen.

5.1. Enzymatic assays

A number of enzymatic assays are commercially available to quantify levels of specific sugars and related metabolic intermediates. Although initially developed for use in mammalian systems, many of these assays have been successfully co-opted for use in *Drosophila.* Care should be taken, however, to properly validate each enzymatic assay for a particular experimental system and/or developmental stage.

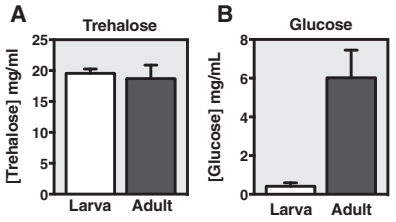

Fig. 1. Circulating trehalose and glucose levels in larvae and adults (A) Circulating trehalose is approximately equivalent and abundant during larval and adult stages. (B) In contrast, circulating glucose is low in larvae and is elevated during adulthood. Hemolymph was collected from w^{1118} mid-third instar larvae and 5 day old adults maintained on a standard cornmeal-based lab medium by puncturing the cuticle with a tungsten needle followed by centrifugation through glass wool into a collection tube. Circulating trehalose and glucose concentrations were determined using the HK assay kit.

5.1.1. Glucose

Two enzymatic-based methods have been widely used to measure free glucose levels in flies. The first of these utilizes the enzyme Hexokinase (HK) to phosphorylate glucose, producing glucose-6-phosphate [57]. Subsequent oxidation of glucose-6-phosphate by glucose-6-phosphate dehydrogenase produces 6-phosphogluconate and NADH. Spectrophotometric readings at 340 nm can then be used to assess the amount of NADH produced, as it naturally absorbs ultraviolet light at this wavelength. With this method, NADH production is directly proportional to the starting glucose concentration. Alternatively, free glucose levels can be measured through a colorimetric-based enzymatic assay. This method employs Glucose Oxidase (GO) activity to catalyze the oxidation of glucose to hydrogen peroxide and gluconic acid [58]. Subsequently, the hydrogen peroxide and an added compound, o-dianisidine, react to produce an oxidized form of o-dianisidine (orange color) in the presence of peroxidase. Sulfuric acid is then added to stop the reaction and convert the color to a pink hue, which can be quantified at an absorbance of 540 nm.

In our hands, the GO assay cannot be used to accurately quantify carbohydrates in pupae; rather, the HK protocol should be followed when studying this stage in development (W. Barry, unpublished results). This finding emphasizes the need to carefully validate the use of metabolite assays in new experimental contexts prior to their use. In addition, when using either the GO or HK protocol, it is important to keep the samples of homogenized tissue cold and to move rapidly prior to heat inactivation, which is essential to prevent the enzymatic breakdown of glycogen and trehalose into glucose by endogenous enzymes in the extract. Similar to the TAG assay described above, 10 μl of homogenate should be removed prior to heat inactivation and reserved for Bradford quantification of protein levels, providing a means to internally normalize glucose levels (although, as discussed above, effects of a mutation on protein levels may require another method for normalization).

5.1.2. Protocol: glucose quantification

(1) Collect samples (25 mid-second instar larvae; 5 adult flies).
(2) Rinse several times with 1 ml cold PBS to remove all traces of food that might be attached to the outside of the animal. Larvae can be washed in a 1.5 ml microfuge tube, but adults should be rinsed in a 9-well glass plate. Transfer adult flies to a 1.5 ml microfuge tube. Carefully remove all liquid. For larvae, centrifuge at 3000×*g* and remove all remnants of PBS. Snap freeze animals in liquid nitrogen for later homogenization or add 100 μl cold PBS.
(3) Rapidly homogenize animals in PBS with a pellet pestle (Kontes; 749521-1500) on ice. A motor can be used to facilitate homogenization (Kontes; 749540-0000). Frozen samples should be kept on dry ice until addition of PBS. If samples are not kept cold, glycogen and trehalose will be enzymatically degraded into free glucose by endogenous enzymes and skew the final analysis.
(4) Remove 10 μl of homogenized sample to measure protein content with a Bradford assay. Keep samples on ice and do not heat-treat. Protein samples can be frozen and stored at −80 °C for later analysis.
(5) Heat supernatant for 10 min at 70 °C, then centrifuge for 3 min at maximum speed in a refrigerated tabletop centrifuge that has been prechilled to 4 °C.
(6) Pipette the resulting supernatant into a new 1.5 ml microfuge tube. At this time, the heat-inactivated sample can be frozen and stored at −80 °C, if desired.
(7) Prepare glucose standards: Dilute 16 μl of 1 mg/ml glucose with 84 μl PBS (100 μl final volume) for 0.16 mg/ml standard. Do four 2-fold serial dilutions into PBS (50 μl 0.16 mg/ml + 50 μl PBS for 0.08 mg/ml standard, etc.) to generate 0.01, 0.02, 0.04, 0.08, and 0.16 mg/ml glucose standards. These assays are linear from 0.01 to 0.16 mg/ml glucose. Glucose stock solutions can be stored at −20 °C or 4 °C.
(8) Add 30 μl of glucose standards and a PBS blank to the first row of a clear-bottom 96 well plate. In the next row, add 30 μl of each sample into an individual well (after diluting them 1:4–1:8 with PBS).
(9a) For GO assay: Add 100 μl of GO reagent (Sigma; GAGO-20) to each well with a multichannel pipette. Seal the wells with parafilm to prevent evaporation and incubate the plate at 37 °C for 30–60 min. Stop the reaction by adding 100 μl of 12 N H_2SO_4 (the samples should visibly change color from yellow/orange to pink). Centrifuge the plate in an appropriate swing-bucket rotor to clear condensate from the sides of the wells and to remove any air bubbles present in the samples. Use a plate reader to measure absorbance at 540 nm. Determine the free glucose concentration by comparing the free glucose measurements for each sample to the glucose standard curve.
(9b) For HK assay: Add 100 μl of HK reagent (Sigma; GAHK20) to each well with a multichannel pipette. Seal the wells with parafilm to prevent evaporation and incubate the plate at room temperature for 15 min. Centrifuge the plate in an appropriate swing-bucket rotor to clear condensate from the sides of the wells and to remove any air bubbles present in the samples. Use a plate reader to measure absorbance at 340 nm. Determine the free glucose concentration by comparing the free glucose measurements for each sample to the glucose standard curve.

Glucose transporters are bidirectional, and thus free glucose will travel freely between intracellular and extracellular compartments. As a result, most free glucose is found in the circulating fluid rather than within cells. Measurements of free glucose from whole animal homogenates therefore provide an approximate assessment of circulating glucose levels. As always, however, accurate measurements of circulating trehalose or glucose can only be made by using hemolymph samples (see below).

5.1.3. Trehalose

Trehalose represents the major circulating sugar in *Drosophila* and, together with glucose, provides essential information about the metabolic state of an animal. Trehalose is quantified by an assay that is based on the protocol for measuring glucose levels, described above [59,60]. The difference is that trehalase is added to the extract to digest the trehalose into free glucose, which can then

be quantified by standard assays and compared to the background level of glucose present in the original sample.

5.1.4. Protocol: trehalose quantification

(1) Collect samples (25 mid-second instar larvae; 5 adult flies).
(2) Rinse several times with 1 ml cold PBS to remove all traces of food that might be attached to the outside of the animal. Larvae can be washed in a 1.5 ml microfuge tube, but adults should be rinsed in a 9-well glass plate. Transfer adult flies to a 1.5 ml microfuge tube. Carefully remove all liquid. For larvae, centrifuge at 3000×*g* and remove all remnants of PBS. Snap freeze animals in liquid nitrogen for later homogenization or add 100 μl cold Trehalase Buffer (TB) (5 mM Tris pH 6.6, 137 mM NaCl, 2.7 mM KCl).
(3) Rapidly homogenize animals in TB with a pellet pestle (Kontes; 749521-1500) on ice. A motor can be used to facilitate homogenization (Kontes; 749540-0000). Frozen samples should be kept on dry ice until addition of TB. If samples are not kept cold, glycogen and trehalose will be enzymatically degraded into free glucose by endogenous enzymes and skew the final analysis.
(4) Remove 10 μl of homogenized sample to measure protein content with a Bradford assay. Keep samples on ice and do not heat-treat. Protein samples can be frozen and stored at −80 °C for later analysis.
(5) Heat supernatant for 10 min at 70 °C, then centrifuge for 3 min at maximum speed in a refrigerated tabletop centrifuge that has been prechilled to 4 °C.
(6) Pipette the resulting supernatant into a new 1.5 ml microfuge tube. At this time, the heat-inactivated sample can be frozen and stored at −80 °C, if desired.
(7) Prepare the trehalase stock (TS) by diluting 3 μl porcine trehalase (Sigma; T8778-1UN) in 1 ml TB.
(8) Generate glucose and trehalose standards for standard curves:
For glucose standards, dilute 16 μl of 1 mg/ml glucose stock solution with 84 μl TB (100 μl final volume) to generate a 0.16 mg/ml standard. Conduct a series of 2-fold serial dilutions of the 0.16 mg/ml standard using TB (50 μl 0.16 mg/ml + 50 μl TB for 0.08 mg/ml standard) to generate 0.01, 0.02, 0.04, 0.08, and 0.16 mg/ml glucose standards. Aliquots of glucose stock solution can be stored at −20 °C or 4 °C.
For trehalose standards, dilute 16 μl of 1 mg/ml trehalose (Sigma; 90208) with 50 μl TS and 34 μl TB (100 μl final volume) for 0.16 mg/ml standard. Conduct a series of 2-fold serial dilutions of the 0.16 mg/ml standard using a 1:1 mix of TB and TS (e.g., 50 μl 0.16 mg/ml + 50 μl TB + TS for 0.08 mg/ml standard) to generate 0.01, 0.02, 0.04, 0.08, and 0.16 mg/ml trehalose standards. Aliquots of trehalose stock solution can be stored at −20 °C or 4 °C.
(9) Add 30 μl of TB blank or glucose standards to 30 μl TB in 1.5 ml microfuge tubes.
(10) Add 30 μl of TB blank or trehalose standards to two sets of 1.5 ml microfuge tubes. In one set, add 30 μl of TB to determine free glucose. In other set, add 30 μl TS to digest trehalose to glucose.
(11) If necessary, dilute fly samples between 1:2 and 1:4 in TB. Larval samples do not need diluting at this step unless analyzing a mutant that possesses particularly high trehalose levels.
(12) Add 30 μl of each fly sample to two 1.5 ml microfuge tubes. In the first tube, add 30 μl of TB to determine the background level of free glucose. In the second tube, add 30 μl of TS to digest trehalose into free glucose.
(13) Incubate all standards and samples at 37 °C for 18–24 h.
(14) Centrifuge at maximum speed in a tabletop centrifuge for 3 min. Transfer 30 μl of each sample into an individual well of a 96-well plate for analysis and use either the GO or HK assay to measure free glucose.
(15) Free glucose concentration in each sample is calculated based on the glucose standard curve. For trehalose measurements, first subtract the absorbance measured for free glucose in the untreated samples from the absorbance of the samples that have been digested with trehalase. The trehalose content in each sample is then calculated based on the trehalose standard curve. This method is linear from 0.01 to 0.16 mg/ml trehalose.

5.1.5. Hemolymph

While analysis of whole animal homogenates provides a relatively easy and high throughput approach for quantifying glucose and trehalose, this method does not distinguish between circulating and stored sugars, and can be complicated by the presence of food within the gut. Therefore, hemolymph samples are used to directly assay circulating sugars. Several alternate methods for hemolymph collection have been described for both larvae and adults [61–64]. Protocols based on filtration by centrifugation and capillary-based collection of hemolymph are most widely used. The centrifugation approach requires approximately 30–50 adult females (adult males contain less hemolymph per fly and thus require larger numbers) carefully punctured in the thorax using a tungsten needle. Punctured flies are placed in a 0.5 ml microfuge tube that contains a hole at the bottom of the tube, which is packed with glass wool. This tube is then placed within a 1.5 ml collection tube and centrifuged at 9000×*g* for 5 min at 4 °C, yielding approximately 1.5 μl of hemolymph. Longer centrifugation times, higher speeds, and more flies can increase yield, but may also increase cellular or intestinal contamination. One way to detect possible contamination from intestinal contents is to add food coloring to the medium and check the collected hemolymph for the absence of the dye. Additionally, hemolymph can be analyzed under a dissection scope for the absence of cellular debris.

Hemolymph can also be collected by immobilizing an adult fly wing-side down on a piece of double-sided tape and carefully puncturing the head cuticle with a tungsten needle [64]. Gentle pressure is applied to the thorax with a blunt object, and a capillary tube or pipette tip is used to collect the small drop of hemolymph that is forced out of the puncture site. While this method is labor intensive and not well suited for the collection of large numbers of samples, it minimizes potential hemolymph contamination.

Regardless of which method is used, a 1 μl aliquot of the collected hemolymph is diluted in 99 μl of trehalase buffer (1:100), followed by heat treatment for 5 min at 70 °C to inactivate endogenous trehalase. After heat treatment, the sample is split into two 50 μl aliquots, one of which is diluted further with an equal volume of trehalase buffer alone, and the other with trehalase buffer plus trehalase [3 μl of porcine trehalase (Sigma; T8778-1UN) per 1 ml of buffer]. The resulting sample will have a final dilution of 1:200. These diluted samples are then placed at 37 °C for 18–24 h to allow for breakdown of trehalose into free glucose. A 30 μl aliquot of each sample (+/−trehalase) is then loaded onto a 96 well plate to measure the concentration of hemolymph trehalose and glucose using the enzymatic assays described above. As previously mentioned, the ideal dilution will depend on dietary conditions, genetic background and developmental stage.

5.1.6. Glycogen

Most carbohydrate in the fly is stored in the form of glycogen, which provides a large and accessible energy source during times of fasting and intense activity. Most glycogen in the adult fly is stored in the fat body, flight muscle, halteres, and gut, while larval

glycogen is primarily located in the body wall muscle [3,65]. Although periodic acid/Schiff staining can be used to visually assess glycogen deposits, the easiest and most quantitative method uses an enzymatic assay that breaks down glycogen into molecules of free glucose, which is then quantified using the GO or HK assays described above [66]. As with the other assays above, homogenized tissue samples must be kept cold and moved rapidly to the heat treatment step to prevent the breakdown of glycogen into free glucose by endogenous enzymes present in the extract. Due to the high level of glycogen in the samples, the resulting supernatant should be appropriately diluted to ensure that the concentrations of all samples are within the linear range of the assay. If the concentration of any sample exceeds that of the 0.16 mg/ml glycogen standard, then the assay should be repeated using more dilute samples. Although either the GO or HK assays can be used to measure glycogen, the HK assay is preferred for glycogen measurements in pupae, when the GO kit can be unreliable.

5.1.7. Protocol: glycogen quantification using the GO kit

(1) Collect samples (25 mid-second instar larvae; 5 adult flies).
(2) Rinse several times with 1 ml cold PBS to remove all traces of food that might be attached to the outside of the animal. Larvae can be washed in a 1.5 ml microfuge tube, but adults should be rinsed in a 9-well glass plate. Transfer adult flies to a 1.5 ml microfuge tube. Carefully remove all liquid. For larvae, centrifuge at 3000×*g* and remove all remnants of PBS. Snap freeze animals in liquid nitrogen for later homogenization or add 100 μl cold PBS.
(3) Rapidly homogenize animals in PBS with a pellet pestle (Kontes; 749521-1500) on ice. A motor can be used to facilitate homogenization (Kontes; 749540-0000). Frozen samples should be kept on dry ice until addition of PBS. If samples are not kept cold, glycogen and trehalose will be enzymatically degraded into free glucose by endogenous enzymes and skew the final analysis.
(4) Remove 10 μl of homogenized sample to measure protein content with a Bradford assay. Keep samples on ice and do not heat-treat. Protein samples can be frozen and stored at −80 °C for later analysis.
(5) Heat supernatant for 10 min at 70 °C, then centrifuge for 3 min at maximum speed in a refrigerated tabletop centrifuge that has been prechilled to 4 °C.
(6) Pipette the resulting supernatant into a new 1.5 ml microfuge tube. At this time, the heat-inactivated sample can be frozen and stored at −80 °C, if desired.
(7) Set up glucose and glycogen standards. Using 1 mg/ml glucose or glycogen stock solutions, make a dilution series of glucose or glycogen standards in PBS, both in the range of 0–0.16 mg/ml, as outlined in glucose assay protocol. Glycogen stock solutions can be stored at −20 °C or 4 °C.
(8) Add 30 μl of each glycogen standard (including PBS blank) to the top row of a clear-bottom 96 well plate. Similarly, add 30 μl of each glucose standard in the next row down.
(9) Dilute heat-treated fly samples for glycogen measurements 1:5 in PBS (the required dilution may range from 1:5 to 1:20 depending on experimental conditions) and load 30 μl into each well. Samples should be loaded in duplicate rows such that one row will be used to measure glycogen + glucose (treated with amyloglucosidase) and the adjacent row will be used to measure glucose alone (no amyloglucosidase).
(10) Prepare the GO reagent (see glucose assay protocol) for your glycogen measurements by adding 1 μl amyloglucosidase (Sigma A1602; 25 mg) per 1 ml of GO reagent.
(11) Using a multichannel pipette, add 100 μl of GO reagent + amyloglucosidase to the glycogen standards and the first row of each set of duplicate samples. Then add 100 μl of GO reagent alone (without amyloglucosidase) to the glucose standards and the remaining samples.
(12) Seal the wells with parafilm to prevent evaporation and incubate the plate at 37 °C for 30–60 min. Briefly centrifuge the plate in an appropriate swing-bucket rotor to clear condensate from the sides of the wells and remove any air bubbles present in the samples. Then add 100 μl of 12 N sulfuric acid and measure absorbance at 540 nm using a plate reader.
(13) Free glucose concentration in each sample is calculated based on the glucose standard curve. For glycogen measurements, first subtract the absorbance measured for free glucose in the untreated samples from the absorbance of the samples that have been digested with amyloglucosidase. The glycogen content in each sample is then calculated based on the glycogen standard curve. This method is linear from 0.01 to 0.16 mg/ml glycogen.

5.1.8. Protocol: glycogen quantification using the HK kit

(1) Collect samples (25 mid-second instar larvae; 5 adult flies).
(2) Rinse several times with 1 ml cold PBS to remove all traces of food that might be attached to the outside of the animal. Larvae can be washed in a 1.5 ml microfuge tube, but adults should be rinsed in a 9-well glass plate. Transfer adult flies to a 1.5 ml microfuge tube. Carefully remove all liquid. For larvae, centrifuge at 3000×*g* and remove all remnants of PBS. Snap freeze animals in liquid nitrogen for later homogenization or add 100 μl cold PBS.
(3) Rapidly homogenize animals in PBS with a pellet pestle (Kontes; 749521-1500) on ice. A motor can be used to facilitate homogenization (Kontes; 749540-0000). Frozen samples should be kept on dry ice until addition of PBS. If samples are not kept cold, glycogen and trehalose will be enzymatically degraded into free glucose by endogenous enzymes and skew the final analysis.
(4) Remove 10 μl of homogenized sample to measure protein content with a Bradford assay. Keep samples on ice and do not heat-treat. Protein samples can be frozen and stored at −80 °C for later analysis.
(5) Heat supernatant for 10 min at 70 °C, then centrifuge for 3 min at maximum speed in a refrigerated tabletop centrifuge that has been prechilled to 4 °C.
(6) Pipette the resulting supernatant into a new 1.5 ml microfuge tube. At this time, the heat-inactivated sample can be frozen and stored at −80 °C, if desired.
(7) Prepare amyloglucosidase stock (AS) solution by adding 1.5 μl amyloglucosidase (Sigma A1602; 25 mg) to 1 ml of PBS.
(8) Set up glycogen standards by diluting 16 μl of glycogen stock (1 mg/ml) with 50 μl of AS solution and 34 μl of PBS (100 μl final volume) for 0.16 mg/ml standard. Do four 2-fold serial dilutions into 1:1 mix of AS and 1×PBS (50 μl 0.16 mg/ml + 50 μl AS + PBS for 0.08 mg/ml standard, etc.) to generate 0.01, 0.02, 0.04, 0.08, and 0.16 mg/ml glycogen standards. Glucose standards should be diluted as outlined in the glucose assay protocol (no amyloglucosidase added).
(9) In 1.5 ml microfuge tubes, dilute the heat-treated fly samples 1:3 in PBS (this dilution can range from 1:2 to 1:5 depending on experimental conditions) by combining 20 μl of sample with 40 μl PBS. Aliquot 20 μl of these diluted samples into two separate tubes, one containing 20 μl of AS solution, and the other containing 20 μl of PBS (final sample dilution will equal 1:6).

(10) Add 30 μl of each glycogen standard (including PBS blank) to one row at the top of the plate. Add 30 μl of the glucose standards (and PBS blank) to the next row.
(11) Load 30 μl of each diluted sample to the plate. Samples should be loaded in duplicate rows such that one row will be used to measure glycogen + glucose (amyloglucosidase treated) and the adjacent row will be used to measure glucose alone (no amyloglucosidase).
(12) Seal the wells with parafilm and incubate the plate at 37 °C for 60 min to digest the glycogen. Spin briefly to clear the condensate from the sides of the wells.
(13) Add 100 μl of HK reagent to each well with a multichannel pipette and incubate at room temperature for 15 min. Measure absorbance at 340 nm using a plate reader.
(14) Free glucose concentration in each sample is calculated based on the glucose standard curve.

For glycogen measurements, first subtract the absorbance measured for free glucose in the untreated samples from the absorbance of the samples that have been digested with amyloglucosidase. The glycogen content in each sample is then calculated based on the glycogen standard curve. This method is linear from 0.01 to 0.16 mg/ml glycogen.

6. ATP

ATP measurements represent a direct readout of cellular energy levels and thus can provide important insights into metabolic phenotypes. This analysis can be conducted with a luciferase-based assay kit that uses endogenous ATP to generate light [67]. Because ATP is so unstable, a chaotropic buffer is used to preserve as much of the intact metabolite as possible.

6.1. Protocol: fluorescence assay for ATP quantification

(1) Collect samples (25 mid-second instar larvae; 5 adult flies).
(2) Rinse several times with 1 ml cold PBS to remove all traces of food that might be attached to the outside of the animal. Larvae can be washed in a 1.5 ml microfuge tube, but adults should be rinsed in a 9-well glass plate. Transfer adult flies to a 1.5 ml microfuge tube. Carefully remove all liquid. For larvae, centrifuge at 3000×*g* and remove all remnants of PBS.
(3) Prior to homogenizing the samples, prepare the ATP reaction mix (Molecular Probes ATP kit; A22066) by mixing 3.56 ml ddH_20, 200 μl 20× reaction buffer, 40 μl 0.1 M DTT, 200 μl 10 mM D-luciferin, and 1 μl firefly luciferase. The resulting mix is sufficient for 40 reactions, and should be kept on ice and protected from light.
(4) Animals are rapidly homogenized in 100 μl of homogenization buffer [6 M guanidine HCl, 100 mM Tris (pH 7.8), 4 mM EDTA] with a pellet pestle (Kontes; 749521-1500) on ice. A motor can be used to facilitate homogenization (Kontes; 749540-0000).
(5) Remove 10 μl of homogenized sample to measure protein content with a Bradford assay. Keep samples on ice and do not heat-treat. Protein samples can be frozen and stored at −80 °C for later analysis.
(6) The remaining samples are boiled for 5 min and centrifuged for 3 min at maximum speed in a refrigerated tabletop centrifuge that has been prechilled to 4 °C.
(7) Transfer 10 μl of the supernatant into a 1.5 ml microfuge tube and dilute 1:10 with 90 μl dilution buffer [25 mM Tris (pH 7.8), 100 μM EDTA], then transfer 10 μl of the diluted supernatant to a second 1.5 ml tube and dilute 1:75 by adding 740 μl of dilution buffer (final dilution of 1:750). The diluted homogenate is centrifuged at 20,000×*g*, and 10 μl of the supernatant is transferred to individual wells of a white, opaque 96 well plate (Corning; 3362).
(8) Prepare a series of ATP standards by diluting the 5 mM ATP stock solution provided with the assay kit with ddH_2O (0, 0.01, 0.05, 0.1, 0.5, 1 μM). Add 10 μl of each ATP standard solution to the first row of the plate to provide a standard curve. ATP standards can be stored at −20 °C for several weeks.
(9) Start the assay by adding 100 μl of the luciferase reaction mix with a multichannel pipette and immediately begin measuring luminescence with a plate reader. A minimum of three sequential measurements should be made for the entire plate, and the results should be averaged.
(10) Determine the ATP concentration by comparing the luminescence measurements for each sample to the ATP standard curve.

7. Metabolomics

The emerging field of metabolomics provides an unprecedented opportunity to simultaneously measure hundreds of metabolic compounds in animal extracts. This technique has proven to be a powerful tool for conducting studies in the fly [17,68–71]. In addition, when combined with classical genetic analysis, metabolomics can be used to precisely identify metabolic reactions that are affected by a mutation, providing key insights into gene function. The field of metabolomics is too large to summarize in a single review because a variety of methods have been developed to assay several classes of metabolites, ranging from small, charged molecules to lipids. Rather, we provide here a relatively simple protocol that allows users to quantify ~100 small, polar molecules, which includes the basic amino acids, sugars, and intermediates in glycolysis and the TCA cycle. This range of compounds is sufficient to provide insights into the metabolic state of the corresponding animal.

7.1. Genetic background

Metabolomic analysis is particularly sensitive to genetic background effects. An example of this is the use of *rosy* mutant strains as a control for transgenic lines that were established by scoring for rescue of the eye phenotype. *ry* mutations render animals unable to synthesize uric acid, which not only results in elevated levels of purine-related intermediates [72], but also induces significant changes in a diverse group of metabolites, including tryptophan, kynurenine, and related compounds [73]. Studies of transgenic lines in which the *ry* background is not controlled would therefore inaccurately identify widespread metabolic defects. Similarly, *yellow* mutants exhibit defects in lysine metabolism [74], and other widely-used mutant lines, such as *white* or *vermillion*, may produce similar metabolomic artifacts. Therefore, the same genetic background should be used for all samples, ideally using multiple control genotypes for internal confirmation.

7.2. Sample collection

The amount of material required for a successful metabolomics experiment varies depending on the developmental stage and type of analysis. For a basic survey of small, polar metabolites using GC-MS, samples should contain at least 300 embryos, 25 second-instar larvae, and 20 mature adult males. All samples, except for larvae, are collected in screw-cap tubes that contain 1.4 mm ceramic beads (MoBio; 13113-50) and flash frozen in liquid nitrogen. These tubes are designed for the Omni Bead Ruptor, described below. Embryos do not need to be dechorionated prior to collection, but

should be washed gently with a paintbrush on a piece of Whatman filter paper soaked in PBS. Larvae are collected in a 1.5 ml tube, repeatedly washed with ice-cold PBS, and flash frozen in liquid nitrogen. The frozen pellet is then dislodged by gently flicking the tube and transferred into a pre-chilled screw cap tube with ceramic beads.

7.3. Sample processing for GC–MS

All samples should be stored at −80 °C until processing, at which point they are transferred to an enzyme-type carrier caddy (Nunc Lab-Top cooler) that has been chilled to −20 °C. Add 800 μl of prechilled 90% methanol containing 1.25 μg/ml succinic-*d*4 acid (Sigma–Aldrich; 293075) and 6.25 μg/ml U-13C, U-15N amino acid mix (Cambridge Isotope; CDNLM-6784) to each tube with a positive displacement pipette. These stable-isotope labeled internal standards provide a means to normalize samples, provide quality control, and allow for the monitoring of instrument efficiency across batches. Additionally, negative controls that contain no fly tissue should be prepared to detect chemical contamination and false-positive peaks during the subsequent GC-MS analysis.

The hard cuticle of the fly is difficult to homogenize and requires a strong physical disruption to efficiently release metabolites. We have found that the Omni Bead Ruptor 24 homogenizer (Omni International) is ideally suited to rapidly and efficiently disrupt fly tissue, with samples homogenized for 30 sec at 6.45 m/sec. While a variety of bead-filled tubes can be used for this purpose, screw-cap tubes containing 1.4 mm ceramic beads are optimal for removing extraction solvent after processing. Homogenized samples are incubated at −20 °C for 1 h to enhance protein precipitation and centrifuged at 20,000×*g* for 5 min at 4 °C to remove the resulting precipitate. The supernatant is transferred to a 1.5 ml microfuge tube and the solvent removed with a Speed-Vac (Genevac).

7.4. GC–MS analysis

We perform GC–MS analysis with a Waters GCT Premier mass spectrometer fitted with an Agilent 6890 gas chromatograph and a Gerstel MPS2 autosampler. Dried samples are suspended in 40 μl of 40 mg/ml O-methoxylamine hydrochloride (MOX) (MP Biomedicals; 155405) in pyridine solution (EMD Millipore; PX2012-7) and incubated for 1 h at 30 °C. Samples are then centrifuged for 5 min at 20,000×*g* to remove particulate matter, and 25 μl of the supernatant is placed in an autosampler vial (Agilent; 8010-0172 and 5181-1215) with a 250 μl deactivated glass microvolume liner (Agilent; 5183–2086). Forty microliters of N-methyl-N-trimethylsilyltrifluoracetamide containing 1% TMCS (MSTFA) (Thermo Scientific; TS-48915) is added automatically via a Gerstal autosampler and the samples are incubated for 60 min at 37 °C with shaking. Following incubation, 3 μl of a fatty acid methyl ester standard solution (FAMES; Table 2) is added via the autosampler and 1 μl of the prepared sample is injected to the gas chromatograph inlet at a 10:1 split ratio with the inlet temperature held at 250 °C. Fatty acid methyl esters do not occur naturally, but will elute in a highly reproducible manner across the entire chromatogram. The retention time curve of FAMES solution, therefore, allows for the building of reliable retention time libraries of metabolites. Furthermore, this solution is used to assess column quality because a degraded column will exhibit peak tailings of the FAMES standards.

The gas chromatograph is set to an initial temperature of 95 °C for one minute followed by a 40 °C/min ramp to 110 °C and a hold time of 2 min. This is followed by a 5 °C/min ramp to 250 °C and a third ramp to 330 °C with a final hold time of 3 min. A 30 meter Phenomex ZB5-5 MSi column with a 5 meter long guard column is employed for chromatographic separation. For each analysis, instrument performance is assessed by analyzing the negative control samples, which only contain the internal standard. Experimental samples are only processed if the instrument passes a preset sensitivity and peak shape criteria. Finally, samples are run in a randomized order, except for quality control samples, which are analyzed every nine samples.

Table 2
Components of FAMES solution (0.1 mg/ml for each compound).

Compound	Sigma Aldrich catalog #
Methyl heptanoate	75218
Methyl caprylate	21719
Methyl caprate	21479
Methyl laurate	61689
Methyl myristate	70129
Methyl palmitate	76159
Methyl stearate	85769
Methyl arachidate	10941
Methyl behenate	11940
Methyl tetracosanoate	87115

7.5. Data analysis

An initial dataset is prepared using a targeted approach to identify known metabolites. Chromatograms are analyzed using the MassLynx utility QuanLynx, and metabolites are identified based on known retention times and mass fragmentation patterns. The peak area for each metabolite is recorded, and the data is exported to Excel. For our analyses, metabolite identity in QuanLynx is experimentally established using pure, purchased standards, and in limited cases by the commercially available NIST library (National Institute of Standards and Technology; version 11). MarkerLynx is used for peak identification during a second, non-targeted analysis of the chromatograms, and the formatted data is transferred to SIMCA-P+ for principle component analysis (PCA) and partial least squares-discriminate (PLS-DA) analysis. If the PCA analysis identifies significant separation between the experimental groups, PLS-DA analysis is employed to detect significantly altered metabolites. The peaks of unknown metabolites are quantified and the resulting data is exported to Excel. Statistical analysis can be performed with any number of software packages that are available for uni- and multivariate analysis, including JMP and Statistica.

Acknowledgements

We thank L.P. Musselman, A.-F. Ruaud, and M. Sieber for their contributions to these protocols, and D. Bricker, M. Horner, S. Marxreiter, and R. Somer for helpful comments on the manuscript. This work was supported by an NIH K99/R00 Pathway to Independence Award to J.M.T. (K99GM101341), an NIH Developmental Biology Training Grant to W.B. (5T32 HD07491), and NIH R01 DK075607 (C.S.T.).

References

[1] S. O'Brien, R. MacIntyre, in: M. Ashburner, T. Wright (Eds.), The Genetics and Biology of *Drosophila*, Academic Press, New York, 1978, pp. 396–551.
[2] G. Beadle, E. Tatum, Am. Nat. 75 (1941) 107–116.
[3] V. Wigglesworth, J. Exp. Biol. 26 (1949) 150–163.
[4] M.R. Clare, Biol. Bull. 49 (1925) 440–460.
[5] J.H. Bodine, P.R. Orr, Biol. Bull. 48 (1925) 1–14.
[6] K.D. Baker, C.S. Thummel, Cell Metab. 6 (2007) 257–266.
[7] R.T. Birse, R. Bodmer, Crit. Rev. Biochem. Mol. Biol. 46 (2011) 376–385.
[8] R.P. Kuhnlein, Results Probl. Cell Differ. 52 (2010) 159–173.
[9] P. Leopold, N. Perrimon, Nature 450 (2007) 186–188.
[10] A.A. Teleman, Biochem. J. 425 (2010) 13–26.

[11] N. Alic, M.P. Hoddinott, A. Foley, C. Slack, M.D. Piper, L. Partridge, PLoS One 7 (2012) e45367.
[12] J.L. Buescher, L.P. Musselman, C.A. Wilson, T. Lang, M. Keleher, T.J. Baranski, J.G. Duncan, Dis. Model Mech. 6 (2013) 1123–1132.
[13] L.M. Matzkin, S. Johnson, C. Paight, T.A. Markow, PLoS One 8 (2013) e59530.
[14] M.A. Horner, K. Pardee, S. Liu, K. King-Jones, G. Lajoie, A. Edwards, H.M. Krause, C.S. Thummel, Genes Dev. 23 (2009) 2711–2716.
[15] M.Y. Pasco, P. Leopold, PLoS One 7 (2012) e36583.
[16] E. Havula, M. Teesalu, T. Hyotylainen, H. Seppala, K. Hasygar, P. Auvinen, M. Oresic, T. Sandmann, V. Hietakangas, PLoS Genet. 9 (2013) e1003438.
[17] D.K. Bricker, E.B. Taylor, J.C. Schell, T. Orsak, A. Boutron, Y.C. Chen, J.E. Cox, C.M. Cardon, J.G. Van Vranken, N. Dephoure, C. Redin, S. Boudina, S.P. Gygi, M. Brivet, C.S. Thummel, J. Rutter, Science 337 (2012) 96–100.
[18] L.P. Musselman, J.L. Fink, K. Narzinski, P.V. Ramachandran, S.S. Hathiramani, R.L. Cagan, T.J. Baranski, Dis. Model Mech. 4 (2011) 842–849.
[19] J. Na, L.P. Musselman, J. Pendse, T.J. Baranski, R. Bodmer, K. Ocorr, R. Cagan, PLoS Genet. 9 (2013) e1003175.
[20] A.S. Kunte, K.A. Matthews, R.B. Rawson, Cell Metab. 3 (2006) 439–448.
[21] R.T. Birse, J. Choi, K. Reardon, J. Rodriguez, S. Graham, S. Diop, K. Ocorr, R. Bodmer, S. Oldham, Cell Metab. 12 (2010) 533–544.
[22] L.K. Reed, S. Williams, M. Springston, J. Brown, K. Freeman, C.E. DesRoches, M.B. Sokolowski, G. Gibson, Genetics 185 (2010) 1009–1019.
[23] W.C. Lee, C.A. Micchelli, PLoS One 8 (2013) e67308.
[24] M.D. Piper, E. Blanc, R. Leitao-Goncalves, M. Yang, X. He, N.J. Linford, M.P. Hoddinott, C. Hopfen, G.A. Soultoukis, C. Niemeyer, F. Kerr, S.D. Pletcher, C. Ribeiro, L. Partridge, Nat. Methods 11 (2013) 100–105.
[25] R.S. Edgecomb, C.E. Harth, A.M. Schneiderman, J. Exp. Biol. 197 (1994) 215–235.
[26] R.C. King, L.P. Wilson, J. Exp. Zool. 130 (1955) 71–82.
[27] G.B. Carvalho, P. Kapahi, S. Benzer, Nat. Methods 2 (2005) 813–815.
[28] D.J. Seay, C.S. Thummel, J. Biol. Rhythms 26 (2011) 497–506.
[29] W.W. Ja, G.B. Carvalho, E.M. Mak, N.N. de la Rosa, A.Y. Fang, J.C. Liong, T. Brummel, S. Benzer, Proc. Natl. Acad. Sci. USA 104 (2007) 8253–8256.
[30] R. Wong, M.D. Piper, B. Wertheim, L. Partridge, PLoS One 4 (2009) e6063.
[31] P.M. Itskov, C. Ribeiro, Front. Neurosci. 7 (2013) 12.
[32] A. Hildebrandt, I. Bickmeyer, R.P. Kuhnlein, PLoS One 6 (2011) e23796.
[33] A. Rietveld, S. Neutz, K. Simons, S. Eaton, J. Biol. Chem. 274 (1999) 12049–12054.
[34] A.G. Clark, W. Gellman, *Drosophila* Info. Serv. 61 (1985) 190.
[35] S. Gronke, M. Beller, S. Fellert, H. Ramakrishnan, H. Jackle, R.P. Kuhnlein, Curr. Biol. 13 (2003) 603–606.
[36] B. Al-Anzi, K. Zinn, PLoS One 5 (2010) e12353.
[37] C.M. Williams, R.H. Thomas, H.A. MacMillan, K.E. Marshall, B.J. Sinclair, J. Ins. Phys. 57 (2011) 1602–1613.
[38] P.P. Van Veldhoven, J.V. Swinnen, M. Esquenet, G. Verhoeven, Lipids 32 (1997) 1297–1300.
[39] H. Chiang, Am. Midland Nat. 70 (1963) 329–338.
[40] M.M. Bradford, Anal. Biochem. 72 (1976) 248–254.
[41] M. Carvalho, D. Schwudke, J.L. Sampaio, W. Palm, I. Riezman, G. Dey, G.D. Gupta, S. Mayor, H. Riezman, A. Shevchenko, T.V. Kurzchalia, S. Eaton, Development 137 (2010) 3675–3685.
[42] X. Huang, J.T. Warren, J. Buchanan, L.I. Gilbert, M.P. Scott, Development 134 (2007) 3733–3742.
[43] M.H. Sieber, C.S. Thummel, Cell Metab. 15 (2012) 122–127.
[44] S.P. Voght, M.L. Fluegel, L.A. Andrews, L.J. Pallanck, Cell Metab. 5 (2007) 195–205.
[45] T. Reis, M.R. Van Gilst, I.K. Hariharan, PLoS Genet. 6 (2010) e1001206.
[46] J.P. Parvy, L. Napal, T. Rubin, M. Poidevin, L. Perrin, C. Wicker-Thomas, J. Montagne, PLoS Genet. 8 (2012) e1002925.
[47] S.K. Tiefenbock, C. Baltzer, N.A. Egli, C. Frei, EMBO J. 29 (2010) 171–183.
[48] R.L. Seecof, S. Dewhurst, Cell Differ. 3 (1974) 63–70.
[49] F.M. Butterworth, D. Bodenstein, R.C. King, J. Exp. Zool. 158 (1965) 141–153.
[50] L. Palanker, J.M. Tennessen, G. Lam, C.S. Thummel, Cell Metab. 9 (2009) 228–239.
[51] E. Gutierrez, D. Wiggins, B. Fielding, A.P. Gould, Nature 445 (2007) 275–280.
[52] I. Zinke, C. Kirchner, L.C. Chao, M.T. Tetzlaff, M.J. Pankratz, Development 126 (1999) 5275–5284.
[53] S. Gronke, A. Mildner, S. Fellert, N. Tennagels, S. Petry, G. Muller, H. Jackle, R.P. Kuhnlein, Cell Metab. 1 (2005) 323–330.
[54] K.K. Brooks, B. Liang, J.L. Watts, PLoS One 4 (2009) e7545.
[55] E.J. O'Rourke, A.A. Soukas, C.E. Carr, G. Ruvkun, Cell Metab. 10 (2009) 430–435.
[56] L.K. Schroeder, S. Kremer, M.J. Kramer, E. Currie, E. Kwan, J.L. Watts, A.L. Lawrenson, G.J. Hermann, Mol. Biol. Cell 18 (2007) 995–1008.
[57] A. Kunst, B. Draeger, J. Ziegenhorn, Methods of Enzymatic Analysis, third ed., Academic Press, New York, 1984.
[58] H.U. Bergmeyer, E. Bernt, Methods of Enzymatic Analysis, second ed., Academic Press, New York, 1974.
[59] A.A. Teleman, Y.W. Chen, S.M. Cohen, Dev. Cell 9 (2005) 271–281.
[60] Q. Chen, E. Ma, K.L. Behar, T. Xu, G.G. Haddad, J. Biol. Chem. 277 (2002) 3274–3279.
[61] G. Lee, J.H. Park, Genetics 167 (2004) 311–323.
[62] E.J. Rulifson, S.K. Kim, R. Nusse, Science 296 (2002) 1118–1120.
[63] S.C. Piyankarage, D.E. Featherstone, S.A. Shippy, Anal. Chem. 84 (2012) 4460–4466.
[64] A.T. Haselton, Y.W. Fridell, J. Vis. Exp. 52 (2011) e2722.
[65] A.F. Ruaud, G. Lam, C.S. Thummel, Mol. Endocrinol. 25 (2011) 83–91.
[66] A.G. Clark, L.E. Keith, Biochem. Genet. 27 (1989) 263–277.
[67] J. Park, S.B. Lee, S. Lee, Y. Kim, S. Song, S. Kim, E. Bae, J. Kim, M. Shong, J.M. Kim, J. Chung, Nature 441 (2006) 1157–1161.
[68] J.M. Tennessen, K.D. Baker, G. Lam, J. Evans, C.S. Thummel, Cell Metab. 13 (2011) 139–148.
[69] Y. Li, D. Padmanabha, L.B. Gentile, C.I. Dumur, R.B. Beckstead, K.D. Baker, PLoS Genet. 9 (2013) e1003230.
[70] V.R. Chintapalli, M. Al, PLoS One 8 (2013) e78066.
[71] J.M. Knee, T.Z. Rzezniczak, A. Barsch, K.Z. Guo, T.J. Merritt, J. Chromatogr. B. Anal. Technol. Biomed. Life Sci. 936 (2013) 63–73.
[72] A.J. Hilliker, B. Duyf, D. Evans, J.P. Phillips, Proc. Natl. Acad. Sci. USA 89 (1992) 4343–4347.
[73] M.A. Kamleh, Y. Hobani, J.A. Dow, D.G. Watson, FEBS Lett. 582 (2008) 2916–2922.
[74] M.A. Bratty, V.R. Chintapalli, J.A. Dow, T. Zhang, D.G. Watson, FEBS Open Bio. 2 (2012) 217–221.

CHAPTER 3

THE *DROSOPHILA* HNF4 NUCLEAR RECEPTOR PROMOTES GLUCOSE-STIMULATED INSULIN SECRETION AND MITOCHONDRIAL FUNCTION IN ADULTS

Originally published as – Barry, W.B. and Thummel, C.S. (2016). The *Drosophila* HNF4 nuclear receptor promotes glucose-stimulated insulin secretion and mitochondrial function in adults. 5:e11183

eLIFE elifesciences.org

RESEARCH ARTICLE

The *Drosophila* HNF4 nuclear receptor promotes glucose-stimulated insulin secretion and mitochondrial function in adults

William E Barry, Carl S Thummel*

Department of Human Genetics, University of Utah School of Medicine, Salt Lake City, United States

Abstract Although mutations in *HNF4A* were identified as the cause of Maturity Onset Diabetes of the Young 1 (MODY1) two decades ago, the mechanisms by which this nuclear receptor regulates glucose homeostasis remain unclear. Here we report that loss of *Drosophila HNF4* recapitulates hallmark symptoms of MODY1, including adult-onset hyperglycemia, glucose intolerance and impaired glucose-stimulated insulin secretion (GSIS). These defects are linked to a role for dHNF4 in promoting mitochondrial function as well as the expression of *Hex-C*, a homolog of the MODY2 gene *Glucokinase. dHNF4* is required in the fat body and insulin-producing cells to maintain glucose homeostasis by supporting a developmental switch toward oxidative phosphorylation and GSIS at the transition to adulthood. These findings establish an animal model for MODY1 and define a developmental reprogramming of metabolism to support the energetic needs of the mature animal.
DOI: 10.7554/eLife.11183.001

***For correspondence:** carl.thummel@genetics.utah.edu

Competing interests: The authors declare that no competing interests exist.

Funding: See page 22

Received: 27 August 2015
Accepted: 12 April 2016
Published: 17 May 2016

Reviewing editor: Utpal Banerjee, University of California, Los Angeles, United States

Introduction

The global rise in the prevalence of diabetes has prompted increased efforts to advance our understanding of metabolic systems and how they become disrupted in the diseased state. Although genetics and environment have a significant impact on diabetes susceptibility, severity, and care, the causal factors are often complex and unclear. Several cases of familial diabetes have been identified, however, that show clear patterns of heritability due to monogenic disease alleles, highlighting these genes as critical factors for glycemic control. To date, mutations in 13 genes have been shown to cause autosomal dominant inheritance of Maturity Onset Diabetes of the Young (MODY1-13), representing the most common forms of monogenic diabetes. MODY patients typically present with hyperglycemia and impaired glucose-stimulated insulin secretion (GSIS) by young adulthood, while having normal body weight and lacking β-cell autoimmunity (***Fajans and Bell, 2011***). Consistent with this, several genes associated with MODY have well-characterized functions in glucose homeostasis, including the glycolytic enzyme *Glucokinase* (GCK/MODY2), and *Insulin* (INS/MODY10). Mechanistic insight into the anti-diabetic roles of other MODY genes, however, remains limited.

The genetic basis for the first MODY subtype was reported two decades ago, identifying loss-of-function mutations in *Hepatocyte Nuclear Factor 4A* (*HNF4A*) as responsible for MODY1 (***Yamagata et al., 1996***). HNF4A is a member of the nuclear receptor superfamily of ligand-regulated transcription factors, which play important roles in the regulation of growth, development, and metabolic homeostasis. Studies in mice demonstrated a critical requirement for *Hnf4A* in early development, with null mutants dying during embryogenesis due to defects in gastrulation (***Chen et al., 1994***). Heterozygotes, however, show no apparent phenotypes. As a result, tissue-specific genetic

eLife digest Diabetes is a complex disease that is caused by a combination of factors, including the person's habits and environment, as well as their genetic make-up. However, there are some rare forms of diabetes that are caused simply by mutations in single genes and are directly inherited. For example, it has been known for twenty years that a type of diabetes called "Maturity Onset Diabetes of the Young type 1" (or MODY1 for short) occurs when a gene called *HNF4* is mutated or deleted. The symptoms of MODY1 usually appear during early adulthood and include abnormally high levels of sugar in the blood, as well as the pancreas not being able to release the hormone insulin properly in response to these sugars.

Previous studies in mice have tried to understand how losing the HNF4 gene leads to MODY1. However, these mouse models did not fully recreate the symptoms of this disorder and the precise role of HNF4 in preventing diabetes remains unclear. Barry and Thummel have now used the fruit fly, because it is a model organism with simple genetics, to help shed light on this question. Furthermore, flies and mammals use many of the same pathways to control metabolism, making the fly a good model for the disease in humans.

Barry and Thummel deleted the *HNF4* gene in fruit flies and observed that the flies had all the symptoms that are typical in people with MODY1. These symptoms included high sugar levels and decreased production of insulin-like hormones. The experiments also showed that *HNF4* normally supports the proper expression of another gene called *Hex-C*; this gene encodes a protein that senses how much sugar is available and helps to keep the amount of sugar circulating the body within normal levels. Barry and Thummel went on to discover that the *HNF4* gene is required for the expression of some genes in structures called mitochondria, which provide most of the energy used by animal cells. Lastly, the *HNF4* gene became more active as the flies matured, and appeared to help the metabolism of a developing fruit fly transition towards that of an adult.

Together these findings show that *HNF4* protects against MODY1 by influencing several components of sugar metabolism in fruit flies. In the future, more studies are needed to understand how exactly *HNF4* acts in mitochondria and to explore if similar results are seen in mammals.

DOI: 10.7554/eLife.11183.002

studies were used to investigate the functions of *Hnf4A* in key tissues where it is expressed, including the liver, kidney, intestine, and pancreatic β-cells. Two groups generated adult mice deficient for *Hnf4A* in β-cells with the goal of modeling MODY1 (**Gupta et al., 2005**; **Miura et al., 2006**). Although both studies reported impaired glucose tolerance in *Hnf4A* deficient mice, along with defects in GSIS, neither study observed sustained hypoinsulinemic hyperglycemia – the defining symptom that brings MODY1 patients to the clinic. As a result, we still have a limited understanding of the mechanisms by which *Hnf4A* maintains carbohydrate homeostasis and the molecular basis for MODY1.

Studies in *Drosophila* have revealed a high degree of conservation with major pathways that regulate cellular metabolism and systemic physiology in humans (**Diop and Bodmer, 2015**; **Owusu-Ansah and Perrimon, 2014**; **Padmanabha and Baker, 2014**; **Teleman et al., 2012**). This includes a central role for the insulin-signaling pathway in maintaining proper levels of circulating sugars through nutrient-responsive secretion of *Drosophila* insulin-like peptides (DILPs) from neuroendocrine cells in the fly brain (**Nassel et al., 2015**). Destruction of these insulin-producing cells (IPCs) results in elevated levels of circulating sugars, analogous to type 1 diabetes (**Rulifson et al., 2002**). In addition, nutrient-sensing mechanisms for insulin release are conserved in adult *Drosophila*, including roles for the Glut1 glucose transporter, mitochondrial metabolism, and ATP-sensitive potassium channels in the IPCs, which respond to the anti-diabetic sulfonylurea drug glibenclamide (**Fridell et al., 2009**; **Kreneisz et al., 2010**; **Park et al., 2014**). Consistent with these similarities, an increasing number of studies in *Drosophila* have proven relevant to mammalian insulin signaling and metabolic homeostasis, highlighting the potential to provide insight into human metabolic disorders such as diabetes (**Alfa et al., 2015**; **Owusu-Ansah and Perrimon, 2014**; **Park et al., 2014**; **Ugrankar et al., 2015**; **Xu et al., 2012**).

Here we describe our functional studies of *Drosophila* HNF4 (dHNF4) with the goal of defining its roles in maintaining carbohydrate homeostasis. dHNF4 is a close ortholog of human HNF4A, with 89% amino acid identity in the DNA-binding domain and 61% identity in the ligand-binding domain. The spatial expression patterns of the fly and mammalian receptors are also conserved through evolution, raising the possibility that they share regulatory activities (**Palanker et al., 2009**). In support of this, our previous studies of *dHNF4* mutant larvae demonstrated a critical role in fatty acid catabolism, leading to defects in lipid homeostasis that are similar to those caused by liver-specific *HNF4A* deficiency in mammals (**Palanker et al., 2009**). Here we report the first functional study of *dHNF4* mutants at the adult stage of development. Our studies show that adult *dHNF4* mutants display the hallmark symptoms of MODY1, including hyperglycemia, glucose intolerance and impaired GSIS. Metabolomic analysis of *dHNF4* mutants revealed coordinated changes in metabolites that are indicative of diabetes, along with an unexpected effect on mitochondrial activity. This was further evident in our RNA-seq and ChIP-seq studies, which indicate that *dHNF4* is required for the proper transcription of both nuclear and mitochondrial genes involved in oxidative phosphorylation (OXPHOS). A homolog of mammalian *GCK, Hex-C*, is also under-expressed in mutants. *dHNF4* appears to act through these pathways to promote GSIS in the IPCs and glucose clearance by the fat body. In addition, we show that *dHNF4* expression increases dramatically at the onset of adulthood, along with its downstream transcriptional programs. These studies suggest that *dHNF4* triggers a developmental transition that establishes the metabolic state of the adult fly, promoting GSIS and OXPHOS to support the energetic needs of the mature animal.

Results

dHNF4 mutants are sugar intolerant and display hallmarks of diabetes

All genetic studies used a transheterozygous combination of *dHNF4* null alleles ($dHNF4^{\Delta 17}$/$dHNF4^{\Delta 33}$) and genetically-matched controls that were transheterozygous for precise excisions of the EP2449 and KG08976 P-elements, as described previously (**Palanker et al., 2009**). Consistent with this earlier study, *dHNF4* null mutants die as young adults, with most mutants failing to emerge properly from the pupal case when raised under standard lab conditions (**Figure 1A**) (**Palanker et al., 2009**). While testing for potential dietary effects on *dHNF4* mutant viability, we discovered that sugar levels have a dramatic influence on their survival. When reared on either standard cornmeal food or a medium containing 15% sugar (2:1 glucose to sucrose, 8% yeast), less than 30% of mutant animals survive though eclosion, and the rest die primarily during the first day of adulthood (**Figure 1A,B**). In contrast, a five-fold reduction in dietary sugar content is sufficient to rescue most *dHNF4* mutants through eclosion and allow them to survive as adults for several weeks (**Figure 1B,C**). Sugar intolerance persists through adulthood, indicating that *dHNF4* plays a critical role in carbohydrate metabolism at this stage (**Figure 1C**). Notably, this dietary response is specific to alterations in carbohydrate levels, as calorically matched changes in dietary protein did not affect mutant viability (**Figure 1—figure supplement 1**).

To examine the effects of sugar consumption on the metabolic state of *dHNF4* mutants, major metabolites were measured in adult males raised on the low 3% sugar diet and transferred to the 3%, 9% or 15% sugar diet for three days. Although *dHNF4* mutants display elevated levels of triglycerides, similar to our observations in mutant larvae, these levels are not affected by the different sugar diets (**Figure 1—figure supplement 2A**). Similarly, while *dHNF4* mutants have reduced glycogen stores and a modest decrease in total protein, the severity of these phenotypes does not correlate with the improved viability due to decreasing dietary sugar (**Figure 1—figure supplement 2B, C**). In contrast, the abundance of free glucose is greatly elevated in *dHNF4* mutants on the 15% sugar diet, but is progressively reduced in mutants exposed to decreasing amounts of dietary sugar, similar to the response of diabetics to a low carbohydrate diet (**Figure 1D**). As expected, the accumulation of free glucose in *dHNF4* mutants represents increased levels in circulation and is accompanied by elevated levels of the glucose disaccharide trehalose (**Figure 1E,F**). Taken together, these results demonstrate that *Drosophila* HNF4 is required for proper glycemic control.

To assess whether the hyperglycemia in *dHNF4* mutants arises due to impaired glucose clearance, adult flies were subjected to an oral glucose tolerance test. Control and mutant animals were reared on the low sugar diet, fasted overnight, transferred to a glucose diet for one hour, and then

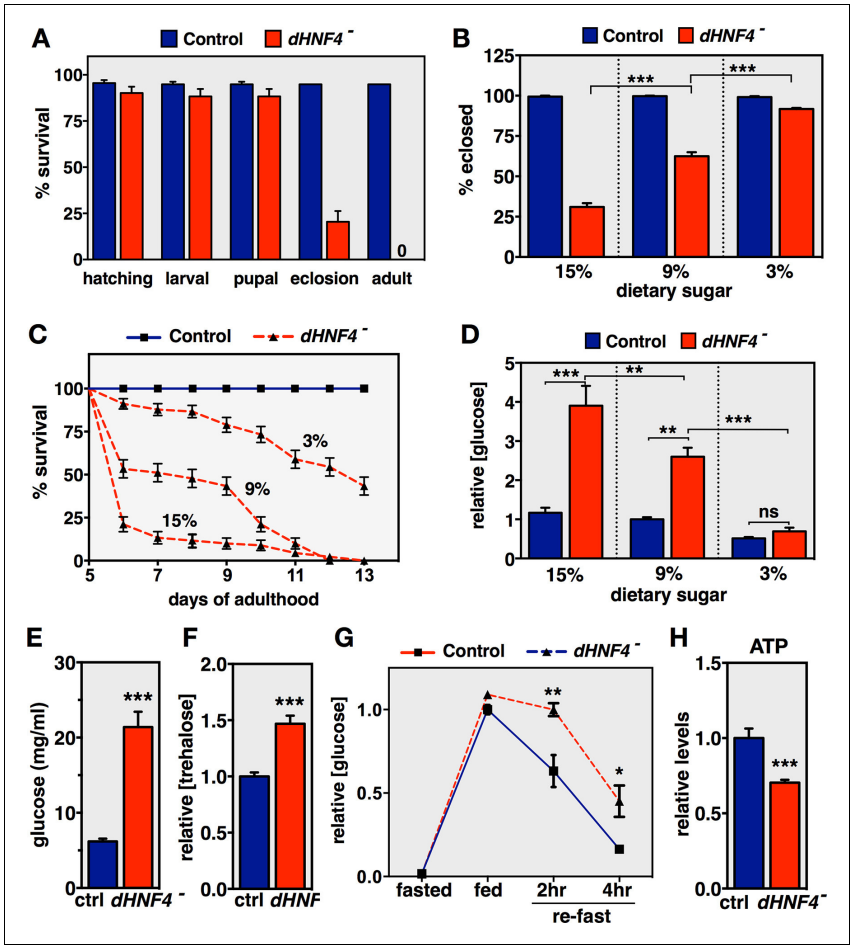

Figure 1. *dHNF4* mutants are sugar intolerant and display hallmarks of diabetes. (**A**) Percent survival of genetically-matched controls and *dHNF4* mutants at each stage of development when raised on standard media. Adult viability represents survival past the first day of adulthood. (**B**) Percent of control and *dHNF4* mutants that successfully eclose when reared on the 15%, 9%, or 3% sugar diet. (**C**) Controls and *dHNF4* mutants were reared on the 3% sugar diet until 5 days of adulthood, transferred to the indicated diet, and scored for survival. (**D**) Free glucose levels measured from whole animal lysates of controls and *dHNF4* mutants raised on the 3% sugar diet and transferred to the indicated diet for three days. (**E**) Circulating free glucose levels were measured from hemolymph extracted from control and *dHNF4* mutant adults raised on the 3% sugar diet and transferred to the 15% sugar diet for 1 day prior to analysis. (**F**) Trehalose levels measured from whole animal lysates of controls and *dHNF4* mutants raised on the 3% sugar diet and transferred to the 15% sugar diet for three days. (**G**) Oral-glucose tolerance test performed on adults raised on the 3% sugar diet, fasted overnight, fed on 15% glucose media for 1 hr, and then re-fasted for either 2 or 4 hr. Data represents relative free glucose levels from whole animal homogenates. (**H**) Relative ATP levels in control and *dHNF4* mutant adults raised on the 3% sugar diet and transferred to sugar-only medium (10% sucrose) for 1 day prior to analysis. Data is plotted as the mean ± SEM. ***p≤0.001, **p≤0.01, *p≤0.05.

DOI: 10.7554/eLife.11183.003

The following figure supplements are available for figure 1:

Figure 1 continued on next page

Figure 1 continued

Figure supplement 1. Dietary sugar, but not protein, correlates with reduced *dHNF4* mutant survival.
DOI: 10.7554/eLife.11183.004
Figure supplement 2. Profiling of major metabolites in *dHNF4* mutant adults fed different levels of dietary sugar.
DOI: 10.7554/eLife.11183.005

re-fasted for 2 or 4 hr. Although *dHNF4* mutants display a normal postprandial spike in free glucose levels after feeding, glucose clearance is significantly impaired in mutant animals at both 2 and 4 hr, indicating glucose intolerance (***Figure 1G***). Taken together, these data demonstrate that *dHNF4* mutant adults display hallmarks of diabetes and may provide an animal model of MODY1.

dHNF4 mutants display defects in glycolysis and mitochondrial metabolism

Small-molecule gas chromatography/mass spectrometry (GC/MS) metabolomic analysis was used to further characterize the metabolic state of *dHNF4* mutants fed a 3% or 15% sugar diet (***Figure 2***). This study confirmed and extended our observations of their diabetic phenotype and revealed underlying defects in glucose homeostasis that are independent of dietary sugar content. Consistent with hyperglycemia, *dHNF4* mutants accumulate glycolytic metabolites on both diets. These include elevated glucose-6-phosphate, dihydroxyacetone phosphate (DHAP), and serine, which is produced from 3-phosphoglycerate, although the increased DHAP was only observed on the 15% sugar diet (***Figure 2***). Several other glucose-derived metabolites are aberrantly increased in *dHNF4* mutants, including sorbitol and fructose, which are intermediates in the polyol pathway (***Figure 2*** and ***Figure 2—figure supplement 1***). This pathway provides an alternate route for cellular glucose uptake under conditions of sustained hyperglycemia. As a result, these metabolites can accumulate to high levels in diabetics and correlate with neuropathy and nephropathy (***Gabbay, 1975***). *dHNF4* mutants also display increased levels of inosine, adenine, xanthine, hypoxanthine, and uric acid, which are purine metabolites that are associated with increased diabetes risk and diabetic nephropathy (***Figure 2***) (***Johnson et al., 2013***). Taken together, these findings reveal additional similarities between the *dHNF4* mutant phenotype and the metabolic complications of diabetes in humans. Finally, in addition to elevated carbohydrates, we observed increased levels of pyruvate and lactate accompanied by decreased levels of ATP, suggesting a potential defect in mitochondrial respiration (***Figure 1H***, ***2***).

To further assess mitochondrial metabolism, *dHNF4* mutant adults were maintained on 10% sucrose medium for three days and analyzed for TCA cycle intermediates using GC/MS metabolomics. This approach was aimed at restricting the ability of dietary amino acids to replenish TCA cycle intermediates by anapleurosis to provide more robust detection of underlying defects in this pathway. Interestingly, *dHNF4* mutants display specific alterations in these metabolites, with increased abundance of citrate, aconitate, isocitrate, fumarate and malate, along with decreased levels of alpha-ketoglutarate and succinate, suggesting a specific block in TCA cycle progression (***Figure 3—figure supplement 1***). Taken together, these metabolite changes suggest that mitochondrial function is impaired in *dHNF4* mutants, providing a possible primary cause for their glucose intolerance.

dHNF4 regulates nuclear and mitochondrial gene expression

As a first step toward identifying transcriptional targets of dHNF4 that mediate its effects on glucose homeostasis, we performed RNA-seq profiling in control and mutant adults. A total of 1370 genes are differentially expressed in *dHNF4* mutants (≥1.5-fold change, 1% FDR), with just over half of these genes showing reduced abundance (726 down, 644 up) (***Supplementary file 1***). Gene ontology analysis revealed that the majority of the down-regulated genes correspond to metabolic functions, with the most significant category corresponding to oxidoreductases (***Supplementary file 2***). In contrast, the up-regulated genes largely correspond to the innate immune response, reflecting a possible inflammatory response in *dHNF4* mutants (***Supplementary file 2***). Interestingly, most of the transcripts encoded by the mitochondrial genome (mtDNA) are expressed at greatly reduced levels in mutant animals (***Supplementary file 1***). In *Drosophila*, as in humans, the mitochondrial genome contains 13 protein-coding genes, all of which encode critical components of the electron transport chain (ETC) that contribute to oxidative phosphorylation (OXPHOS). Further analysis of these

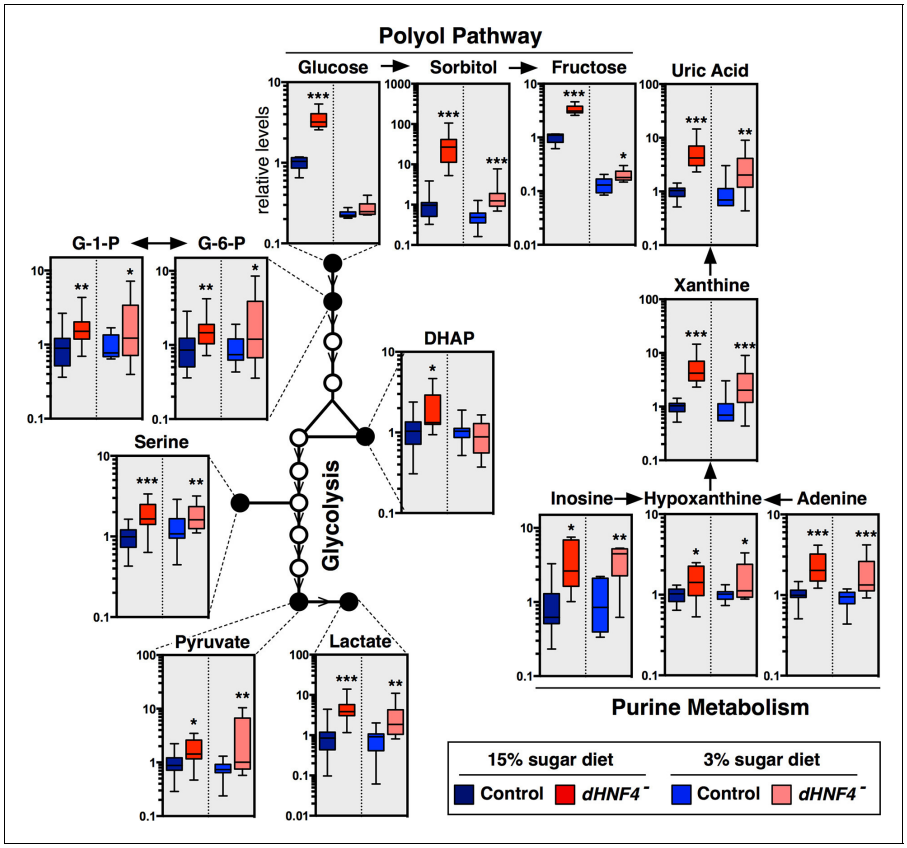

Figure 2. *dHNF4* mutants display defects in glycolysis and mitochondrial metabolism. GC/MS metabolomic profiling of controls and *dHNF4* mutants raised to adulthood on the 3% sugar diet, transferred to the indicated diet for 3 days, and subjected to analysis. Data were obtained from three independent experiments consisting of 5–6 biological replicates per condition and values were normalized to control levels on the 15% sugar diet. Box plots are presented on a log scale, with the box representing the lower and upper quartiles, the horizontal line representing the median, and the error bars representing the minimum and maximum data points. ***p≤0.001, **p≤0.01, *p≤0.05.

DOI: 10.7554/eLife.11183.006

The following figure supplement is available for figure 2:

Figure supplement 1. *dHNF4* mutants show broad defects in carbohydrate homeostasis.

DOI: 10.7554/eLife.11183.007

transcripts by northern blot hybridization confirmed their reduced expression in *dHNF4* mutants, corresponding to mtDNA genes involved in Complex I (*mt:ND1, mt:ND2, mt:ND4, mt:ND5*), Complex IV (*mt:Cox1, mt:Cox2, mt:Cox3*) and Complex V/ATP synthase (*mt:ATPase6, mt:ATPase8*), along with reduced levels of the mitochondrial large ribosomal RNA (*mt:lrRNA*) (***Figure 3A***, ***Supplementary file 1***). Importantly, not all mtDNA genes are misregulated, as the expression of *mt:Cyt-b* is consistently unaltered in mutants (***Figure 3A***). In addition, the copy number of mtDNA is

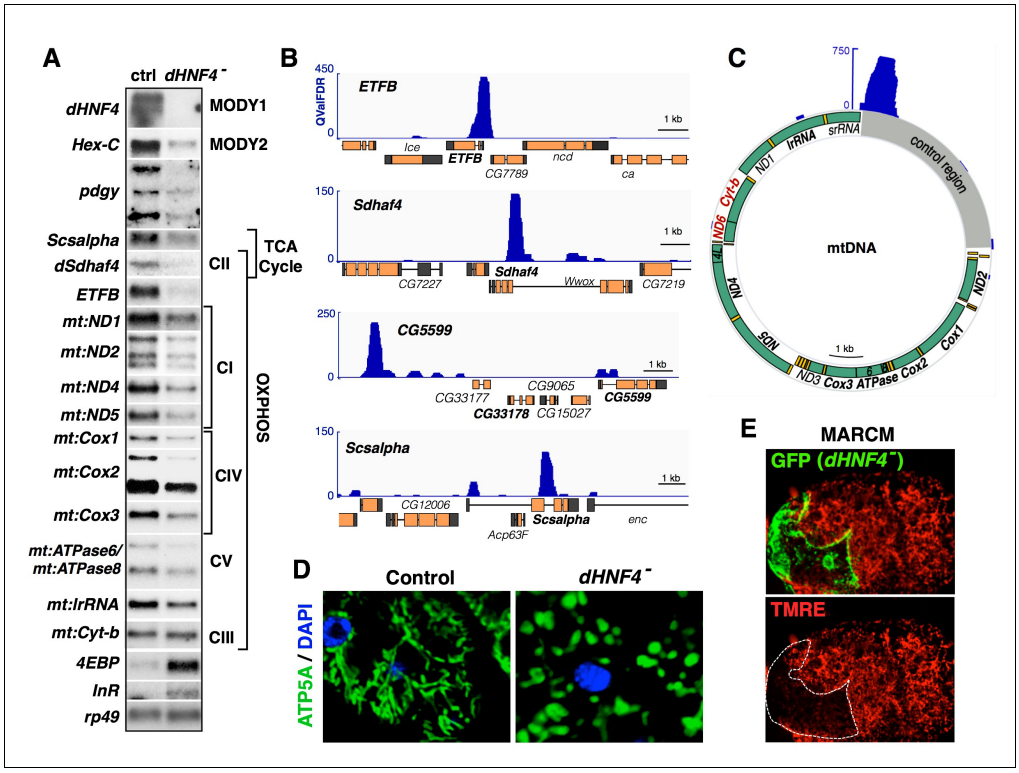

Figure 3. dHNF4 regulates nuclear and mitochondrial gene expression. (**A**) Validation of RNA-seq data by northern blot using total RNA extracted from control and *dHNF4* mutant adults. Affected transcripts include those involved in glucose homeostasis (*Hex-C*, *pdgy*), the electron transport chain (*Sdhaf4*, *mt:ND1*, *mt:ND2*, *mt:ND4*, *mt:ND5*, *mt:CoxI*, *mt:Cox2*, *mt:Cox3*, *mt:ATPase6/8*, *mt:Cyt-b* and *mt:lrRNA*), the TCA cycle (*Scsalpha*, *dSdhaf4*), and insulin signaling (*4EBP*, *InR*). *rp49* is included as a control for loading and transfer. Mitochondrial-encoded transcripts are indicated by the prefix '*mt*'. Depicted results were consistent across multiple experiments. (**B–C**) ChIP-seq analysis performed on adult flies for endogenous dHNF4 genomic binding shows direct association with both nuclear (**B**) and mitochondrial-encoded (**C**) genes involved in OXPHOS. Data tracks display *q* value FDR (QValFDR) significance values (*y*-axis) compared to input control, where QValFDR 50 corresponds to $P=10^{-5}$ and 100 corresponds to $P=10^{-10}$. Gene names in bold represent those expressed at reduced levels in *dHNF4* mutants by RNA-seq and/or northern blot analysis. Gene names in red (*ND6*, *Cyt-B*) denote the mtDNA-encoded transcriptional unit confirmed to show no change in *dHNF4* mutants. (**D**) Whole-mount immunostaining of adult fat body tissue for ATP5A (green) to detect mitochondria and DAPI (blue) to mark nuclei, showing fragmented mitochondrial morphology in *dHNF4* mutants. (E) Analysis of *dHNF4* mutant MARCM clones (GFP+) shows reduced mitochondrial membrane potential by TMRE staining of live fat body tissue from adult flies maintained on the 15% sugar diet.

DOI: 10.7554/eLife.11183.008

The following figure supplements are available for figure 3:

Figure supplement 1. *dHNF4* mutants display changes in TCA cycle intermediates that correlate with changes in gene expression.

DOI: 10.7554/eLife.11183.009

Figure supplement 2. *dHNF4* mutants display mitochondrial defects.

DOI: 10.7554/eLife.11183.010

Figure supplement 3. Predicted functions of dHNF4 target genes.

DOI: 10.7554/eLife.11183.011

unaffected in *dHNF4* mutants, suggesting that mitochondrial abundance is normal in these animals (***Figure 3—figure supplement 2A***).

Several nuclear-encoded OXPHOS genes also require *dHNF4* for their maximal expression, including genes that encode the alpha and beta subunits of the electron transfer flavoprotein (*ETFA* and *ETFB*), ETF-ubiquinone oxidoreductase (*ETF-QO*), and the Complex II (succinate dehydrogenase, SDH) assembly factor *dSdhaf4* (***Figure 3A***, ***Supplementary file 1***). Similar to flies lacking *dSdhaf4, dHNF4* mutants display reduced steady-state levels of SDH complex as assayed by western blot (***Figure 3—figure supplement 1***) (***Van Vranken et al., 2014***). These observations are thus consistent with impaired mitochondrial SDH function, and suggest that *dSdhaf4* is a critical functional target of dHNF4. Additional genes involved in the TCA cycle are misexpressed in *dHNF4* mutants, including *Succinyl-CoA synthetase alpha (Scsalpha), CG5599* (which encodes a protein with homology to the E2 subunit of the α-ketoglutarate dehydrogenase complex (α-KGDHC) as well as the E2 subunit of the branched-chain alpha-ketoacid dehydrogenase complex), *CG1544* (which encodes a homolog of α-KGDHC E1), as well as *Isocitrate dehydrogenase* (*IDH*, $NADP^+$-dependent) (***Figure 3A***, ***Supplementary file 1***). These changes in gene expression are consistent with the observed changes in the levels of TCA cycle intermediates in *dHNF4* mutants, suggesting that they are functionally relevant to the mutant metabolic phenotype (***Figure 3—figure supplement 1***).

Notably, *dHNF4* mutants also have decreased expression of the *GCK* homolog *Hexokinase-C (Hex-C)* (***Figure 3A***). GCK is a tissue-specific glycolytic enzyme that is required for glucose sensing by pancreatic β-cells and glucose clearance by the liver. These activities, combined with the association of *GCK* mutations with MODY2, make *Hex-C* a candidate for mediating the effects of *dHNF4* on carbohydrate metabolism. The glucose transporter *CG1213* is also down-regulated in *dHNF4* mutants, along with *phosphoglucomutase (pgm)*, which is involved in glycogen metabolism, and *transaldolase* and *CG17333*, which are involved in the pentose phosphate shunt. Additionally, the gluconeogenesis genes *Pyruvate carboxylase (CG1514)* and *Phosphoenolpyruvate carboxykinase (Pepck, CG17725)* show reduced expression in mutant animals, similar to their dependence on *Hnf4A* for expression in the mammalian liver (***Supplementary file 1***) (***Chavalit et al., 2013***; ***Yoon et al., 2001***). Finally, *dHNF4* mutants display transcriptional signatures of reduced insulin signaling, including up-regulation of the dFOXO-target genes *4EBP* and *InR* (***Figure 3A***, ***Supplementary file 1***). Taken together, these findings indicate an important role for dHNF4 in mitochondrial OXPHOS and glucose metabolism, and suggest that it acts through multiple pathways to maintain glycemic control.

Chromatin immunoprecipitation followed by high-throughput sequencing (ChIP-seq) was performed to identify direct transcriptional targets of the receptor. Through this analysis, forty-seven genes were identified as high confidence targets by fitting the criteria of showing proximal dHNF4 binding along with reduced transcript abundance in mutant animals (≥1.5 fold change, 1% FDR) (***Figure 3—figure supplement 3***, ***Supplementary file 3***). These include nuclear-encoded OXPHOS genes such as *ETFB, ETF-QO, dSdhaf4,* and genes that encode TCA cycle factors *Scsalpha* and *CG5599* (***Figure 3B***). We also observed abundant and specific binding of dHNF4 within the control region of the mitochondrial genome (***Figure 3C*** and ***Supplementary file 3***). Taken together with our other results, these data suggest that dHNF4 is required to maintain normal mitochondrial function. Consistent with this, mitochondrial morphology is severely fragmented in mutant animals, and MARCM clonal analysis in the adult fat body shows reduced mitochondrial membrane potential in *dHNF4* mutant cells (***Figure 3D,E*** and ***Figure 3—figure supplement 2B,C***). In contrast, we were unable to detect changes in reactive oxygen species (ROS) in *dHNF4* mutant clones by DHE staining (***Figure 3—figure supplement 2D***). This might be due to the decreased levels of ROS-generating ETC complexes in *dHNF4* mutants, along with no detectable effect on the transcripts that encode ROS-scavenging enzymes, such as catalase and SOD (***Supplementary file 1***). Taken together, these data support the model that dHNF4 regulates both nuclear and mitochondrial gene expression to promote OXPHOS and maintain mitochondrial integrity.

dHNF4 acts through multiple tissues and pathways to control glucose homeostasis

Tissue-specific RNAi was used to disrupt *dHNF4* expression in the IPCs, fat body, and intestine to examine the contributions of *dHNF4* in these tissues to systemic glucose homeostasis. This revealed a requirement in both the IPCs and fat body for glucose homeostasis, consistent with the well-

established roles of these tissues in insulin signaling and the regulation of circulating sugar levels (***Figure 4A***, ***Figure 4—figure supplement 1B***). Our initial functional analysis of *dHNF4* target genes supports these tissue-specific activities and provides insights into the molecular mechanisms of *dHNF4* action. Tissue-specific inactivation of *Hex-C* by RNAi demonstrates that it is required in the fat body, but not the IPCs, to maintain normal levels of circulating glucose (***Figure 4B,C***). This is consistent with the important role of mammalian *GCK* for glucose clearance by the liver as well as its association with MODY2 (***Postic et al., 1999***). In contrast, both fat body and IPC-specific RNAi for the direct target of dHNF4, *CG5599*, significantly impaired glucose homeostasis (***Figure 4B,C***). This indicates that *CG5599* is required in each of these tissues for glycemic control, similar to dHNF4, suggesting that it is a key downstream target of the receptor. Although technical limitations prevent us from performing tissue-specific RNAi studies of mitochondrial-encoded transcripts, disruption of ETC Complex I by targeting a critical assembly factor, CIA30 (Complex I intermediate-associated protein 30 kDa) (***Cho et al., 2012***) in either the IPCs or fat body produced elevated levels of free

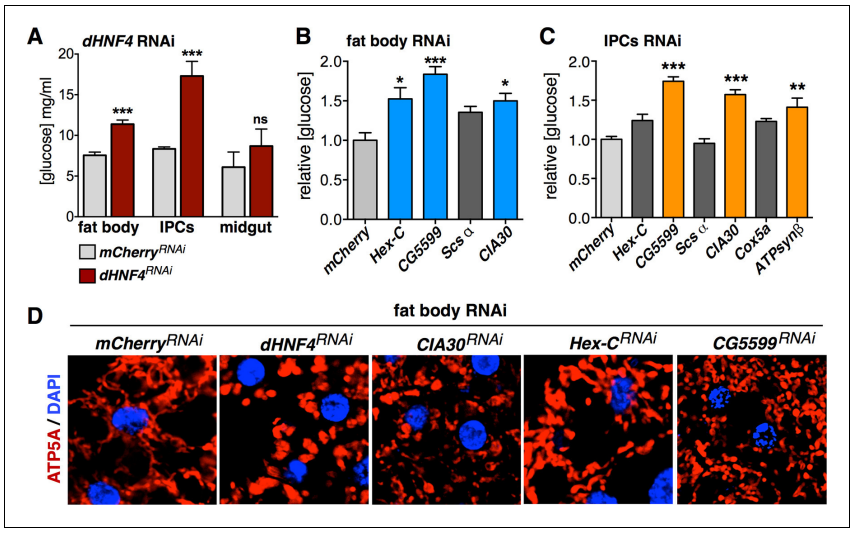

Figure 4. dHNF4 acts through multiple tissues and pathways to control glucose homeostasis. (**A**) Circulating glucose levels in adult males expressing tissue-specific RNAi against *mCherry* (TRiP 35785, grey bars) or *dHNF4* (TRiP 29375, dark red bars) in the fat body (*r4-GAL4*), IPCs (*dilp2-GAL4*), or midgut (*mex-GAL4*). (**B–C**) Relative free glucose levels in adult males on the 15% sugar diet expressing fat body (*r4-GAL4*, B) or IPC (*dilp2-GAL4*, C)-specific RNAi compared to *mCherry* RNAi controls (light grey bars). RNAi lines directed against *Hex-C*, *CG5599*, *Scsα*, *CIA30*, *Cox5a*, and *ATPsynβ* were obtained from the TRiP RNAi collection. Blue and orange bars depict significant changes in glucose levels. Dark grey bars are not significant. Data represents the mean ± SEM. ***p≤0.001, **p≤0.01, *p≤0.05. (**D**) Confocal imaging of mitochondrial morphology (marked by ATP5A immunostaining, red) in the adult fat body from animals expressing fat-body specific RNAi (*r4-GAL4*). The extended network of mitochondria seen in controls is disrupted and appears more punctate upon RNAi for *dHNF4*, *CIA30*, or *CG5599*, indicative of mitochondrial fragmentation. No effect is seen upon RNAi for *Hex-C*.

DOI: 10.7554/eLife.11183.012

The following figure supplements are available for figure 4:

Figure supplement 1. *dHNF4* is required in the insulin-producing cells and fat body to maintain glucose homeostasis.

DOI: 10.7554/eLife.11183.013

Figure supplement 2. Fat body-specific disruption of the electron transport chain causes sugar intolerance.

DOI: 10.7554/eLife.11183.014

Figure supplement 3. Additional RNAi lines confirming the importance of *Hex-C* in the fat body for glycemic control.

DOI: 10.7554/eLife.11183.015

glucose (**Figure 4B,C**). Fat body-specific RNAi for *dHNF4, CIA30, or CG5599* resulted in fragmented mitochondrial morphology, consistent with previous reports of CIA30 loss of function and the onset of mitochondrial dysfunction (**Figure 4D**) (**Cho et al., 2012**). In contrast, RNAi for *Hex-C* had no detectable effect on mitochondrial morphology (**Figure 4D**).

While RNAi for Complex V (*ATPsynβ* RNAi) in the fat body caused lethality prior to eclosion, IPC-specific RNAi produced viable adults that appeared normal but displayed significant hyperglycemia (**Figure 4C**). In contrast, disruption of ETC Complex IV in the IPCs (*Cox5a* RNAi) failed to produce hyperglycemia, while RNAi in the fat body caused lethality prior to adulthood, similar to *ATPsynβ*. This premature lethality was accompanied by severe developmental delay and more than 50% of the animals dying prior to puparium formation when raised on the 15% sugar diet. Interestingly, we discovered that these animals are sugar intolerant, similar to *dHNF4* mutants, such that rearing them on the 3% sugar diet allowed for 100% survival to puparium formation while also alleviating the developmental delay (**Figure 4—figure supplement 2**). Although adult viability was not achievable through dietary intervention, these findings demonstrate that ETC function in the fat body is important for sugar tolerance during development, similar to the requirement for dHNF4. Taken together, these data reveal important roles for *dHNF4* in both the IPCs and fat body to maintain glucose homeostasis, likely in part by promoting *Hex-C* expression in the fat body for glucose clearance and supporting mitochondrial function and OXPHOS in both the IPCs and fat body.

dHNF4 is required for glucose-stimulated DILP2 secretion

The requirement for *dHNF4* function in the IPCs for systemic glucose homeostasis fits with the important roles for *Hnf4A* in mouse pancreatic β-cells as well as the contribution of β-cell physiology to the onset of MODY1. Accordingly, we examined if *dHNF4* mutants display defects in GSIS. We used an experimental approach developed for this purpose in *Drosophila* larvae, assaying for the steady-state levels of DILP2 peptide in the IPCs using a fasting/refeeding paradigm (**Geminard et al., 2009**). As expected, DILP2 accumulates in the IPCs of fasted control animals and is effectively released into circulation in response to glucose feeding (**Figure 5A,B**). In contrast, while DILP2 accumulates normally in fasted *dHNF4* mutants, it fails to respond to dietary glucose stimulation, despite these animals having normal IPC number and morphology (**Figure 5A,B**). Peripheral insulin signaling is also reduced in *dHNF4* mutants relative to controls, consistent with their reduced GSIS (**Figure 5C**). This defect in GSIS is due to a tissue-specific requirement for *dHNF4* in the IPCs since IPC-specific RNAi for *dHNF4* resulted in impaired DILP2 secretion into the hemolymph, along with reduced peripheral insulin signaling (**Figure 5D,E** and **Figure 5—figure supplement 1**) (**Park et al., 2014**). Taken together, these data demonstrate that impaired GSIS plays a central role in the diabetic phenotype of *dHNF4* mutants.

dHNF4 is required to establish the metabolic state of adult *Drosophila*

As we reported in our prior study of *dHNF4*, the receptor is not expressed in the larval IPCs (**Figure 6A**) (**Palanker et al., 2009**). It is, however, expressed in the IPCs of the adult fly, consistent with its central roles at this stage in GSIS, insulin signaling, and glucose homeostasis (**Figure 6B**). Interestingly, this cell-type specific switch in *dHNF4* expression correlates with a developmental change in IPC physiology. Unlike mammalian β-cells, larval IPCs fail to secrete DILPs in response to dietary glucose (**Geminard et al., 2009**). Adult IPCs, however, display calcium influx, membrane depolarization, and DILP2 secretion in response to glucose, analogous to β-cells (**Alfa et al., 2015**; **Fridell et al., 2009**; **Kreneisz et al., 2010**; **Park et al., 2014**). Along with the temporal induction of dHNF4 expression in adult IPCs, these results suggest that there is a developmental switch in the response to glucose at the onset of adulthood. Consistent with this, glucose feeding activates insulin signaling in adult flies, but not in larvae (**Figure 6C**). This correlates with a ~ten-fold increase in the basal circulating levels of glucose in adults compared to larvae, which first becomes apparent during the final stages of pupal development (**Figure 6D**) (**Tennessen et al., 2014a**). Moreover, *dHNF4* mutants maintain euglycemia on a normal diet during larval and early pupal stages, but display hyperglycemia just prior to eclosion (**Figure 6D**). Taken together, these observations point to a switch in IPC physiology and glucose homeostasis as *Drosophila* transition into maturity.

The induction of *dHNF4* in the adult IPCs and the adult onset of hyperglycemia in *dHNF4* mutants raise the interesting possibility that this receptor may play a role in coordinating the metabolic

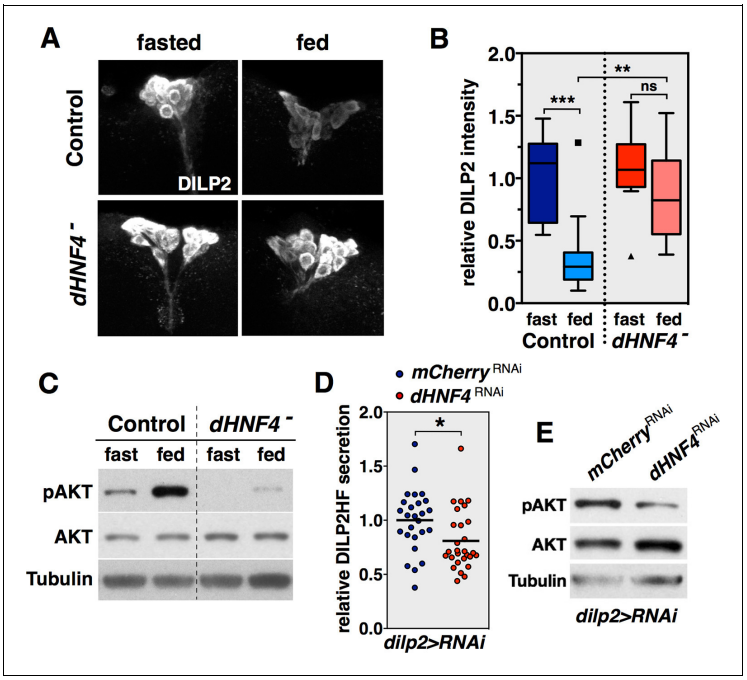

Figure 5. *dHNF4* is required for glucose-stimulated DILP2 secretion by the insulin-producing cells. (**A**) Whole-mount staining for DILP2 peptide in brains dissected from adult control and *dHNF4* mutants that were either fasted overnight or re-fed glucose for two hours. (**B**) Quantification of relative DILP2 fluorescent intensity in the IPCs of fasted and glucose-fed controls and *dHNF4* mutants. Data is plotted as a Tukey boxplot with outliers denoted as individual data points (n= 11 ± 3 brains per-condition). Results were consistent between three independent experiments. (**C**) Western blot analysis to detect phosphorylated AKT (pAKT), total AKT, and Tubulin in extracts from controls and *dHNF4* mutants that were either fasted overnight or re-fed glucose for two hours. (**D**) Levels of circulating HA-FLAG-tagged DILP2 (DILP2HF) were assayed in animals with IPC-specific RNAi (TRiP) against either *mCherry* as a control (blue) or *dHNF4* (red) using the *dilp2-GAL4* driver (*dilp2>RNAi*). Data is combined from five independent experiments, each containing 5–6 biological replicates per genotype. The horizontal lines depict the mean value. (**E**) Western blot analysis to detect phosphorylated AKT (pAKT), total AKT, and Tubulin in extracts from *ad libitum* fed adult males with IPC-specific RNAi against either *mCherry* as a control or *dHNF4* using the *dilp2-GAL4* driver (*dilp2>RNAi*). ***p≤0.001, **p≤0.01, *p≤0.05.

DOI: 10.7554/eLife.11183.016

The following figure supplement is available for figure 5:

Figure supplement 1. *dHNF4* RNAi in the IPCs causes reduced levels of circulating DILP2-HF.

DOI: 10.7554/eLife.11183.017

switch toward GSIS and OXPHOS at this stage. Indeed, northern blot analysis of RNA samples isolated from staged wild-type larvae, pupae, and young adults, demonstrate that *dHNF4* expression increases dramatically at the onset of adulthood (***Figure 6E***). Moreover, this temporal pattern of expression is accompanied by increased expression of both nuclear and mitochondrial-encoded *dHNF4* target genes that contribute to OXPHOS as well as *Hex-C*. The expression of these target genes is also reduced in staged *dHNF4* mutants, consistent with our earlier findings that their maximal expression depends on receptor function (***Figure 6E***). Taken together, our results support the

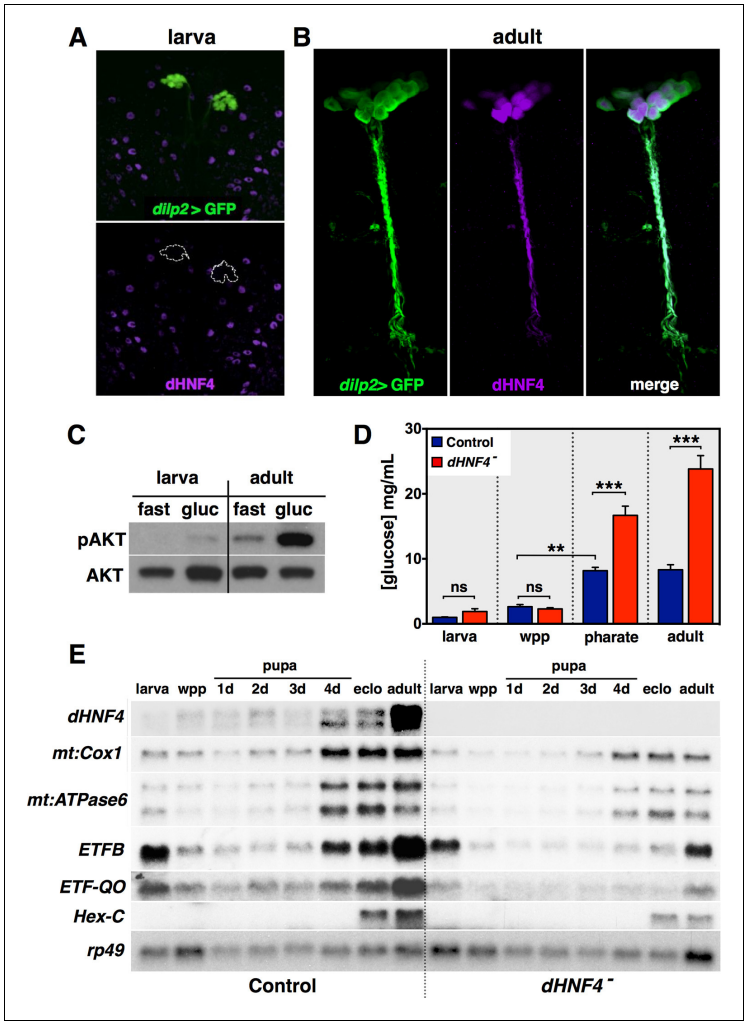

Figure 6. *dHNF4* supports a developmental transition toward GSIS and OXPHOS in adult *Drosophila*. (**A–B**) Whole-mount immunostaining of larval (**A**) or adult (**B**) brains to detect dHNF4 protein (magenta) or GFP, which marks the IPCs (*dilp2>GFP*, green). (**C**) Western blot analysis to detect phosphorylated AKT (pAKT) and total AKT in extracts from w^{1118} third-instar larvae or mature adults that were fasted overnight and re-fed 10% glucose for two hours. (**D**) Relative levels of free glucose in controls and *dHNF4* mutants staged as either feeding third-instar larvae (larva), white prepupae (wpp), pharate adults (~4 day-old pupae), or mature adults. Data is plotted as the mean ± SEM. ***p≤0.001, **p≤0.01, *p≤0.05. (**E**) Northern blot analysis of RNA extracted from feeding third-instar larvae (larva), white prepupae (wpp), pupae at one-day intervals, mid-eclosion (eclo), and mature adults. *rp49* is included as a control for loading and transfer.

DOI: 10.7554/eLife.11183.018

model that dHNF4 contributes to a metabolic switch in glucose homeostasis at the onset of adulthood that promotes GSIS and OXPHOS to meet the energy demands of the adult fly.

Discussion

The association of MODY subtypes with mutations in specific genes provides a framework for understanding the monogenic heritability of this disorder as well as the roles of the corresponding pathways in systemic glucose homeostasis. In this paper, we investigate the long-known association between *HNF4A* mutations and MODY1 by characterizing a whole-animal mutant that recapitulates the key symptoms associated with this disorder. We show that *Drosophila* HNF4 is required for both GSIS and glucose clearance in adults, acting in distinct tissues and multiple pathways to maintain glucose homeostasis. We also provide evidence that dHNF4 promotes mitochondrial OXPHOS by regulating nuclear and mitochondrial gene expression. Finally, we show that the expression of *dHNF4* and its target genes is dramatically induced at the onset of adulthood, contributing to a developmental switch toward GSIS and oxidative metabolism at this stage in development. These results provide insights into the molecular basis of MODY1, expand our understanding of the close coupling between development and metabolism, and establish the adult stage of *Drosophila* as an accurate context for genetic studies of GSIS, glucose clearance, and diabetes.

dHNF4 acts through multiple pathways to regulate glucose homeostasis

Drosophila HNF4 mutants display late-onset hyperglycemia accompanied by sensitivity to dietary carbohydrates, glucose intolerance, and defects in GSIS – hallmarks of MODY1. These defects arise from roles for *dHNF4* in multiple tissues, including a requirement in the IPCs for GSIS and a role in the fat body for glucose clearance. The regulation of GSIS by *dHNF4* is consistent with the long-known central contribution of pancreatic β-cells to the pathophysiology of MODY1 (***Fajans and Bell, 2011***). Similarly, several MODY-associated genes, including *GCK*, *HNF1A* and *HNF1B*, are important for maintaining normal hepatic function. These distinct tissue-specific contributions to glycemic control may explain why single-tissue *Hnf4A* mutants in mice do not fully recapitulate MODY1 phenotypes and predict that a combined deficiency for the receptor in both the liver and pancreatic β-cells of adults would produce a more accurate model of this disorder.

We used metabolomics, RNA-seq, and ChIP-seq to provide initial insights into the molecular mechanisms by which dHNF4 exerts its effects on systemic metabolism. These studies revealed several downstream pathways, each of which is associated with maintaining homeostasis and, when disrupted, can contribute to diabetes. These include genes identified in our previous study of *dHNF4* in larvae that act in lipid metabolism and fatty acid β-oxidation, analogous to the role of *Hnf4A* in the mouse liver to maintain normal levels of stored and circulating lipids (***Hayhurst et al., 2001***; ***Palanker et al., 2009***). Extensive studies have linked defects in lipid metabolism with impaired β-cell function and peripheral glucose uptake and clearance, suggesting that these pathways contribute to the diabetic phenotypes of *dHNF4* mutants (***Prentki et al., 2013***; ***Qatanani and Lazar, 2007***). An example of this is *pudgy*, which is expressed at reduced levels in *dHNF4* mutants and encodes an acyl-CoA synthetase that is required for fatty acid oxidation (***Figure 3A***) (***Xu et al., 2012***). Interestingly, *pudgy* mutants have elevated triglycerides, reduced glycogen, and increased circulating sugars, similar to *dHNF4* mutants, suggesting that this gene is a critical downstream target of the receptor. It is important to note, however, that our metabolomic, RNA-seq, and ChIP-seq studies were conducted on extracts from whole animals rather than individual tissues. As a result, some of our findings may reflect compensatory responses between tissues, and some tissue-specific changes in gene expression or metabolite levels may not be detected by our approach. Further studies using samples from dissected tissues would likely provide a more complete understanding of the mechanisms by which *dHNF4* maintains systemic physiology.

Notably, the *Drosophila* GCK homolog encoded by *Hex-C* is expressed at reduced levels in *dHNF4* mutants (***Figure 3A***). The central role of GCK in glucose sensing by pancreatic β-cells as well as glucose clearance by the liver places it as an important regulator of systemic glycemic control. Our functional data supports these associations by showing that *Hex-C* is required in the fat body for proper circulating glucose levels, analogous to the role of GCK in mammalian liver (***Figure 4B***) (***Postic et al., 1999***). Unlike mice lacking *GCK* in the β-cells, however, we do not see an effect on

glucose homeostasis when *Hex-C* is targeted by RNAi in the IPCs. This is possibly due to the presence of a second *GCK* homolog in *Drosophila*, Hex-A, which could act alone or redundantly with Hex-C to mediate glucose sensing by the IPCs. In mammals, *GCK* expression is differentially regulated between hepatocytes and β-cells through the use of two distinct promoters, and studies in rats have demonstrated a direct role for HNF4A in promoting *GCK* expression in the liver (**Roth et al., 2002**). Our findings suggest that this relationship has been conserved through evolution. In addition, the association between *GCK* mutations and MODY2 raise the interesting possibility that defects in liver GCK activity may contribute to the pathophysiology of both MODY1 and MODY2.

Interestingly, gene ontology analysis indicates that the up-regulated genes in *dHNF4* mutants correspond to the innate immune response pathways in *Drosophila* (**Supplementary file 2**). This response parallels that seen in mice lacking *Hnf4A* function in enterocytes, which display intestinal inflammation accompanied by increased sensitivity to DSS-induced colitis and increased permeability of the intestinal epithelium, similar to humans with inflammatory bowel disease (**Ahn et al., 2008**; **Babeu and Boudreau, 2014**; **Cattin et al., 2009**). Disruption of *Hnf4A* expression in Caco-2 cells using shRNA resulted in changes in the expression of genes that act in oxidative stress responses, detoxification pathways, and inflammatory responses, similar to the effect we see in *dHNF4* mutants (**Marcil et al., 2010**). Moreover, mutations in human *HNF4A* are associated with chronic intestinal inflammation, irritable bowel disease, ulcerative colitis, and Crohn's disease, suggesting that these functions are conserved through evolution (**UK IBD Genetics Consortium et al., 2009**; **Marcil et al., 2012**; **van Sommeren et al., 2011**). Taken together, these results support the hypothesis that *dHNF4* plays an important role in suppressing an inflammatory response in the intestine. Future studies are required to test this hypothesis in *Drosophila*. In addition, further work is required to better define the regulatory functions of HNF4 that are shared between *Drosophila* and mammals. Although our work described here suggests that key activities for this receptor have been conserved in flies and mammals, corresponding to the roles of HNF4 in the IPCs (β-cells) for GSIS, fat body (liver) for lipid metabolism and glucose clearance, and intestine to suppress inflammation, there are likely to be divergent roles as well. One example of this is the embryonic lethality of *Hnf4A* mutant mice, which is clearly distinct from the early adult lethality reported here for *dHNF4* mutants. Further studies are required to dissect the degree to which the regulatory functions of this receptor have been conserved through evolution.

It is also important to note that mammalian *Hnf4A* plays a role in hepatocyte differentiation and proliferation in addition to its roles in metabolism (**Bonzo et al., 2012**; **Li et al., 2000**). This raises the possibility that early developmental roles for *dHNF4* could impact the phenotypes we report here in adults. Indeed, all of our studies involve zygotic *dHNF4* null mutants that lack function throughout development. In an effort to address this possibility and distinguish developmental from adult-specific functions, we are constructing a conditional *dHNF4* mutant allele using CRISPR/Cas9 technology. Future studies using this mutation should allow us to conduct a detailed phenotypic analysis of this receptor at different stages of *Drosophila* development.

It is also interesting to speculate that our functional studies of *dHNF4* uncover more widespread roles for MODY-associated genes in glycemic control, in addition to the link with MODY2 described above. *HNF1A* and *HNF1B*, which are associated with MODY3 and MODY5, respectively, act together with *HNF4A* in an autoregulatory circuit in an overlapping set of tissues, with HNF4A proposed to be the most upstream regulator of this circuit (**Boj et al., 2001**; **Nagaki and Moriwaki, 2008**). The observation that *Drosophila* do not have identifiable homologs for *HNF1A* and *HNF1B* raises the interesting possibility that *dHNF4* alone replaces this autoregulatory circuit in more primitive organisms. The related phenotype of these disorders is further emphasized by cases of MODY3 that are caused by mutation of an HNF4A binding site within the *HNF1A* promoter (**Gragnoli et al., 1997**). Consistent with this link, MODY1, MODY3 and MODY5 display similar features of disease complication and progression, and studies of HNF1A and HNF4A in INS-1 cells have implicated roles for these transcription factors in promoting mitochondrial metabolism in β-cells (**Wang et al., 2002**). In line with this, mitochondrial diabetes is clearly age progressive, as are MODY1, 3, and 5, but not MODY2, which represents a more mild form of this disorder. Furthermore, the severity and progression of MODY3 is significantly enhanced when patients carry an additional mutation in either HNF4A or mtDNA (**Forlani et al., 2010**). Overall, these observations are consistent with the well-established multifactorial nature of diabetes, with multiple distinct metabolic insults contributing to disease onset.

dHNF4 regulates nuclear and mitochondrial gene expression

Our RNA-seq analysis supports a role for *dHNF4* in coordinating mitochondrial and nuclear gene expression (***Supplementary file 1*** and ***Figure 3A***). This is represented by the reduced expression of transcripts encoded by the mitochondrial genome, along with effects on nuclear-encoded genes that act in mitochondria. In addition, ChIP-seq revealed that several of the nuclear-encoded genes are direct targets of the receptor. Mitochondrial defects have well-established links to diabetes-onset, with mutations in mtDNA causing maternally-inherited diabetes and mitochondrial OXPHOS playing a central role in both GSIS and peripheral glucose clearance (***Sivitz and Yorek, 2010***). Consistent with this, our functional studies indicate that dHNF4 is required to maintain normal mitochondrial function and that defects in this process contribute to the diabetic phenotypes in *dHNF4* mutants.

It is important to note that the number of direct targets for dHNF4 in the nucleus is difficult to predict with our current dataset. A relatively low signal-to-noise ratio in our ChIP-seq experiment allowed us to identify only 37 nuclear-encoded genes as high confidence targets by fitting the criteria of proximal dHNF4 binding along with reduced expression in *dHNF4* mutants (***Figure 3B*** and ***Supplementary file 3***). Future ChIP-seq studies will allow us to expand this dataset to gain a more comprehensive understanding of the scope of the dHNF4 regulatory circuit and may also reveal tissue-restricted targets that are more difficult to detect. Nonetheless, almost all of the genes identified as direct targets for dHNF4 regulation correspond to genes involved in mitochondrial metabolism, including the TCA cycle, OXPHOS, and lipid catabolism, demonstrating that this receptor has a direct impact on these critical downstream pathways that influence glucose homeostasis (***Figure 3—figure supplement 3***, ***Supplementary file 3***).

dHNF4 is required for mitochondrial function

An unexpected and significant discovery in our studies is that dHNF4 is required for mitochondrial gene expression and function. Several lines of evidence support the model that dHNF4 exerts this effect through direct regulation of mitochondrial transcription, although a number of additional experiments are required to draw firm conclusions on this regulatory connection. First, most of the 13 protein-coding genes in mtDNA are underexpressed in *dHNF4* mutants (***Figure 3A***, ***Supplementary file 1***). Our lab and others have conducted RNA-seq studies of *Drosophila* nuclear transcription factor mutants and, to our knowledge, similar effects on mitochondrial gene expression have not been reported previously. Second, dHNF4 protein is abundantly bound to the control region of the mitochondrial genome, representing the fifth strongest enrichment peak in our ChIP-seq dataset (***Figure 3C***). Although the promoters in *Drosophila* mtDNA have not yet been identified, the site bound by dHNF4 corresponds to a predicted promoter region for *Drosophila* mitochondrial transcription and coincides with the location of the major divergent promoters in human mtDNA (***Garesse and Kaguni, 2005***; ***Roberti et al., 2006***). It is unlikely that the abundance of mtDNA relative to nuclear DNA had an effect on our ChIP-seq peak calling because the MACS2 platform used for our analysis accounts for local differences in read depth across the genome (including the abundance of mtDNA). In addition, although the D-loop in mtDNA has been proposed to contribute to possible false-positive ChIP-seq peaks in mammalian studies (***Marinov et al., 2014***), the D-loop structure is not present in *Drosophila* mtDNA (***Rubenstein et al., 1977***). Nonetheless, additional experiments are required before we can conclude that this apparent binding is of regulatory significance for mitochondrial function. Third, the effects on mitochondrial gene expression do not appear to be due to reduced mitochondrial number in *dHNF4* mutants (***Figure 3—figure supplement 2A***). This is consistent with the normal expression of *mt:Cyt-b* in *dHNF4* mutants (***Figure 3A***), which has a predicted upstream promoter that drives expression of the *mt:Cyt-b* and mt:*ND6* operon (although we could not detect *mt:ND6* RNA in our northern blot studies) (***Berthier et al., 1986***; ***Roberti et al., 2006***). Fourth, immunostaining for dHNF4 shows cytoplasmic protein that overlaps with the mitochondrial marker ATP5A, in addition to its expected nuclear localization (***Figure 3—figure supplement 2B***). Some of the cytoplasmic staining, however, clearly fails to overlap with the mitochondrial marker, making it difficult to draw firm conclusions from this experiment. Multiple efforts to expand on this question biochemically with subcellular fractionation studies have been complicated by abundant background proteins that co-migrate with the receptor in mitochondrial extracts. We are currently developing new reagents to detect the relatively low levels of endogenous dHNF4 protein in

mitochondria, including use of the CRISPR/Cas9 system for the addition of specific epitope tags to the endogenous *dHNF4* locus. Finally, we observe multiple hallmarks of mitochondrial dysfunction, including elevated pyruvate and lactate, specific alterations in TCA cycle metabolites, reduced mitochondrial membrane potential, reduced levels of ATP, and fragmented mitochondrial morphology. These phenotypes are consistent with the reduced expression of key genes involved in mitochondrial OXPHOS (***Figure 3A*** and ***Supplementary file 1***), and studies showing that decreased mitochondrial membrane potential and ATP production are commonly associated with mitochondrial fragmentation (***Mishra and Chan, 2014***; ***Toyama et al., 2016***).

Although unexpected, our proposal that dHNF4 may directly regulate mitochondrial gene expression is not unprecedented. A number of nuclear transcription factors have been localized to mitochondria, including ATFS-1, MEF2D, CREB, p53, STAT3, along with several nuclear receptors, including the estrogen receptor, glucocorticoid receptor, and the p43 isoform of the thyroid hormone receptor (***Leigh-Brown et al., 2010***; ***Nargund et al., 2015***; ***Szczepanek et al., 2012***). The significance of these observations, however, remains largely unclear, with few studies demonstrating regulatory functions within mitochondria. In addition, these factors lack a canonical mitochondrial localization signal at their amino-terminus, leaving it unclear how they achieve their subcellular distribution (***Marinov et al., 2014***). In contrast, one of the five mRNA isoforms encoded by *dHNF4, dHNF4-B*, encodes a predicted mitochondrial localization signal in its 5'-specific exon, providing a molecular mechanism to explain the targeting of this nuclear receptor to this organelle. Efforts are currently underway to conduct a detailed functional analysis of *dHNF4-B* by using the CRISPR/Cas9 system to delete its unique 5' exon, as well as establishing transgenic lines that express a tagged version of *dHNF4-B* under UAS control. Future studies using these reagents, along with our *dHNF4* mutants, should allow us to dissect the nuclear and mitochondrial functions of this nuclear receptor and their respective contributions to systemic physiology.

Finally, it is interesting to speculate whether the role for dHNF4 in mitochondria is conserved in mammals. A few papers have described the regulation of nuclear-encoded mitochondrial genes by HNF4A (***Rodriguez et al., 1998***; ***Wang et al., 2000***). In addition, several studies have detected cytoplasmic *Hnf4A* by immunohistochemistry in tissue sections, including in postnatal pancreatic islets (***Miura et al., 2006***; ***Nammo et al., 2008***) and hepatocytes (***Bell and Michalopoulos, 2006***; ***Soutoglou et al., 2000***; ***Sun et al., 2007***; ***Yanger et al., 2013***). Moreover, the regulation of nuclear/cytoplasmic shuttling of HNF4A has been studied in cultured cells (***Soutoglou et al., 2000***). The evolutionary conservation of the physiological functions of HNF4A, from flies to mammals, combined with these prior studies, argue that more effort should be directed at defining the subcellular distribution of HNF4A protein and its potential roles within mitochondria. Taken together with our studies in *Drosophila*, this work could provide new directions for understanding HNF4 function and MODY1.

dHNF4 contributes to an adult switch in metabolic state

Physiological studies by George Newport in 1836 noted that holometabolous insects reduce their respiration during metamorphosis leading to a characteristic "U-shaped curve" in oxygen consumption (***Needham, 1929***; ***Newport, 1836***). Subsequent classical experiments in *Lepidoptera, Bombyx, Rhodnius* and *Calliphora* showed that this reduction in mitochondrial respiration during metamorphosis and dramatic rise in early adults is seen in multiple insect species, including *Drosophila* (***Bodine, 1925***; ***Merkey et al., 2011***). Consistent with this, the activity of oxidative enzyme systems and the levels of ATP also follow a "U-shaped curve" during development as the animal transitions from a non-feeding pupa to a motile and reproductively active adult fly (***Agrell, 1953***). Although first described over 150 years ago, the regulation of this developmental increase in mitochondrial activity has remained undefined. Here we show that this temporal switch is dependent, at least in part, on the dHNF4 nuclear receptor. The levels of *dHNF4* expression increase dramatically at the onset of adulthood, accompanied by the expression of downstream genes that act in glucose homeostasis and mitochondrial OXPHOS (***Figure 6E***). This coordinate transcriptional switch is reduced in *dHNF4* mutants, indicating that the receptor plays a key role in this transition. Importantly, the timing of this program correlates with the onset of *dHNF4* mutant phenotypes in young adults, including sugar-dependent lethality, hyperglycemia, and defects in GSIS, indicating that the upregulation of *dHNF4* expression in adults is of functional significance. It should also be noted, however, that *dHNF4* target genes are still induced at the onset of adulthood in *dHNF4* mutants, albeit at lower levels, indicating that other regulators contribute to this switch in metabolic state (***Figure 6E***). Nonetheless, the

timing of the induction of *dHNF4* and its target genes in early adults, and its role in promoting OXPHOS, suggest that this receptor contributes to the end of the "U-shaped curve" and directs a systemic transcriptional switch that establishes an optimized metabolic state to support the energetic demands of adult life.

Interestingly, a similar metabolic transition towards OXPHOS was recently described in *Drosophila* neuroblast differentiation, mediated by another nuclear receptor, EcR (**Homem et al., 2014**). Although this occurs during early stages of pupal development, prior to the *dHNF4*-mediated transition at the onset of adulthood, the genes involved in this switch show a high degree of overlap with *dHNF4* target genes that act in mitochondria, including *ETFB*, components of Complex IV, *pyruvate carboxylase*, and members of the α-ketoglutarate dehydrogenase complex. This raises the possibility that *dHNF4* may contribute to this change in neuroblast metabolic state and play a more general role in supporting tissue differentiation by promoting OXPHOS.

To our knowledge, only one other developmentally coordinated switch in systemic metabolic state has been reported in *Drosophila* and, intriguingly, it is also regulated by a nuclear receptor. *Drosophila* Estrogen-Related Receptor (dERR) acts in mid-embryogenesis to directly induce genes that function in biosynthetic pathways related to the Warburg effect, by which cancer cells use glucose to support rapid proliferation (**Tennessen et al., 2011**; **Tennessen et al., 2014b**). This switch toward aerobic glycolysis favors lactate production and flux through biosynthetic pathways over mitochondrial OXPHOS, supporting the ~200-fold increase in mass that occurs during larval development. Taken together with our work on dHNF4, these studies define a role for nuclear receptors in directing temporal switches in metabolic state that meet the changing physiological needs of different stages in development. Further studies should allow us to better define these regulatory pathways as well as determine how broadly nuclear receptors exert this role in coupling developmental progression with systemic metabolism.

Although little is known about the links between development and metabolism, it is likely that coordinated switches in metabolic state are not unique to *Drosophila*, but rather occur in all higher organisms in order to meet the distinct metabolic needs of an animal as it progresses through its life cycle. Indeed, a developmental switch towards OXPHOS in coordination with the cessation of growth and differentiation appears to be a conserved feature of animal development. Moreover, as has been shown for cardiac hypertrophy, a failure to coordinate metabolic state with developmental context can have an important influence on human disease (**Lehman and Kelly, 2002**).

Adult *Drosophila* as a context for genetic studies of GSIS and diabete

In addition to promoting a transition toward systemic oxidative metabolism in adult flies, *dHNF4* also contributes to a switch in IPC physiology that supports GSIS. dHNF4 is not expressed in larval IPCs, but is specifically induced in these cells at adulthood (**Figure 6A,B**). Similarly, the fly homologs of the mammalian ATP-sensitive potassium channel subunits, Sur1 and Kir6, which link OXPHOS and ATP production to GSIS, are not expressed in the larval IPCs but are expressed during the adult stage (**Fridell et al., 2009**; **Kim and Rulifson, 2004**). They also appear to be active at this stage as cultured IPCs from adult flies undergo calcium influx and membrane depolarization upon exposure to glucose or the anti-diabetic sulfonylurea drug glibenclamide (**Kreneisz et al., 2010**). In addition, reduction of the mitochondrial membrane potential in adult IPCs by ectopic expression of an uncoupling protein is sufficient to reduce IPC calcium influx, elevate whole-animal glucose levels, and reduce peripheral insulin signaling (**Fridell et al., 2009**). This switch in IPC physiology is paralleled by a change in the nutritional signals that trigger DILP release. Amino acids, and not glucose, stimulate DILP2 secretion by larval IPCs (**Geminard et al., 2009**). Rather, glucose is sensed by the corpora cardiaca in larvae, a distinct organ that secretes adipokinetic hormone, which acts like glucagon to maintain carbohydrate homeostasis during larval stages (**Kim and Rulifson, 2004**; **Lee and Park, 2004**). Interestingly, this can have an indirect effect on the larval IPCs, triggering DILP3 secretion in response to dietary carbohydrates (**Kim and Neufeld, 2015**). Adult IPCs, however, are responsive to glucose for DILP2 release (**Park et al., 2014**) (**Figure 5A,D**). In addition, *dHNF4* mutants on a normal diet maintain euglycemia during larval and early pupal stages, but display hyperglycemia at the onset of adulthood, paralleling their lethal phase on a normal diet (**Figure 6D**). Taken together, these observations support the model that the IPCs change their physiological state during the larval-to-adult transition and that *dHNF4* contributes to this transition toward GSIS. The observation that glucose is a major circulating sugar in adults, but not larvae, combined with its ability to

stimulate DILP2 secretion from adult IPCs, establishes this stage as an experimental context for genetic studies of glucose homeostasis, GSIS, and diabetes. Functional characterization of these pathways in adult *Drosophila* will allow us to harness the power of model organism genetics to better understand the regulation of glucose homeostasis and the factors that contribute to diabetes.

Materials and methods

Drosophila strains and media

All genetic studies used a transheterozygous combination of *dHNF4* null alleles ($dHNF4^{\Delta 17}$/$dHNF4^{\Delta 33}$) and genetically-matched controls that were transheterozygous for precise excisions of the EP2449 and KG08976 P-elements, as described previously (**Palanker et al., 2009**). Sugar diets were made using 8% yeast, 1% agar, 0.05% $MgSO_4$, 0.05% $CaCl_2$, and either 3%, 9% or 15% dietary sugar (2:1 ratio of glucose to sucrose, percentages represent weight/final food volume. 10 ml/L tegosept and 6 ml/L propionic acid were added just prior to pouring). Fasting was achieved by using 1% agar as a medium. For adult studies, 8–10 day old males were selected for all studies unless otherwise indicated.

GAL4/UAS lines for tissue-specific RNAi studies

The following GAL4 driver lines were used for tissue-specific expression experiments: Fat body: *r4-GAL4* (**Lee and Park, 2004**), midgut: *mex-GAL4* (**Phillips and Thomas, 2006**), IPCs: *yw; UAS-Dicer2; $dilp2^{1}$ dilp2HF dilp2-GAL4* (**Park et al., 2014**). RNAi lines used in this study include: $UAS\text{-}dHNF4^{RNAi}$ (TRiP 29375 used in **Figure 4A**, **Figure 4—figure supplement 1A**, **Figure 5D,E**; VDRC 12692 used in **Figure 4—figure supplement 1A–B**, **Figure 5—figure supplement 1**), $UAS\text{-}mCherry^{RNAi}$ (TRiP 35785), $UAS\text{-}Cox5a^{RNAi}$ (TRiP 27548), $UAS\text{-}CIA30^{RNAi}$ (TRiP 55660), $UAS\text{-}ATPsyn\beta^{RNAi}$ (TRiP 28056), $UAS\text{-}Scs\text{-}\alpha^{RNAi}$ (TRiP 51807), $UAS\text{-}CG5599^{RNAi}$ (TRiP 32876), and $UAS\text{-}HexC^{RNAi}$ (TRiP 57404 used in **Figure 4B–D**, and VDRC 35337 and VDRC 35338 used in **Figure 4—figure supplement 3**).

Lifespan studies

The *dHNF4* mutant lethal phase was assessed by raising 50–60 newly hatched first instar larvae in vials of standard laboratory media at 25˚C and scoring for survival through embryonic hatching, wandering third instar, puparium formation, eclosion, and survival through the first day of adulthood (**Figure 1A**). Eclosion rates were scored in a similar manner for *dHNF4* mutants and genetically matched controls raised on the 3%, 9% or 15% sugar diets. For adult survival studies on different diets (**Figure 1C**), 50–60 newly hatched first instar larvae were placed in vials with the 3% sugar diet and raised until five days of adulthood. These mature adults were then transferred to fresh vials of 3%, 9%, or 15% dietary sugar with approximately 25 males and 25 females per vial at 25˚C and scored daily for lethality. Flies were transferred to fresh vials every 2–3 days. At least three replicate vials were analyzed per condition and each experiment was repeated at least three times with similar results.

Developmental staging

For the developmental time course northern blot, we collected 0–12 hr feeding third instar larvae, pupae at 24, 48 or 72 hr after puparium formation, stage P12 males (newly formed pharate adult with visible sex combs) for 4 day pupae, and males at mid-eclosion from the pupal case (to ensure that all *dHNF4* mutants were alive) (n=15 animals per sample). Animals collected for developmental RNA and glycemia measurements (**Figure 6D–E**) were raised on the 15% sugar diet, except for the adults, which were reared on the 3% sugar diet and transferred to the 15% sugar diet after eclosion.

Metabolic assays

Glycogen, trehalose, and free glucose levels were determined using the Hexokinase (HK) and/or Glucose Oxidase (GO) assay kits (Sigma GAHK20, GAGO20) as previously described, with approximately six biological replicates (n=5 animals per sample) assayed per condition (**Tennessen et al., 2014a**). Total protein levels were determined in parallel by Bradford assay to control for potential variations in sample homogenization and/or animal size. Hemolymph glucose measurements were determined by centrifuging 60–100 adult males in a prepared zymogen barrier column (Zymo

Research Corporation C1006) at 9000 g for 5 min at 4˚C, as described (**Park et al., 2014**). The hemolymph flow-though was diluted 1:100 in 1xPBS prior to heat treatment, followed by analysis using the HK assay kit.

ATP assay

Mature adult males were placed on 10% sucrose + 1% agar overnight prior to analysis. Six biological replicates per genotype (n=5 males per sample) were analyzed for ATP levels by using a luminescence assay kit (Molecular Probes ATP kit; A22066,) as described (**Tennessen et al., 2014a**).

GC/MS Metabolomic analysis

Animals were raised on the 3% sugar diet until five days of adulthood and transferred to a fresh vial with either the 3% or 15% sugar diet for three days prior to collection. Twenty adult males per sample were snap-frozen in liquid nitrogen and prepared for analysis by gas chromatography-mass spectrometry (GC/MS) as described (**Tennessen et al., 2014a**). Data is presented from three independent experiments, each consisting of 5–6 biological replicates per condition. Sample preparation and GC/MS analysis were performed by the Metabolomics Core Research Facility at the University of Utah School of Medicine.

Immunostaining

Tissues were dissected in cold 1xPBS, fixed in 4% paraformaldehyde for 20-30 min at room temperature, and washed once quickly followed by three washes for 20 min each in PBS, 0.2% Triton-X100. Samples were blocked using 5% normal goat serum for 1–2 hr at room temperature and incubated with primary antibodies for a minimum of 24 hr at 4˚C, washed, and incubated with secondary antibody at 4˚C for 24 hr. Images were acquired using an Olympus FV1000 confocal microscope and analyzed by Volocity software to generate Z-stack projections and overlay images. The following antibodies were used for immunofluorescence studies: rat anti-dHNF4 (**Palanker et al., 2009**), rat anti-DILP2 (a gift from P. Leopold), rabbit anti-GFP (Molecular Probes A-6455), chicken anti-GFP (Abcam 13970), and mouse anti-ATP5A (Abcam 14748).

Quantification of DILP2 fluorescence

Dissected brains stained for DILP2 peptide were mounted in SlowFade® Gold (Life Technologies) and imaged using an Olympus FV1000 confocal microscope and 60X water-immersion objective. Scan settings were fixed to be identical for all captured images, with Z-stack limits set to encompass the entire depth of DILP2 fluorescence for each brain. Maximum projection Z-stacks were analyzed using Volocity software to calculate mean pixel intensity of DILP2 fluorescence within the IPCs (selected by ROI tool) for each set of IPCs analyzed.

Northern blot analysis

Total RNA was extracted from groups of 10–20 animals using TriPure isolation reagent (Roche). RNA was fractionated by 1% formaldehyde gel electrophoresis at a constant voltage (70V) for ~3.5 hr prior to transfer to a nylon membrane overnight. After transfer, RNA was UV cross-linked to the membrane and placed in hybridization buffer (5 mls formamide, 2 mls 10x PIPES buffer, pH 6.5, 2 mls ddH_20, 1 ml 10% SDS, 100 µl sheared herring sperm ssDNA) for two hours at 42˚C prior to the addition of radiolabeled probe. Probes were generated by Klenow-mediated random primer amplification of purified template DNA corresponding to approximately 100–500 bp of the transcript of interest, allowing incorporation of ^{32}P radiolabeled-nucleotide (dCTP, PerkinElmer). Probes were incubated with membranes overnight, and the hybridized membranes were washed and exposed to X-ray film at -80˚C using two intensifying screens.

RNA-seq

dHNF4 mutants and genetically-matched controls were reared on the 3% sugar diet for five days of adulthood and transferred to the 15% sugar diet for 3 days prior to extracting total RNA. Eight biological replicates per genotype (n=20 males per sample) were collected using TriPure isolation reagent (Roche). Pairs of biological replicates were pooled to obtain four biological replicates for further purification using an RNeasy kit (QIAGEN). RNA quality was subsequently analyzed using an

Agilent Bioanalyzer RNA 6000. PolyA-selected RNAs from each biological replicate were then assembled into barcoded libraries and pooled into a single-flow cell lane for Illumina HighSeq2000 50-cycle single-read sequencing, which produced ≥21.9 million reads per sample. Standard replicate RNA-seq analysis was performed using USeq and DESeq analysis packages with alignment to the *Drosophila melanogaster* dm3 genome assembly. Transcripts meeting a cutoff of ≥1.5 fold difference in mRNA abundance and FDR ≤1% were considered as differentially expressed genes. RNA quality control, library preparation, sequencing, and data analysis were performed at the University of Utah High Throughput Genomics and Bioinformatics Core Facilities. Although *mt:Cyt-b* and *mt:ND6* are included among the down-regulated genes in our RNA-Seq dataset (***Supplementary file 1***), these represent false positives as demonstrated by subsequent repeated northern blot hybridization studies for *mt:Cyt-b* (***Figure 3A***). We are also unable to detect *mt:ND6* mRNA in either mutant or control flies, consistent with a previous report (***Berthier et al., 1986***).

ChIP-seq

Chromatin isolation and immunoprecipitation were performed as described (***Schwartz et al., 2003***). w^{1118} flies were reared on standard cornmeal-based lab medium and 1–1.5 g of mature adults were homogenized in ice-cold buffer A (0.3 M sucrose, 2 mM MgOAc, 3 mM $CaCl_2$, 10 mM Tris-Cl [pH 8], 0.3% Triton X-100, 0.5 mM dithiothreitol, 1 Roche protease inhibitor tablet per 10 ml) for 1.5 min using a Brinkmann Homogenizer Polytron PT 10/35. The homogenate was filtered through a layer of 100 µm-pore nylon mesh into a pre-chilled glass-Teflon homogenizer, stroked on ice 35 times using a B pestle, and filtered through two layers of 40-µm-pore nylon mesh prior to adding one volume of warm cross-linking buffer (0.1 M NaCl, 1 mM EDTA, 0.5 mM EGTA, 50 mM Tris [pH 8], pre-warmed to 40˚C) to bring the sample to room temperature for crosslinking (0.3% formaldehyde for 3 min). 2.5 M glycine was added to a final concentration of 125 mM to stop the crosslinking after 3 min. The mixture was pelleted for resuspension into 10 ml of RIPA buffer (140 mM NaCl, 10 mM Tris-Cl [pH 8.0], 1 mM EDTA, 1% Triton, 0.3% SDS, 0.1% sodium deoxycholate, and Roche protease inhibitor cocktail) for sonication. The sonicated material was centrifuged at 20,000 *g*, and the supernatant was distributed into 500 µl aliquots that were snap frozen in liquid nitrogen. To each aliquot, 1 ml of cold RIPA buffer (without SDS) was added prior to removing 150 µl for an input control, and then 5 µl of polyclonal affinity-purified anti-dHNF4 antibody was added to each sample for immunoprecipitation overnight at 4˚C (***Palanker et al., 2009***). 50 µl of prepared Protein G Dynabeads (Life Technologies) were added to each sample and incubated for 4 hr at 4˚C prior to wash and elution using a magnetic stand. Washes were performed for 3 min each at 4˚C with 1 ml of the following ice-cold solutions: three times in low salt wash buffer (0.1% SDS, 1% Triton X-100, 2 mM EDTA, 20 mM Tris-Cl [pH 8.0], 150 mM NaCl), one time in high salt wash buffer (0.1% SDS, 1% Triton X-100, 2 mM EDTA, 20 mM Tris-Cl [pH 8.0], 500 mM NaCl), once in LiCl wash buffer (0.25 M LiCl, 1% NP-40, 1% deoxycholate, 1 mM EDTA, 10 mM Tris-Cl [pH 8.0]), and twice with Tris-EDTA. Protein-DNA complexes were eluted in 1.5 ml DNA-low bind tubes (Eppendorf) using two 15-minute washes with 250 µl elution buffer (1% SDS, 0.1 M NaHCO3). NaCl was added to a final concentration of 0.2 M to reverse the crosslinks of IP and input control samples, followed by an overnight incubation at 65˚C. dHNF4-bound DNA was purified by using PCR-purification columns (Qiagen), and pooled to acquire four replicates of dHNF4-IP chromatin and input controls. Barcoded libraries for dHNF4-IP and input control samples were generated by the University of Utah High Throughput Genomics core facility and sequenced in a single lane Illumina HiSeq 50-cycle single-read sequencing. Data analysis was performed by the Bioinformatics Core at the University of Utah School of Medicine using USeq SanSeqs (FDR80) as well as Model-based Analysis for ChIP-seq 2.0 (MACS2) (***Zhang et al., 2008***) with an FDR cutoff of 1% (FDR20), identifying 68 enrichment regions. Nearest neighboring genes were compiled using USeq FindNeighboringGenes and UCSC dm3 EnsGenes gene tables and were compared to our RNA-seq dataset to identify proximal genes that are also misexpressed in *dHNF4* mutants, highlighting these as direct targets of dHNF4.

Immunoblotting

Samples were homogenized in Laemmli sample buffer with protease and phosphatase inhibitor cocktails, resolved by SDS-PAGE (10% acrylamide), transferred to PVDF membrane overnight at 4˚C, and blocked with 5% BSA prior to immunoblotting. Antibodies used for western blots include rabbit

anti-pAKT (Cell Signaling #4054), rabbit anti-AKT (Cell Signaling #4691), mouse anti-SDHA (Abcam 137756), rabbit anti-SDHB (a generous gift from D. Winge, generated against yeast SDH2/SDHB), mouse anti-ATP5A (Abcam 14748), and mouse anti-βTubulin (Chemicon MAB380).

DILP2HF ELISA for measuring circulating DILP2

Transgenic lines expressing HA-FLAG tagged DILP2 (DILP2-HF) peptide were used for ELISA assays, essentially as described (**Park et al., 2014**). The indicated *UAS-RNAi* line or w^{1118} controls (**Figure 5D** and **Figure 5—figure supplement 1**) were crossed to *yw; UAS-Dcr2; dilp2*^{1} *DILP2HF dilp2-GAL4* flies. Adult male progeny were either fed *ad libitum* (**Figure 5—figure supplement 1**) or fasted overnight and then re-fed the 15% sugar diet for 45 min prior to analysis (**Figure 5D**). The posterior end of the abdomen was removed using micro-dissection scissors and placed in 60 µl of PBS, using 10 males per biological replicate. Tubes were vortexed for 20 min, after which 50 µl of supernatant was collected in a fresh tube. Samples were homogenized in 600 µl of PBS, 1% Triton X-100. HA-FLAG peptide standards from 0, 20, 40 80, 160, 320 and 640 pg/ml were generated for a linear standard curve. 50 µl of circulating DILP2HF, total DILP2HF, or peptide standards were added to 50 µl of anti-HA-peroxidase (5 ng/ml, Roche 3F10) in PBS (with or without 1% Triton X-100) and then pipetted into a 96-well ELISA plate (Thermo Scientific MaxiSorp Immulon 4 HBX, Cat# 3855) coated with mouse anti-FLAG antibody (Sigma F1804, M2 monoclonal). Samples were incubated at 4˚C overnight and washed 6 times with PBS, 0.2% Tween-20. 100 µl of 1-Step Ultra TMB ELISA Substrate (Thermo Scientific 34029) was added to the plate and incubated at room temperature for 30 min. 100 µl of 2M sulfuric acid was added to stop the reaction and the absorbance was measured immediately at 450 nm. Circulating DILP2HF (pg/fly) versus total remaining peptide was calculated to determine the percent secretion relative to controls ($n \geq 4$ biological replicates per condition).

Clonal analysis

Virgin female flies (*yw,hsFLP,UAS-GFP; tub-GAL80,FRT*^{40A}*;tub-GAL4)* were crossed to *w;HNF4*$^{\Delta 33}$*/CyO twi>GFP* males for MARCM analysis. Flies were reared on the 3% sugar diet and heat treated at 37°C for one hour as pharate adults, and again as newly-eclosed adults. Adults were maintained on the 15% sugar diet for 8–10 days prior to analysis.

Tetramethylrhodamine ethyl ester (TMRE) staining

Adult flies were dissected in room temperature Schneider's medium (ThermoFisher 21720024) with microdissection scissors to separate the abdomen from the thorax. The intestine was removed and the abdominal cavity was cut open to allow maximal contact of fat body with the TMRE solution (ThermoFisher T669). Dissected abdomens were placed in freshly-prepared solution of 20 nM TMRE in Schneider's medium and incubated in the dark for 5–7 min. Samples were then washed briefly twice in Schneider's medium, mounted on glass slides in fresh Schneider's medium, and immediately imaged on an Olympus FV1000 confocal microscope with a 60x water objective.

Dihydroethidium (DHE) staining

DHE staining was performed as previously described (**Owusu-Ansah and Banerjee, 2009**). Briefly, adult abdomens were dissected as described for TMRE staining, but instead placed in freshly prepared 30 µM DHE (ThermoFisher D11347) in Schneider's medium and incubated in the dark for 5–7 min. Samples were washed rapidly three times with Schneider's medium, followed by fixation in 4% formaldehyde in 1xPBS for seven minutes. Samples were then washed twice in 1xPBS, mounted in SlowFade Gold (ThermoFisher S36936), and imaged on an Olympus FV1000 confocal microscope with a 20X objective.

Statistics

GraphPad PRISM 6 software was used to plot data and perform statistical analysis. Pairwise comparison *P* values were calculated using a two-tailed Student's *t*-test, multiple comparison *P* values were calculated using one-way ANOVA with Šídák multiple test correction (except **Figure 4B,C** which included Dunnett's correction). Error bars are ± 1xSEM unless otherwise noted. Box plots display the full range of data (error bars), the 25–75th quartiles (box), and the median (midline).

Acknowledgements

We thank J Tennessen for his contributions to the early stages of this project and for valuable discussions, P Leopold for DILP2 antibodies, S Park and S Kim for DILP2 ELISA stocks and reagents, C Doane for his contributions to the glucose tolerance test, J Evans for technical assistance, D Winge for the anti-SDHB antibodies, the University of Utah Metabolomics, Cell Imaging, High-Throughput Sequencing and Bioinformatics cores, the Bloomington Stock Center, VDRC and TRiP for stocks and reagents, and FlyBase for informatics support. This research was supported by the NIH (DK075607) and a NIH Developmental Biology Training Grant to WB (5T32 HD07491).

Additional information

Funding

Funder	Grant reference number	Author
National Institutes of Health	DK075607	Carl S Thummel
National Institutes of Health	5T32 HD07491	William E Barry

The funders had no role in study design, data collection and interpretation, or the decision to submit the work for publication.

Author contributions

WEB, Conceived and designed the study, Acquired the data, Analyzed and interpreted the data, Drafted and revised the paper; CST, Conceived and designed the study, Assisted with data analysis and interpretation, Revised the paper

Author ORCIDs

Carl S Thummel, http://orcid.org/0000-0001-8112-4643

Additional files

Supplementary files

• Supplementary file 1. List of genes identified by RNA-seq that display differential abundance between *dHNF4* mutant adult males and matched controls, meeting an FDR cutoff of 20 (1%) and Log2 ratio of ± 0.6 (>1.5 fold change). Transcripts that show reduced abundance in *dHNF4* mutants are marked in beige, while those with increased abundance are colored blue.
DOI: 10.7554/eLife.11183.019

• Supplementary file 2. List of the gene ontology categories (determined using GOstat) represented in the top 500 down-regulated and 500 up-regulated genes in *dHNF4* mutant adults. The top 10-16 GO categories for each gene set are listed in order of significance along with the number of genes affected in that category, the total number of genes in that category (in parentheses), and the statistical significance of the match.
DOI: 10.7554/eLife.11183.020

• Supplementary file 3. List of genes with transcription start sites (TSS) within 10 kb of dHNF4 enrichment peaks determined by ChIP-seq analysis, meeting an FDR 20 cutoff (1%). The chromosomal region and coordinates are indicated for each enrichment peak with neighboring genes listed below each region. Genes are listed from proximal to distal, where the distance reported represents the number of base pairs from the TSS to the middle of the enrichment peak. Gene symbols and corresponding FlyBase gene ID numbers are reported, along with chromosomal location, gene start and stop sites, strand, and TSS position. Neighboring genes also identified by RNA-seq as being either up- or down-regulated in *dHNF4* mutants are highlighted in blue and beige, respectively.
DOI: 10.7554/eLife.11183.021

Major datasets

The following datasets were generated:

Author(s)	Year	Dataset title	Dataset URL	Database, license, and accessibility information
Barry W, Thummel CS	2015	RNA-seq analysis of dHNF4 mutants	http://www.ncbi.nlm.nih.gov/geo/query/acc.cgi?acc=GSE73523	Publicly available at NCBI Gene Expression Omnibus (accession no: GSE73523)
Barry W, Thummel CS	2015	ChIP-seq analysis of dHNF4	http://www.ncbi.nlm.nih.gov/geo/query/acc.cgi?acc=GSE73675	Publicly available at NCBI Gene Expression Omnibus (accession no: GSE73675)
Thummel CS, Barry WE	2015	Data from: Drosophila HNF4 promotes glucose-stimulated insulin secretion and increased mitochondrial function in adults	http://dx.doi.org/10.5061/dryad.8h8q5	Available at Dryad Digital Repository under a CC0 Public Domain Dedication

Reporting standards: Standard used to collect data: Data was uploaded to the NCBI Gene Expression Omnibus website according to their specifications and guidelines.

References

Agrell I. 1953. The aerobic and anaerobic utilization of metabolic energy during insect metamorphosis. *Acta Physiologica Scandinavica* **28**:306–335. doi: 10.1111/j.1748-1716.1953.tb00984.x

Ahn S-H, Shah YM, Inoue J, Morimura K, Kim I, Yim S, Lambert G, Kurotani R, Nagashima K, Gonzalez FJ, Inoue Y. 2008. Hepatocyte nuclear factor 4α in the intestinal epithelial cells protects against inflammatory bowel disease. *Inflammatory Bowel Diseases* **14**:908–920. doi: 10.1002/ibd.20413

Alfa RW, Park S, Skelly K-R, Poffenberger G, Jain N, Gu X, Kockel L, Wang J, Liu Y, Powers AC, Kim SK. 2015. Suppression of insulin production and secretion by a decretin hormone. *Cell Metabolism* **21**:323–333. doi: 10.1016/j.cmet.2015.01.006

Babeu JP, Boudreau F. 2014. Hepatocyte nuclear factor 4-alpha involvement in liver and intestinal inflammatory networks. *World Journal of Gastroenterology* **20**:22–30. doi: 10.3748/wjg.v20.i1.22

Bell AW, Michalopoulos GK. 2006. Phenobarbital regulates nuclear expression of Hnf-4α in mouse and rat hepatocytes independent of CAR and PXR. *Hepatology* **44**:186–194. doi: 10.1002/hep.21234

Berthier F, Renaud M, Alziari S, Durand R. 1986. RNA mapping *on Drosophila* mitochondrial DNA: Precursors and template strands. *Nucleic Acids Research* **14**:4519–4533. doi: 10.1093/nar/14.11.4519

Bodine JH, Orr PR. 1925. Respiratory metabolism. Physiological studies on respiratory metabolism. *Biological Bulletin* **48**:1–14. doi: 10.2307/1536588

Boj SF, Parrizas M, Maestro MA, Ferrer J. 2001. A transcription factor regulatory circuit in differentiated pancreatic cells. *Proceedings of the National Academy of Sciences* **98**:14481–14486. doi: 10.1073/pnas.241349398

Bonzo JA, Ferry CH, Matsubara T, Kim J-H, Gonzalez FJ. 2012. Suppression of hepatocyte proliferation by hepatocyte nuclear factor 4 in adult mice. *Journal of Biological Chemistry* **287**:7345–7356. doi: 10.1074/jbc.M111.334599

Cattin A-L, Le Beyec J, Barreau F, Saint-Just S, Houllier A, Gonzalez FJ, Robine S, Pincon-Raymond M, Cardot P, Lacasa M, Ribeiro A. 2009. Hepatocyte nuclear factor 4, a key factor for homeostasis, cell architecture, and barrier function of the adult intestinal epithelium. *Molecular and Cellular Biology* **29**:6294–6308. doi: 10.1128/MCB.00939-09

Chavalit T, Rojvirat P, Muangsawat S, Jitrapakdee S. 2013. Hepatocyte nuclear factor 4alpha regulates the expression of the murine pyruvate carboxylase gene through the HNF4-specific binding motif in its proximal promoter. *Biochim Biophys Acta*:987–999 . doi: 10.1016/j.bbagrm.2013.05.001

Chen WS, Manova K, Weinstein DC, Duncan SA, Plump AS, Prezioso VR, Bachvarova RF, Darnell JE. 1994. Disruption of the HNF-4 gene, expressed in visceral endoderm, leads to cell death in embryonic ectoderm and impaired gastrulation of mouse embryos. *Genes & Development* **8**:2466–2477. doi: 10.1101/gad.8.20.2466

Cho J, Hur JH, Graniel J, Benzer S, Walker DW. 2012. Expression of yeast NDI1 rescues a Drosophila complex I assembly defect. *PLoS ONE* **7**:e50644. doi: 10.1371/journal.pone.0050644

Diop SB, Bodmer R. 2015. Gaining insights into diabetic cardiomyopathy from *Drosophila*. *Trends in Endocrinology & Metabolism* **26**:618–627. doi: 10.1016/j.tem.2015.09.009

Fajans SS, Bell GI. 2011. MODY: history, genetics, pathophysiology, and clinical decision making. *Diabetes Care* **34**:1878–1884. doi: 10.2337/dc11-0035

Forlani G, Zucchini S, Di Rocco A, Di Luzio R, Scipione M, Marasco E, Romeo G, Marchesini G, Mantovani V. 2010. Double heterozygous mutations involving both HNF1A/MODY3 and HNF4A/MODY1 genes: A case report. *Diabetes Care* **33**:2336–2338. doi: 10.2337/dc10-0561

Fridell Y-WC, Hoh M, Kréneisz O, Hosier S, Chang C, Scantling D, Mulkey DK, Helfand SL. 2009. Increased uncoupling protein (UCP) activity in *Drosophila* insulin-producing neurons attenuates insulin signaling and extends lifespan. *Aging* **1**:699–713. doi: 10.18632/aging.100067

Gabbay KH. 1975. Hyperglycemia, polyol metabolism, and complications of diabetes mellitus. *Annual Review of Medicine* **26**:521–536. doi: 10.1146/annurev.me.26.020175.002513

Garesse R, Kaguni L. 2005. A *Drosophila* model of mitochondrial DNA replication: Proteins, genes and regulation. *IUBMB Life* **57**:555–561. doi: 10.1080/15216540500215572

Gragnoli C, Lindner T, Cockburn BN, Kaisaki PJ, Gragnoli F, Marozzi G, Bell GI. 1997. Maturity-onset diabetes of the young due to a mutation in the hepatocyte nuclear factor-4 binding site in the promoter of the hepatocyte nuclear factor-1 gene. *Diabetes* **46**:1648–1651. doi: 10.2337/diacare.46.10.1648

Gupta RK, Vatamaniuk MZ, Lee CS, Flaschen RC, Fulmer JT, Matschinsky FM, Duncan SA, Kaestner KH. 2005. The MODY1 gene hnf-4α regulates selected genes involved in insulin secretion. *Journal of Clinical Investigation* **115**:1006–1015. doi: 10.1172/JCI200522365

Géminard C, Rulifson EJ, Léopold P. 2009. Remote control of insulin secretion by fat cells in *Drosophila*. *Cell Metabolism* **10**:199–207. doi: 10.1016/j.cmet.2009.08.002

Hayhurst GP, Lee Y-H, Lambert G, Ward JM, Gonzalez FJ. 2001. Hepatocyte nuclear factor 4 (nuclear receptor 2A1) is essential for maintenance of hepatic gene expression and lipid homeostasis. *Molecular and Cellular Biology* **21**:1393–1403. doi: 10.1128/MCB.21.4.1393-1403.2001

Homem CCF, Steinmann V, Burkard TR, Jais A, Esterbauer H, Knoblich JA. 2014. Ecdysone and mediator change energy metabolism to terminate proliferation in *Drosophila* neural stem cells. *Cell* **158**:874–888. doi: 10.1016/j.cell.2014.06.024

Johnson RJ, Nakagawa T, Sanchez-Lozada LG, Shafiu M, Sundaram S, Le M, Ishimoto T, Sautin YY, Lanaspa MA. 2013. Sugar, uric acid, and the etiology of diabetes and obesity. *Diabetes* **62**:3307–3315. doi: 10.2337/db12-1814

Kim J, Neufeld TP. 2015. Dietary sugar promotes systemic TOR activation in *Drosophila* through AKH-dependent selective secretion of Dilp3. *Nature Communications* **6**:6846. doi: 10.1038/ncomms7846

Kim SK, Rulifson EJ. 2004. Conserved mechanisms of glucose sensing and regulation by *Drosophila* corpora cardiaca cells. *Nature* **431**:316–320. doi: 10.1038/nature02897

Kréneisz O, Chen X, Fridell Y-WC, Mulkey DK. 2010. Glucose increases activity and Ca2+ in insulin-producing cells of adult *Drosophila*. *NeuroReport* **21**:1116–1120. doi: 10.1097/WNR.0b013e3283409200

Lee G, Park JH. 2004. Hemolymph sugar homeostasis and starvation-induced hyperactivity affected by genetic manipulations of the adipokinetic hormone-encoding gene in *Drosophila melanogaster* . *Genetics* **167**:311–323. doi: 10.1534/genetics.167.1.311

Legros F, Malka F, Frachon P, Lombès A, Rojo M. 2004. Organization and dynamics of human mitochondrial DNA. *Journal of Cell Science* **117**:2653–2662. doi: 10.1242/jcs.01134

Lehman JJ, Kelly DP. 2002. Transcriptional activation of energy metabolic switches in the developing and hypertrophied heart. *Clinical and Experimental Pharmacology and Physiology* **29**:339–345. doi: 10.1046/j.1440-1681.2002.03655.x

Leigh-Brown S, Enriquez J, Odom DT. 2010. Nuclear transcription factors in mammalian mitochondria. *Genome Biology* **11**:215. doi: 10.1186/gb-2010-11-7-215

Li J, Ning G, Duncan SA. 2000. Mammalian hepatocyte differentiation requires the transcription factor Hnf-4alpha. *Genes & Development* **14**:464–474.

Marcil V, Seidman E, Sinnett D, Boudreau F, Gendron F-P, Beaulieu J-F, Menard D, Precourt L-P, Amre D, Levy E. 2010. Modification in oxidative stress, inflammation, and lipoprotein assembly in response to hepatocyte nuclear factor 4 knockdown in intestinal epithelial cells. *Journal of Biological Chemistry* **285**:40448–40460. doi: 10.1074/jbc.M110.155358

Marcil V, Sinnett D, Seidman E, Boudreau F, Gendron F-P, Beaulieu J-F, Menard D, Lambert M, Bitton A, Sanchez R, Amre D, Levy E. 2012. Association between genetic variants in the HNF4A gene and childhood-onset Crohn's disease. *Genes and Immunity* **13**:556–565. doi: 10.1038/gene.2012.37

Marinov GK, Wang YE, Chan D, Wold BJ. 2014. Evidence for site-specific occupancy of the mitochondrial genome by nuclear transcription factors. *PLoS ONE* **9**:e84713. doi: 10.1371/journal.pone.0084713

Merkey AB, Wong CK, Hoshizaki DK, Gibbs AG. 2011. Energetics of metamorphosis in *Drosophila melanogaster* . *Journal of Insect Physiology* **57**:1437–1445. doi: 10.1016/j.jinsphys.2011.07.013

Mishra P, Chan DC. 2014. Mitochondrial dynamics and inheritance during cell division, development and disease. *Nature Reviews Molecular Cell Biology* **15**:634–646. doi: 10.1038/nrm3877

Miura A, Yamagata K, Kakei M, Hatakeyama H, Takahashi N, Fukui K, Nammo T, Yoneda K, Inoue Y, Sladek FM, Magnuson MA, Kasai H, Miyagawa J, Gonzalez FJ, Shimomura I. 2006. Hepatocyte nuclear factor-4 is essential for glucose-stimulated insulin secretion by pancreatic beta-cells. *Journal of Biological Chemistry* **281**:5246–5257. doi: 10.1074/jbc.M507496200

Nagaki M, Moriwaki H. 2008. Transcription factor HNF and hepatocyte differentiation. *Hepatology Research* **38**:961–969. doi: 10.1111/j.1872-034X.2008.00367.x

Nammo T, Yamagata K, Tanaka T, Kodama T, Sladek FM, Fukui K, Katsube F, Sato Y, Miyagawa Jun-ichiro, Shimomura I. 2008. Expression of HNF-4α (MODY1), HNF-1β (MODY5), and HNF-1α (MODY3) proteins in the developing mouse pancreas. *Gene Expression Patterns* **8**:96–106. doi: 10.1016/j.modgep.2007.09.006

Nargund AM, Fiorese CJ, Pellegrino MW, Deng P, Haynes CM. 2015. Mitochondrial and nuclear accumulation of the transcription factor ATFS-1 promotes OXPHOS recovery during the UPR(mt). *Molecular Cell* **58**:123–133. doi: 10.1016/j.molcel.2015.02.008

Needham DM. 1929. The chemical changes during the metamorphosis of insects. *Biological Reviews* **4**:307–326. doi: 10.1111/j.1469-185X.1929.tb00613.x
Newport G. 1836. On the respiration of insects. *Philosophical Transactions of the Royal Society of London* **126**: 529–566. doi: 10.1098/rstl.1836.0026
Nässel DR, Liu Y, Luo J. 2015. Insulin/IGF signaling and its regulation in drosophila. *General and Comparative Endocrinology* **221**:255–266. doi: 10.1016/j.ygcen.2014.11.021
Owusu-Ansah E, Banerjee U. 2009. Reactive oxygen species prime drosophila haematopoietic progenitors for differentiation. *Nature* **461**:537–541. doi: 10.1038/nature08313
Owusu-Ansah E, Perrimon N. 2014. Modeling metabolic homeostasis and nutrient sensing in drosophila: Implications for aging and metabolic diseases. *Disease Models & Mechanisms* **7**:343–350. doi: 10.1242/dmm.012989
Padmanabha D, Baker KD. 2014. *Drosophila* gains traction as a repurposed tool to investigate metabolism. *Trends in Endocrinology & Metabolism* **25**:518–527. doi: 10.1016/j.tem.2014.03.011
Palanker L, Tennessen JM, Lam G, Thummel CS. 2009. *Drosophila* HNF4 regulates lipid mobilization and β-oxidation. *Cell Metabolism* **9**:228–239. doi: 10.1016/j.cmet.2009.01.009
Park S, Alfa RW, Topper SM, Kim GES, Kockel L, Kim SK. 2014. A genetic strategy to measure circulating *Drosophila* insulin reveals genes regulating insulin production and secretion. *PLoS Genetics* **10**:e1004555. doi: 10.1371/journal.pgen.1004555
Phillips MD, Thomas GH. 2006. Brush border spectrin is required for early endosome recycling in *Drosophila*. *Journal of Cell Science* **119**:1361–1370. doi: 10.1242/jcs.02839
Postic C, Shiota M, Niswender KD, Jetton TL, Chen Y, Moates JM, Shelton KD, Lindner J, Cherrington AD, Magnuson MA. 1999. Dual roles for glucokinase in glucose homeostasis as determined by liver and pancreatic cell-specific gene knock-outs using Cre recombinase. *Journal of Biological Chemistry* **274**:305–315. doi: 10.1074/jbc.274.1.305
Prentki M, Matschinsky FM, Madiraju SRM. 2013. Metabolic signaling in fuel-induced insulin secretion. *Cell Metabolism* **18**:162–185. doi: 10.1016/j.cmet.2013.05.018
Qatanani M, Lazar MA. 2007. Mechanisms of obesity-associated insulin resistance: Many choices on the menu. *Genes & Development* **21**:1443–1455. doi: 10.1101/gad.1550907
Roberti M, Bruni F, Polosa PL, Gadaleta MN, Cantatore P. 2006. The *Drosophila* termination factor DmTTF regulates *in vivo* mitochondrial transcription. *Nucleic Acids Research* **34**:2109–2116. doi: 10.1093/nar/gkl181
Rodríguez JC, Ortiz JA, Hegardt FG, Haro D. 1998. The hepatocyte nuclear factor 4 (HNF-4) represses the mitochondrial HMG-CoA synthase gene. *Biochemical and Biophysical Research Communications* **242**:692–696. doi: 10.1006/bbrc.1997.8032
Roth U, Jungermann K, Kietzmann T. 2002. Activation of glucokinase gene expression by hepatic nuclear factor 4α in primary hepatocytes. *Biochemical Journal* **365**:223–228. doi: 10.1042/bj20020340
Rubenstein JL, Brutlag D, Clayton DA. 1977. The mitochondrial DNA of drosophila melanogaster exists in two distinct and stable superhelical forms. *Cell* **12**:471–482. doi: 10.1016/0092-8674(77)90123-4
Rulifson EJ, Kim SK, Nusse R. 2002. Ablation of insulin-producing neurons in flies: Growth and diabetic phenotypes. *Science* **296**:1118–1120. doi: 10.1126/science.1070058
Schwartz BE, Larochelle S, Suter B, Lis JT. 2003. Cdk7 is required for full activation of *Drosophila* heat shock genes and RNA polymerase II phosphorylation *in vivo*. *Molecular and Cellular Biology* **23**:6876–6886. doi: 10.1128/MCB.23.19.6876-6886.2003
Sivitz WI, Yorek MA. 2010. Mitochondrial dysfunction in diabetes: From molecular mechanisms to functional significance and therapeutic opportunities. *Antioxidants & Redox Signaling* **12**:537–577. doi: 10.1089/ars.2009.2531
Soutoglou E, Katrakili N, Talianidis I. 2000. Acetylation regulates transcription factor activity at multiple levels. *Molecular Cell* **5**:745–751. doi: 10.1016/S1097-2765(00)80253-1
Sun K, Montana V, Chellappa K, Brelivet Y, Moras D, Maeda Y, Parpura V, Paschal BM, Sladek FM. 2007. Phosphorylation of a conserved serine in the deoxyribonucleic acid binding domain of nuclear receptors alters intracellular localization. *Molecular Endocrinology* **21**:1297–1311. doi: 10.1210/me.2006-0300
Szczepanek K, Lesnefsky EJ, Larner AC. 2012. Multi-tasking: Nuclear transcription factors with novel roles in the mitochondria. *Trends in Cell Biology* **22**:429–437. doi: 10.1016/j.tcb.2012.05.001
Teleman A, Ratzenböck I, Oldham S. 2012. *Drosophila*: A model for understanding obesity and diabetic complications. *Experimental and Clinical Endocrinology and Diabetes* **120**:184–185. doi: 10.1055/s-0032-1304566
Tennessen JM, Baker KD, Lam G, Evans J, Thummel CS. 2011. The *Drosophila* estrogen-related receptor directs a metabolic switch that supports developmental growth. *Cell Metabolism* **13**:139–148. doi: 10.1016/j.cmet.2011.01.005
Tennessen JM, Barry WE, Cox J, Thummel CS. 2014a. Methods for studying metabolism in *Drosophila*. *Methods* **68**:105–115. doi: 10.1016/j.ymeth.2014.02.034
Tennessen JM, Bertagnolli NM, Evans J, Sieber MH, Cox J, Thummel CS. 2014b. Coordinated metabolic transitions during *Drosophila* embryogenesis and the onset of aerobic glycolysis. *G3; Genes|Genomes|Genetics* **4**:839–850. doi: 10.1534/g3.114.010652
Toyama EQ, Herzig S, Courchet J, Lewis TL, Loson OC, Hellberg K, Young NP, Chen H, Polleux F, Chan DC, Shaw RJ. 2016. AMP-activated protein kinase mediates mitochondrial fission in response to energy stress. *Science* **351**:275–281. doi: 10.1126/science.aab4138

Ugrankar R, Berglund E, Akdemir F, Tran C, Kim MS, Noh J, Schneider R, Ebert B, Graff JM. 2015. *Drosophila* glucome screening identifies Ck1alpha as a regulator of mammalian glucose metabolism. *Nature Communications* **6**:7102. doi: 10.1038/ncomms8102

UK IBD Genetics Consortium, Barrett JC, Lee JC, Lees CW, Prescott NJ, Anderson CA, Phillips A, Wesley E, Parnell K, Zhang H, Drummond H, Nimmo ER, Massey D, Blaszczyk K, Elliott T, Cotterill L, Dallal H, Lobo AJ, Mowat C, Sanderson JD, Jewell DP, et al. 2009. Genome-wide association study of ulcerative colitis identifies three new susceptibility loci, including the HNF4A region. *Nature Genetics* **41**:1330–1334. doi: 10.1038/ng.483

van Sommeren S, Visschedijk MC, Festen EAM, de Jong DJ, Ponsioen CY, Wijmenga C, Weersma RK. 2011. Hnf4α and CDH1 are associated with ulcerative colitis in a Dutch cohort. *Inflammatory Bowel Diseases* **17**: 1714–1718. doi: 10.1002/ibd.21541

Van Vranken JG, Bricker DK, Dephoure N, Gygi SP, Cox JE, Thummel CS, Rutter J. 2014. SDHAF4 promotes mitochondrial succinate dehydrogenase activity and prevents neurodegeneration. *Cell Metabolism* **20**:241–252. doi: 10.1016/j.cmet.2014.05.012

Wang H, Hagenfeldt-Johansson K, Otten LA, Gauthier BR, Herrera PL, Wollheim CB. 2002. Experimental models of transcription factor-associated maturity-onset diabetes of the young. *Diabetes* **51**:S333–S342. doi: 10.2337/diabetes.51.2007.S333

Wang H, Maechler P, Antinozzi PA, Hagenfeldt KA, Wollheim CB. 2000. Hepatocyte nuclear factor 4α regulates the expression of pancreatic β-cell genes implicated in glucose metabolism and nutrient-induced insulin secretion. *Journal of Biological Chemistry* **275**:35953–35959. doi: 10.1074/jbc.M006612200

Xu X, Gopalacharyulu P, Seppänen-Laakso T, Ruskeepää A-L, Aye CC, Carson BP, Mora S, Orešič M, Teleman AA. 2012. Insulin signaling regulates fatty acid catabolism at the level of CoA activation. *PLoS Genetics* **8**: e1002478. doi: 10.1371/journal.pgen.1002478

Yamagata K, Furuta H, Oda N, Kaisaki PJ, Menzel S, Cox NJ, Fajans SS, Signorini S, Stoffel M, Bell GI. 1996. Mutations in the hepatocyte nuclear factor-4α gene in maturity-onset diabetes of the young (MODY1). *Nature* **384**:458–460. doi: 10.1038/384458a0

Yanger K, Zong Y, Maggs LR, Shapira SN, Maddipati R, Aiello NM, Thung SN, Wells RG, Greenbaum LE, Stanger BZ. 2013. Robust cellular reprogramming occurs spontaneously during liver regeneration. *Genes & Development* **27**:719–724. doi: 10.1101/gad.207803.112

Yoon JC, Puigserver P, Chen G, Donovan J, Wu Z, Rhee J, Adelmant G, Stafford J, Kahn CR, Granner DK, Newgard CB, Spiegelman BM. 2001. Control of hepatic gluconeogenesis through the transcriptional coactivator PGC-1. *Nature* **413**:131–138. doi: 10.1038/35093050

Zhang Y, Liu T, Meyer CA, Eeckhoute J, Johnson DS, Bernstein BE, Nussbaum C, Myers RM, Brown M, Li W, Liu XS. 2008. Model-based analysis of ChIP-Seq (MACS). *Genome Biology* **9**:R137. doi: 10.1186/gb-2008-9-9-r137

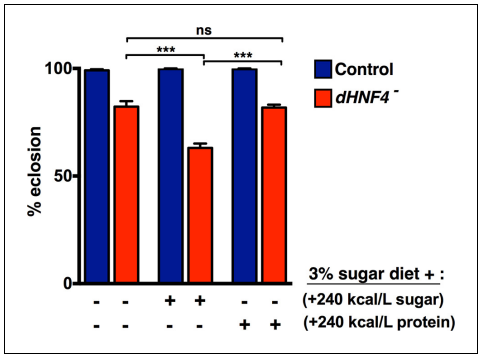

Figure 1—figure supplement 1. Dietary sugar, but not protein, correlates with reduced *dHNF4* mutant survival. Newly hatched first instar larvae were placed in vials (~60 larvae per vial) containing either the 3% sugar diet, the 3% sugar diet + 240 kcal/L extra sugar (2:1 glucose to sucrose, 9% final concentration), or the 3% sugar diet + 240 kcal/L of additional protein (peptone). All diets contained 8% yeast, 1% agar, 0.05% $MgSO_4$, and 0.05% $CaCl_2$, as described in Materials and methods. Animals were reared at 25˚C and successful eclosion was scored as complete emergence from the pupal case. Data is plotted as the mean ± SEM. ***$p \leq 0.001$.
DOI: 10.7554/eLife.11183.004

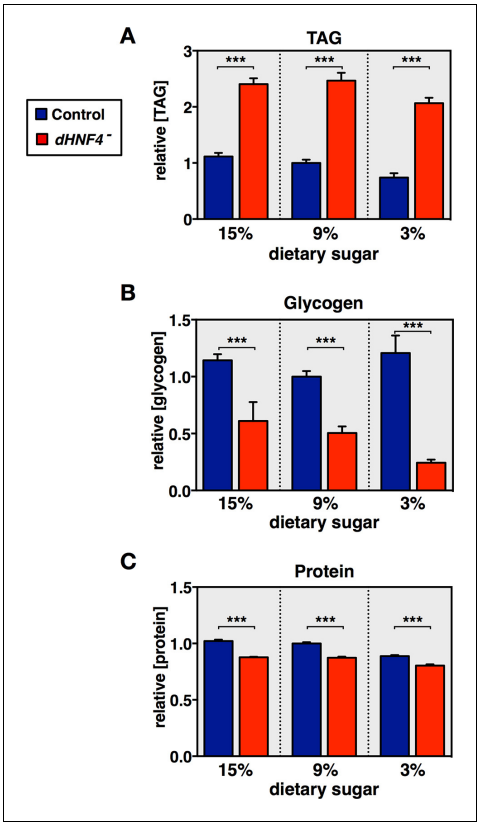

Figure 1—figure supplement 2. Profiling of major metabolites in *dHNF4* mutant adults fed different levels of dietary sugar. Controls and *dHNF4* mutants were raised to adulthood on the 3% sugar diet under density-controlled conditions. Five days after eclosion, mature adult males were transferred to the 3%, 9%, or 15% sugar diets for three days prior to analysis. Whole-animal lysates were analyzed for concentrations of total triacylglycerol (TAG) (**A**), glycogen (**B**), or protein (**C**). All data was normalized to the level in controls on the 9% sugar diet. Data represents six biological replicates each with five animals, and results were consistent between at least three independent experiments. Data is plotted as the mean ± SEM. ***p≤0.001, **p≤0.01, *p≤0.05 Student's *t*-test.
DOI: 10.7554/eLife.11183.005

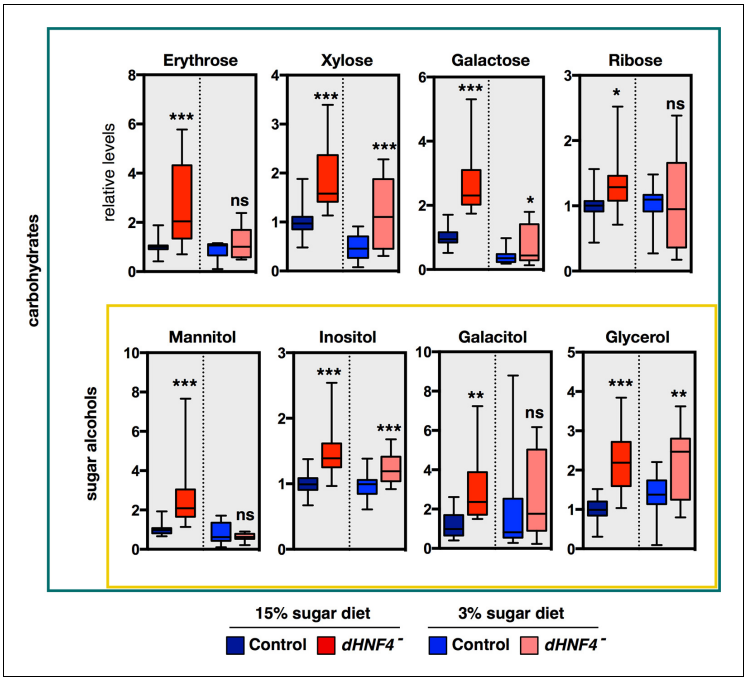

Figure 2—figure supplement 1. *dHNF4* mutants show broad defects in carbohydrate homeostasis. GC/MS metabolomic profiling reveals that a range of sugars and sugar alcohols are increased in *dHNF4* mutants compared to genetically matched controls, indicating that *dHNF4* is required for proper carbohydrate metabolism. Animals were raised to adulthood on the 3% sugar diet prior to being transferred to the indicated diet for 3 days. Data was obtained from three independent experiments consisting of five to six biological replicates per condition and values were normalized to control levels on the 15% sugar diet. Data are graphically represented as a box plot, with the box representing the lower and upper quartiles, the horizontal line representing the median, and the error bars denoting the minimum and maximum data points. ***p≤0.001, **p≤0.01, *p≤0.05.

DOI: 10.7554/eLife.11183.007

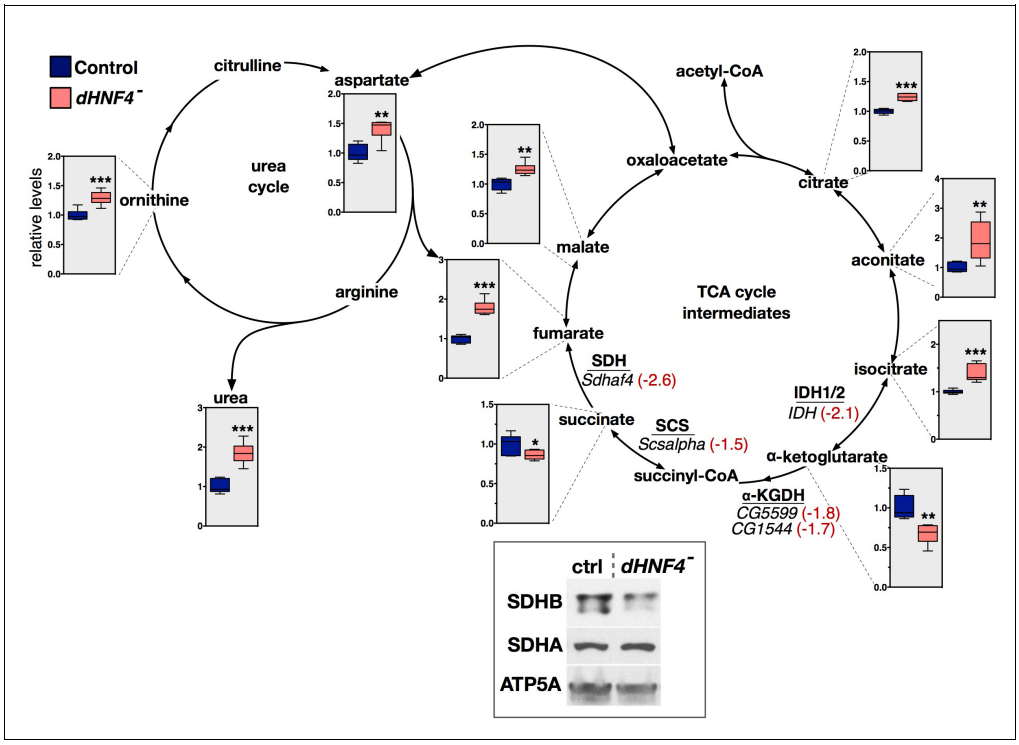

Figure 3—figure supplement 1. *dHNF4* mutants display changes in TCA cycle intermediates that correlate with changes in gene expression. GC/MS metabolomic profiling of adult flies fed a sugar only diet (10% sucrose + 1% agar) reveals defective TCA cycle metabolism in *dHNF4* mutants. Intermediates of the TCA cycle are presented along with genes that are underexpressed in *dHNF4* mutants (in italics). The mRNA abundance for each gene in *dHNF4* mutants is indicated (red text) relative to matched controls from RNA-seq data. These genes are predicted to affect enzymatic complexes for isocitrate dehydrogenase (IDH1/2), alpha-ketoglutarate dehydrogenase (α-KGDH), succinyl-CoA synthetase (SCS), or succinate dehydrogenase (SDH). Consistent with impaired IDH and SCS activity, levels of alpha-ketoglutarate and succinate are reduced, while upstream citrate, aconitate, and isocitrate accumulate. The modest effect on succinate abundance is possibly due to a combined effect of impaired succinate production balanced by decreased succinate oxidation resulting from impaired SDH activity. In addition, intermediates of the urea cycle are broadly accumulated in *dHNF4* mutants including fumarate, which lies at the interface of these two pathways. This may contribute to the elevated levels of fumarate and downstream malate independent of impaired SDH activity. Metabolites lacking graphical data were not detected or could not be measured by GC/MS. Animals were reared on the 3% sugar diet until 5 days of adulthood and then transferred to medium containing 10% sucrose with 1% agar (sugar only) for 3 days prior to analysis. Data represents six biological replicates consisting of 20 males per replicate. ***p≤0.001, **p≤0.01, *p≤0.05. Inset - western blot analysis of whole animal lysates revealed reduced levels of SDHB protein, but no effect on SDHA, in *dHNF4* mutants. ATP5A was detected as a control for loading and transfer.

DOI: 10.7554/eLife.11183.009

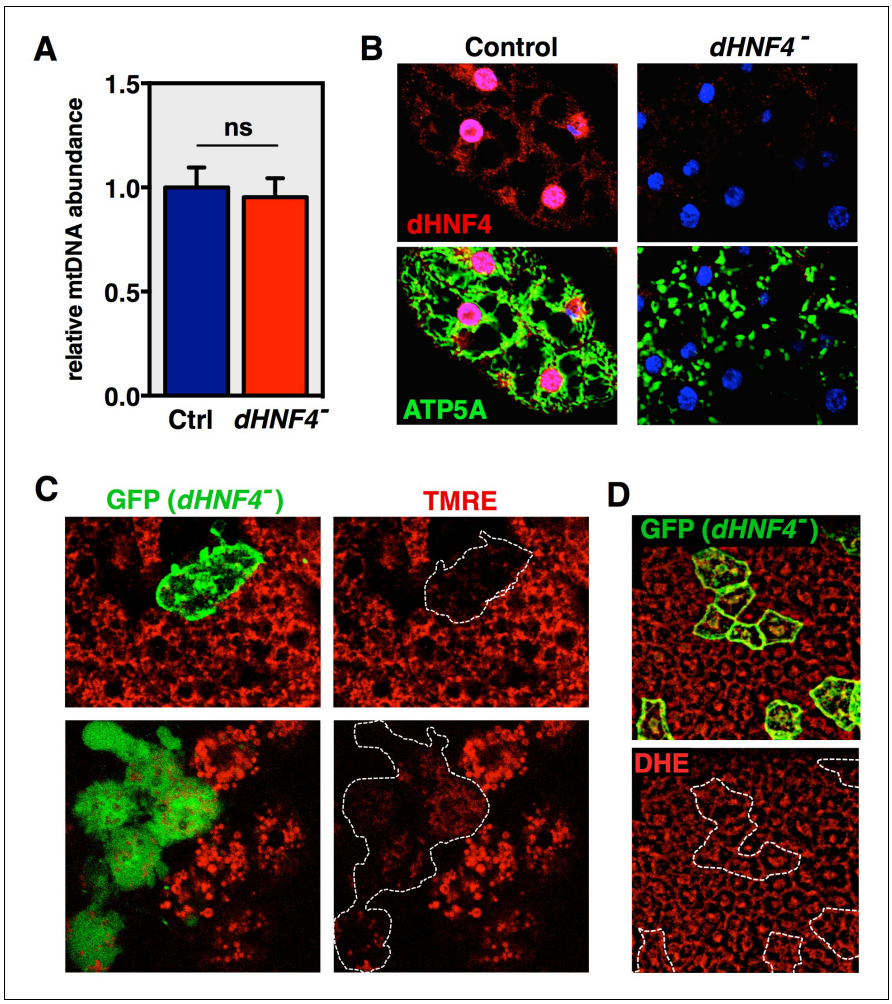

Figure 3—figure supplement 2. *dHNF4* mutants display mitochondrial defects. (**A**) mtDNA abundance relative to nuclear DNA quantified by qPCR in control and *dHNF4* mutant adult males on the 15% sugar diet. (B) Adult fat body tissue from control or *dHNF4* mutants immunostained for ATP5A (green) to detect mitochondria, dHNF4 protein (red), and DAPI (blue) to mark nuclei. (**C**) Analysis of *dHNF4* mutant MARCM clones (GFP+) shows reduced mitochondrial membrane potential by TMRE staining of live fat body tissue from adult flies maintained on the 15% sugar diet. (**D**) MARCM clonal analysis of adult *dHNF4* mutant fat body cells (GFP+) for reactive oxygen species (ROS) by DHE staining shows no detectable difference in ROS levels in mutant cells.
DOI: 10.7554/eLife.11183.010

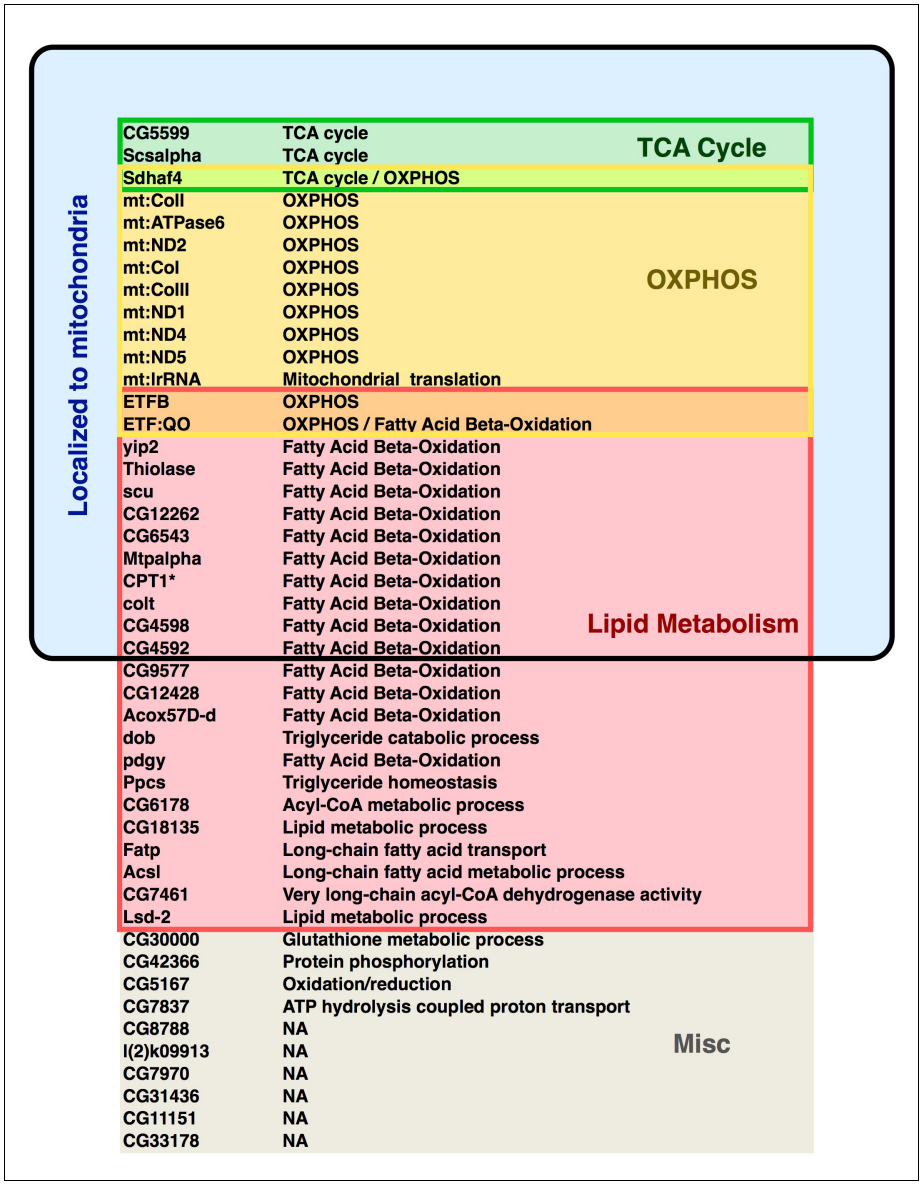
Localized to mitochondria
CG5599 TCA cycle
Scsalpha TCA cycle
TCA Cycle
Sdhaf4 TCA cycle / OXPHOS
mt:CoII OXPHOS
mt:ATPase6 OXPHOS
mt:ND2 OXPHOS
mt:CoI OXPHOS
mt:CoIII OXPHOS
mt:ND1 OXPHOS
mt:ND4 OXPHOS
mt:ND5 OXPHOS
mt:lrRNA Mitochondrial translation
OXPHOS
ETFB OXPHOS
ETF:QO OXPHOS / Fatty Acid Beta-Oxidation
yip2 Fatty Acid Beta-Oxidation
Thiolase Fatty Acid Beta-Oxidation
scu Fatty Acid Beta-Oxidation
CG12262 Fatty Acid Beta-Oxidation
CG6543 Fatty Acid Beta-Oxidation
Mtpalpha Fatty Acid Beta-Oxidation
CPT1* Fatty Acid Beta-Oxidation
colt Fatty Acid Beta-Oxidation
CG4598 Fatty Acid Beta-Oxidation
CG4592 Fatty Acid Beta-Oxidation
Lipid Metabolism
CG9577 Fatty Acid Beta-Oxidation
CG12428 Fatty Acid Beta-Oxidation
Acox57D-d Fatty Acid Beta-Oxidation
dob Triglyceride catabolic process
pdgy Fatty Acid Beta-Oxidation
Ppcs Triglyceride homeostasis
CG6178 Acyl-CoA metabolic process
CG18135 Lipid metabolic process
Fatp Long-chain fatty acid transport
Acsl Long-chain fatty acid metabolic process
CG7461 Very long-chain acyl-CoA dehydrogenase activity
Lsd-2 Lipid metabolic process
CG30000 Glutathione metabolic process
CG42366 Protein phosphorylation
CG5167 Oxidation/reduction
CG7837 ATP hydrolysis coupled proton transport
CG8788 NA
l(2)k09913 NA
CG7970 NA
CG31436 NA
CG11151 NA
CG33178 NA
Misc

Figure 3—figure supplement 3. Predicted functions of dHNF4 target genes. Forty-seven genes identified as high confidence targets for direct regulation by dHNF4 are depicted. These genes fit the criteria of showing proximal dHNF4 binding along with reduced transcript abundance in mutant animals as determined by RNA-seq (≥1.5 fold change, 1% FDR) (Supplementary Tables 1,3).
DOI: 10.7554/eLife.11183.011

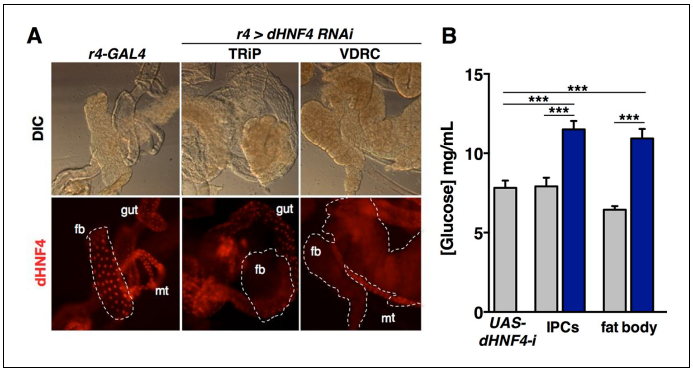

Figure 4—figure supplement 1. *dHNF4* is required in the insulin-producing cells and fat body to maintain glucose homeostasis. (**A**) Tissue-specific RNAi directed against *dHNF4* effectively reduces steady-state levels of dHNF4 protein. Immunostaining was used to detect dHNF4 in organs dissected from third instar larvae that express either the *r4-GAL4* driver alone as a control or fat body-specific RNAi for *dHNF4* (*r4>dHNF4*^{RNAi}) using *UAS-RNAi* constructs from either the TRiP or VDRC stock collections (fb = fat body, mt = Malpighian tubules). (**B**) *dHNF4* function is required in both the IPCs and fat body for glucose homeostasis. This data reproduces that shown in ***Figure 4A*** using a distinct *dHNF4* UAS-RNAi construct. Circulating glucose levels were measured in animals with tissue-specific RNAi against *dHNF4* (VDRC) in the IPCs (*dilp2-GAL4*) or fat body (*r4-GAL4*) compared to GAL4 and UAS lines alone as controls. Controls are represented by grey bars while *dHNF4* RNAi is represented by blue bars. Data represents the mean ± SEM, ***p≤0.001.

DOI: 10.7554/eLife.11183.013

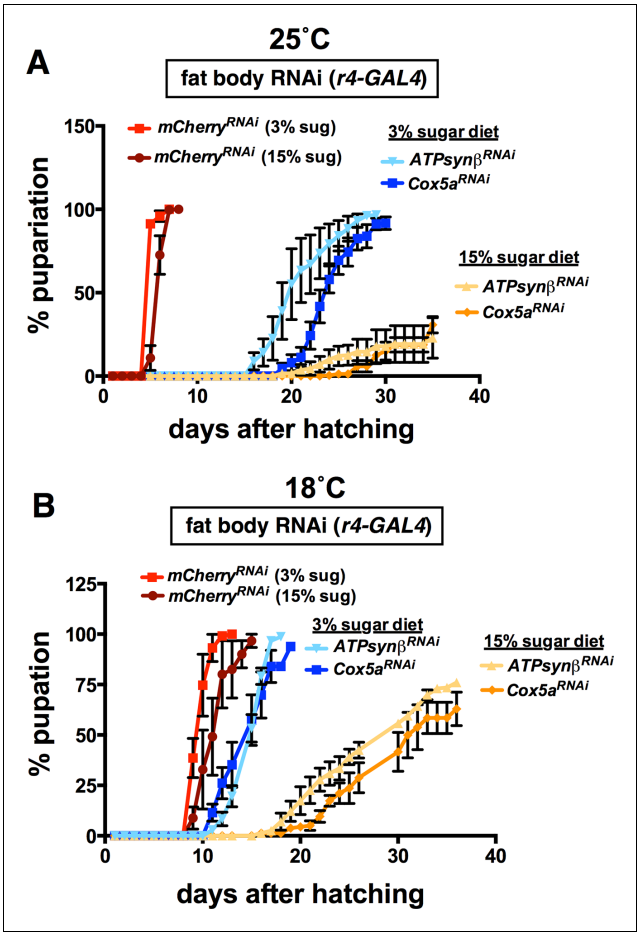

Figure 4—figure supplement 2. Fat body-specific disruption of the electron transport chain causes sugar intolerance. Newly hatched first instar larvae were placed in vials (~60 per vial) containing the 3% or 15% sugar diet and scored for puparium formation when raised at either 25˚C (A) or 18˚C (**B**). Disruption of ETC complex IV (*Cox5a* RNAi) or complex V (*ATPsynβ* RNAi) in the fat body (*r4-GAL4*) results in sugar intolerance as seen by a pronounced developmental delay and reduced survival to puparium formation on the 15% sugar diet. These defects are partially suppressed when reared on the low sugar diet at either temperature; however, the 18˚C condition allows for more robust suppression of the sugar-dependent developmental delay (**B**).
DOI: 10.7554/eLife.11183.014

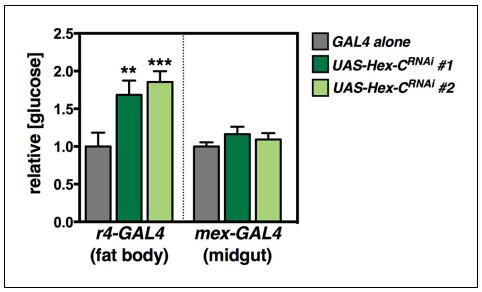

Figure 4—figure supplement 3. Additional RNAi lines confirming the importance of *Hex-C* in the fat body for glycemic control. Tissue-specific RNAi directed against *Hex-C* in the fat body, but not midgut, results in elevated levels of free glucose. RNAi lines against *Hex-C* were obtained from the VDRC RNAi collection (*UAS-Hex-C RNAi#1*: VDRC 35337, and *UAS-Hex-C RNAi#2*: VDRC 35338). Grey bars represent the indicated GAL4 driver line crossed to w^{1118} as a negative control. These results are consistent with those in ***Figure 4B*** showing hyperglycemia upon fat body-specific RNAi for *Hex-C* using a line from the TRiP collection (Bloomington stock #57404).

DOI: 10.7554/eLife.11183.015

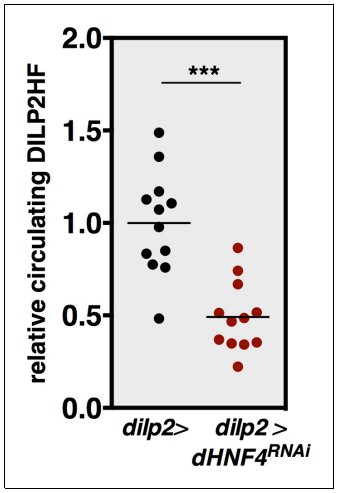

Figure 5—figure supplement 1. *dHNF4* RNAi in the IPCs causes reduced levels of circulating DILP2-HF. This data reproduces that shown in ***Figure 5D*** using a distinct *dHNF4* UAS-RNAi construct (VDRC collection). Levels of circulating HA-FLAG-tagged DILP2 (DILP2HF) were assayed in *ad libitum* fed animals with IPC-specific RNAi against *dHNF4* (VDRC 12692) using the *dilp2-GAL4* driver compared to animals carrying the *dilp2-GAL4* driver alone as a control. Dot plot depicts individual sample values from two independent experiments and the midline represents the mean (n=6 biological replicates per genotype per experiment). ***p≤0.001.

DOI: 10.7554/eLife.11183.017

CHAPTER 4

INVESTIGATION OF A CONSERVED ROLE FOR HNF4 IN REGULATING MITOCHONDRIAL FUNCTION

William E. Barry, Judith A. Simcox, Nathan M. Krah, L. Charles Murtaugh, Claudio J. Villanueva, and Carl S. Thummel

Summary

The nuclear receptor HNF4A is an essential regulator of development and metabolic homeostasis. In humans, haploinsufficiency for *HNF4A* results in diabetes-onset during young adulthood, yet the molecular basis for this remains unclear. My previous studies in *Drosophila* revealed an important role for dHNF4 in promoting mitochondrial function at the transition to adulthood to support insulin secretion and glucose homeostasis in the mature animal. Here I present a collaborative effort to assess the potential evolutionarily conserved role of HNF4 in supporting mitochondrial function. This includes an extended analysis of dHNF4-dependent mitochondrial activity during *Drosophila* development, showing an adult-specific requirement for dHNF4 to maintain mitochondrial integrity and the activity of the electron transport chain (ETC). dHNF4 maintains ETC complex I activity through the regulation of mtDNA-encoded genes and through *CG7461,* a nuclear-encoded acyl-CoA dehydrogenase that is homologous to mammalian *ACAD9*. Mutations in *ACAD9* cause complex I deficiency in humans and HNF4A binds to the *ACAD9* promoter region in the adult mouse liver. HNF4A also associates with *Polrmt*, and *Pink1,* encoding the mitochondrial RNA polymerase gene and a factor necessary for both mitochondrial quality control and ETC activity, respectively. Although HNF4A is dispensable for proper expression of *Polrmt* and *Acad9* under normal conditions, their expression is significantly reduced in *HNF4A* mutant livers under the metabolic stress condition of cold exposure. In contrast, *Pink1* and mtDNA-encoded transcripts require HNF4A for maximal expression at both room temperature and under cold stress. Although mitochondrial localization was not observed for HNF4A in mouse hepatocytes, staining of human pancreas specimens revealed

distinct mitochondrial localization in islets. Taken together, these findings suggest that the role for HNF4A in regulating mitochondrial activity has been conserved through evolution and may represent a critical function of this nuclear receptor to maintain metabolic homeostasis and prevent diabetes.

Introduction

The rising prevalence of metabolic disorders has generated an urgent need to better understand how metabolic systems are regulated to help advance clinical progress. A major focus of these studies is on nuclear receptors, which comprise a family of ligand-regulated transcription factors that play important roles in development and metabolic homeostasis. One of the first nuclear receptors to be associated with a human metabolic disorder is HNF4A, which was linked to a heritable form of diabetes termed Maturity Onset Diabetes of the Young 1 (MODY1) two decades ago (Yamagata et al., 1996). Autosomal dominant inheritance of *HNF4A* mutations results in impaired insulin secretion and hyperglycemia, which typically manifest during young adulthood (Fajans and Bell, 2011). Attempts to model MODY1 have been limited, however, as heterozygous loss of *HNF4A* in mice shows no apparent phenotypes, and null mutants die during early embryogenesis (Chen et al., 1994). Two separate groups have reported studies of adult mice with β-cell specific deletion of *HNF4A*; however, overt diabetes was not observed in either case (Gupta et al., 2005; Miura et al., 2006). Although insulin secretion was found to be impaired in one these studies, there was no impact on sustained glycemic control (Miura et al., 2006). In contrast, hyperinsulinemic hypoglycemia was reported in a separate study of adult mice lacking β-cell HNF4A (Gupta et al., 2005). As a result, the molecular function of HNF4A to support insulin secretion and maintain

systemic glucose homeostasis remains unclear.

Although β-cell dysfunction is thought to be the major cause of MODY1, HNF4A is expressed in several other important metabolic tissues, including the liver, intestine, and kidney. In the liver, HNF4A acts as a master regulator of hepatocyte differentiation and metabolic gene expression. As a result, liver-specific deletion leads to hepatic dedifferentiation, over proliferation, steatosis, reduced glycogen stores, and early lethality (Bonzo et al., 2012; Hayhurst et al., 2001; Walesky et al., 2013a; Walesky et al., 2013b). In the fed state, the liver helps to clear excess circulating glucose by storing it in the form of glycogen. As circulating glucose levels drop during fasting, free glucose is released from the liver through gluconeogenesis and glycogen breakdown to prevent hypoglycemia. Although HNF4A is known to regulate several genes involved in gluconeogenesis, liver-specific disruption of *HNF4A* in an otherwise wild-type background has little effect on circulating glucose levels (Bonzo et al., 2012; Yin et al., 2011; Yoon et al., 2001). RNAi for *HNF4A* in the adult liver, however, exacerbates glucose intolerance in a mouse model of type-2 diabetes, suggesting an important role in this tissue to maintain euglycemia under metabolically stressed conditions (Yin et al., 2011).

In *Drosophila*, null mutants for the single ortholog of *HNF4A*, *dHNF4*, recapitulate the hallmark features of MODY1, including impaired insulin secretion and hyperglycemia (Barry and Thummel, 2016). *dHNF4* mutants display an adult onset form of diabetes due, in part, to a role for dHNF4 in promoting increased mitochondrial function in the mature animal. *dHNF4* mutants also recapitulate several phenotypes of mice carrying liver-specific deletion of *HNF4A,* including triglyceride accumulation and

low glycogen stores (Barry and Thummel, 2016; Palanker et al., 2009). Interestingly, *Drosophila* HNF4 functions in both the fat body and insulin-producing cells to maintain glucose homeostasis. These tissues represent the functional equivalents of mammalian β-cells and the liver, respectively, raising the possibility that HNF4A may act in a similar manner in flies and mammals to support glycemic control.

The developmental-onset of diabetes in *dHNF4* mutant adults relates to the well-established link between mitochondrial activity and cellular development. In contrast to growing and proliferative cells, differentiated tissues are more reliant on mitochondrial oxidative phosphorylation (OXPHOS) for ATP production (Shyh-Chang et al., 2013; Vander Heiden et al., 2009). This likely explains the developmental upregulation of mitochondrial gene expression at the transition to adulthood in *Drosophila*, which requires *dHNF4* (Barry and Thummel, 2016). OXPHOS is also central to the process of insulin secretion from β-cells, where increased ATP production resulting from elevated blood glucose triggers a signaling cascade for insulin release (Aleyassine, 1970; Erecinska et al., 1992; Gerbitz et al., 1996; Sivitz and Yorek, 2010; Soejima et al., 1996; Wiederkehr and Wollheim, 2006). Consistent with this, mutations in the mitochondrial genome (mtDNA), which encodes 13 respiratory chain proteins, result in maternally-inherited diabetes linked to progressive defects in glucose-stimulated insulin secretion (GSIS) (Sivitz and Yorek, 2010). Furthermore, haploinsufficiency for the nuclear-encoded mtDNA transcription factor, *TFB1M*, causes impaired GSIS and diabetes susceptibility in both humans and mice (Koeck et al., 2011) and β-cell-specific deletion of the nuclear-encoded mitochondrial transcription factor *Tfam*, or *Opa1*, a regulator of mitochondrial fusion, results in impaired GSIS and diabetes in mice (Koeck et al., 2011;

Silva et al., 2000; Zhang et al., 2011). In addition, mitochondrial dysfunction in the liver and skeletal muscle has been implicated in the development of insulin resistance, suggesting an important role for mitochondrial function in multiple tissues to protect against diabetes onset (Sivitz and Yorek, 2010).

Here I report evidence for a conserved role for HNF4A to support mitochondrial function in adults. Consistent with the role for *Drosophila* HNF4 to promote increased expression of OXPHOS genes at the transition to maturity, dHNF4 is required in adults, but not larvae, to maintain mitochondrial integrity and activity of the ETC complexes I and IV. dHNF4 supports complex I activity through both mtDNA gene expression and nuclear regulation of *CG7461*, a homolog of the mammalian acyl-CoA dehydrogenase and complex I assembly factor, *ACAD9*. ChIP-seq analysis of HNF4A in the adult mouse liver shows association with the *ACAD9* promoter region, along with several other important regulators of mitochondrial gene expression and function. Consistent with this, HNF4A is required for maximal expression of mtDNA-encoded genes involved in the ETC and *PINK1*, an important factor for mitochondrial quality control and complex I activity. Although HNF4A does not appear to be localized to mitochondria in hepatocytes, HNF4A colocalizes with mitochondria in human islets. Taken together, these data suggest that regulation of mitochondrial function is an evolutionarily conserved function of HNF4A, with defects in this process potentially contributing to the development of MODY1.

Materials and Methods

Fly stocks and maintenance

A transheteroallelic combination of *dHNF4*$^{\Delta 17}$ and *dHNF4*$^{\Delta 33}$ alleles were used for all studies of *dHNF4* loss-of-function and were compared to genetically-matched controls consisting of a transheteroallelic combination of precise excisions of P-elements *EP2449* and *KG08976,* as previously described (Barry and Thummel, 2016; Palanker et al., 2009). RNAi lines were acquired from the Bloomington stock center TRiP RNAi collection. *UAS-RNAi* lines used include: TRiP 55347 (*CG7461*^{RNAi}), TRiP 55660 (*CIA30*^{RNAi}), and TRiP 35785 (m*Cherry*^{RNAi}). Fat body-specific RNAi was achieved by crossing to *r4-GAL4* transgenics (Lee and Park, 2004). Stocks were maintained at room temperature and experimental crosses were set up in vials in a humidified incubator at 25˚C. Animals were reared on the 3% sugar diet as previously described (Barry and Thummel, 2016). For conditioning on the 15% sugar diet, mature adults were transferred to the 15% sugar diet for three days prior to analysis. Diets consist of 0.8-1% agar, 8% yeast, 3% or 15% sugar (2:1 ratio of glucose to sucrose), and 0.5% $MgSO_4$ and 0.5% $CaCl_2$, where percentages represent weight by volume. The media was cooked by microwaving on high power to achieve at least 5 min of rapid boiling and slowly cooled while stirring. After allowing the media to cool to ~50˚C, 10 ml/L tegosept and 6 ml/L propionic acid were added prior to pouring into vials for solidification.

Whole-mount immunostaining of *Drosophila* tissues

Fat body was dissected from either feeding L3 larvae or mature adult males in ice-cold PBS. The dissected tissues were then transferred to 4% paraformaldehyde for fixation at room temperature for either 20 (larval fat body) or 30 (adult) min while

rocking. Samples were quickly washed in PBS+0.2% Triton X-100 and then washed for three additional times for 10-15 min each at room temperature. Samples were blocked for 2 hr at room temperature with 5% normal donkey serum in PBS+0.2% Triton. Primary antibody (mouse anti-ATP5A, Abcam 14748) was added at a dilution of 1:200 in block solution and incubated overnight at 4˚C while rocking. Samples were then washed once quickly with PBS+0.2% Triton and for three additional times for 10-15 min each at room temperature. Secondary antibody was added at a final dilution of 1:1000 (donkey antimouse Cy2, Jackson Immuno) and incubated overnight at 4˚C in the dark. Samples were then washed and mounted in Slowfade Gold (Thermo Fisher Scientific). Imaging was performed with an Olympus FlowView 1000 with a 60x water or oil immersion objective and processed using ImageJ software.

Mitochondrial isolation

Approximately sixty adult male flies were placed in a 15 ml ice-cold dounce homogenizer and stroked approximately 20 times with glass pestle A. Animals were homogenized in 1 ml of cold isolation buffer plus protease inhibitor. The homogenizer and pestle were rinsed with 1 ml of isolation buffer, and the final 2 mls of homogenate was passed through100-micron nylon filter basket. The membrane was washed with 1 ml of buffer, which was subsequently centrifuged through a 10 micron filter at 1000 g for 30 sec. After rinsing the membrane with an additional 1 ml of isolation buffer, the flow through was centrifuged at 1,000 g for 5 min at 4˚C to pellet cell debris. The supernatant was then transferred to a fresh tube and centrifuged for an additional 15 min at 13,000 g. The supernatant was then discarded and the pellet was resuspended in 50-100 µl of hypotonic buffer (0.5 mM NaCl, 25 mM potassium phosphate, pH 7.5) and split into

three separate aliquots before storing at -80˚C.

Electron transport chain complex activity assays

ETC complex activity assays were performed as previously described with minor alterations (Spinazzi et al., 2012). Mitochondrial isolates were subjected to at least four freeze-thaw cycles followed by Bradford assay to quantify mitochondrial protein. Samples were adjusted, if necessary, to achieve comparable protein concentrations and to be sufficiently dilute for accurate pipetting volumes to be used in the assays. For complex I activity, 15-20 ug of mitochondrial extracts were used per assay with three biological replicates analyzed per genotype. Parallel wells were analyzed +/- addition of rotenone to a final concentration of 10 μM. The reaction was initiated by addition of ubiquinone (10 μM final concentration) and the decrease in absorbance at 340 nm was monitored for up to 5 min as a read-out of NADH oxidation. Rotenone-independent activity was quantified and subtracted to determine specific complex I activity.

For complex II activity, approximately 10 μg of mitochondrial protein was assayed. Complex II activity was measured by reading the decrease in absorbance at 600 nm for 5 min to assess oxidation of succinate upon addition of decylubiquinone (50 μM final concentration). Malonate was used at a final concentration of 10 mM to determine SDH-specific activity.

Two μg of mitochondrial protein was used to assay complex IV activity. Baseline activity was determined by assaying the change in absorbance prior to addition of mitochondria. Upon addition of mitochondrial protein, the decrease in absorbance was monitored at 550 nm for 5 min to determine the oxidation of cytochrome C. Specific activity of complex IV was determined by adding KCN (300 μM final concentration) to

parallel replicates.

To examine citrate synthase activity, approximately 4 μg of mitochondrial protein was assayed for oxidation of oxaloacetic acid by monitoring the increase in absorbance at 412 nM for 3 min.

Blue-native polyacrylamide gel electrophoresis

Blue-native PAGE was performed as described previously (Van Vranken et al., 2014). Briefly, isolated mitochondria were resuspended in lysis buffer (50 mM NaCl, 5 mM 6-aminocaproic acid, 50 mM imidazole, 1 mM AEBSF, and protease inhibitor cocktail). Mitochondria were permeabilized with 1% digitonin. Samples were resolved on a 3-13% gradient native gel prior to membrane transfer and subsequent immune blotting.

Antibodies

Antibodies used for immunostaining and blotting were mouse anti-ATP5A (Abcam 14748), rabbit anti-SDHB (generated against yeast SDH2, a generous gift from Dennis Winge), Goat anti-TIM17 (Santa Cruz, sc-13293), mouse anti-NDUFS3 (Abcam, ab14711), and goat anti-HNF4A (Santa Cruz, sc-6556).

Immunostaining of mammalian tissues

Tissue fixation, processing, and immunostaining were performed as previously described (Krah et al., 2015). For staining of mouse liver, the liver was dissected from six week-old adult female mice (CD1 background), washed in cold PBS, then fixed for one hr in 4% paraformaldehyde followed by processing in Paraplast Plus (McCormick Scientific). Human pancreas specimens were de-identified prior to use and therefore do not fall under human subject research according to the US Department of Human and

Health Services regulations guide (45 CDR Part 46). Six μM paraffin sections were cut and stained with primary antibodies against HNF4A and ATP5A. Fluorescently conjugated donkey secondary antibodies were acquired from JacksonImmuno Labs along with DAPI to mark nuclei. Slides were mounted in Fluoromount-G (Southern Biotech) and imaged on an Olympus FV1000 confocal microscope. ImageJ was used for image processing.

Gene expression analysis

Three month-old *HNF4A*$^{flox/flox}$ (Hayhurst et al., 2001)were injected with viral AAV8-TBG-Cre or AAV8-TBG-eGFP (University of Pennsylvania Vector Core, Philadelphia, PA) through the tail-vein. Liver was harvested one week after viral delivery for RNA isolation. Liver samples were homogenized with a TissueLyzer II (Qiagen) and RNA was isolated using Trizol reagent (Invitrogen). Reverse transcription was performed with SuperScript VILO Master Mix (Thermofisher). Quantification of gene expression was performed with KAPA SYBR FAST qPCR 2x Master Mix Rox Low (Kapabiosystems) on an Applied Biosystems QuantStuio 6 Flex Real-Time PCR System, 384-well. Relative expression was calculated by extrapolation from a standard curve for each primer pair that was then normalized to expression of the housekeeping gene *RPL13*. Primer pairs were designed with Universal Probe Library (Roche) or qPrimer Depot (mouseprimerdepot.nci.nih.gov).

Results

Drosophila HNF4 is required for mitochondrial function in adulthood

My previous studies of *Drosophila* HNF4 identified a critical role for this nuclear receptor to support mitochondrial function in adulthood (Barry and Thummel, 2016). The question remains, however, whether dHNF4 is also required during larval development for mitochondrial activity. Examination of mitochondrial morphology in *dHNF4* mutant larvae fed a 15% sugar diet revealed normal mitochondrial structure, in contrast to the severely fragmented morphology of mutant adults (Figure 4.1). Even though dHNF4 is required for the expression of genes involved in mitochondrial β-oxidation during this stage (Palanker et al., 2009), this finding indicates that mitochondrial integrity is not reliant on dHNF4 during larval development. Defects in mitochondrial morphology thus correlate with the susceptibility of *dHNF4* mutants to diabetes-onset in the adult, but not larval stage.

Although mitochondrial morphology is disrupted in *dHNF4* mutant adults fed a 15% sugar diet, this could either represent a secondary effect of diabetes or a predisposing factor for impaired glycemic control (Barry and Thummel, 2016). As an initial approach to address this question, I examined the effect of dietary sugar on mitochondrial integrity. Although *dHNF4* mutants do not display hyperglycemia on a low sugar diet (Barry and Thummel, 2016), mitochondrial morphology is nonetheless severely fragmented, demonstrating a critical role for dHNF4 to maintain mitochondrial integrity independent of dietary sugar content (Figure 4.1). Furthermore, this finding indicates that mitochondrial fragmentation is not a secondary effect of hyperglycemia in

dHNF4 mutants. Rather, mitochondrial dysfunction likely provides a metabolic predisposition to hyperglycemia when dietary sugar is in abundance.

To more directly assess the requirement of dHNF4 for mitochondrial activity during development, ETC complex activities were analyzed from larval and adult mitochondrial extracts. This further confirmed a specific requirement for dHNF4 in adults, but not larvae, for normal ETC function. In contrast to larvae, adult mutants show a severe reduction in complex I activity (Figure 4.2 A). Consistent with this, *dHNF4* mutants also display reduced complex I assembly/stability by blue native-PAGE analysis (Figure 4.3). Interestingly, complex I activity is also elevated in mitochondria from wild-type adults compared to larvae (Figure 4.2 A). This result is not explained by differences in mitochondrial abundance, as the same amount of mitochondrial protein was assayed. Rather, this finding suggests that either the abundance of complex I per mitochondrion is increased in adulthood, or that there is an increase in the inherent activity of the complex. In contrast, complex IV shows no significant difference in enzymatic activity between larval and adult mitochondria, yet dHNF4 is also required for its maximal activity in the adult stage (Figure 4.2 C). The effects on complex I and IV are specific, and not due to general mitochondrial damage during isolation, as the activities of citrate synthase and complex II are unaffected (Figure 4.2 B,D). The normal activity of complex II is unexpected, however, since *dHNF4* mutant adults show reduced steady state levels of SDHB and reduced expression of the complex II assembly factor *dSdhaf4* (Barry and Thummel, 2016) (Figure 4.3). However, these effects were observed under conditions high dietary sugar, while ETC activity was analyzed from animals fed a low sugar diet. Any defects in complex II activity in *dHNF4* mutants might therefore only manifest when

fed a high sugar diet. Nonetheless, these data demonstrate that dHNF4 is required for maximal activity of ETC complexes I and IV in the mature fly. The specific effect on these complexes could relate to impaired mtDNA gene expression in *dHNF4* mutants, as ten of the thirteen protein-coding genes of the mitochondrial genome function in these two complexes of the respiratory chain. Furthermore, these data reveal a developmental increase in complex I activity in adult *Drosophila*, although the basis of this remains unclear.

CG7461 is a direct target of dHNF4 and supports complex I function

Although dHNF4 regulates the expression of several nuclear and mitochondrial-encoded genes involved in OXPHOS, the majority of dHNF4 nuclear targets function in the mitochondrial β-oxidation pathway (Barry and Thummel, 2016; Palanker et al., 2009). One of these, *CG7461*, has two closely related mammalian homologs, *ACAD9* and *ACADVL*. These paraologous genes represent mitochondrial-localized acyl-CoA dehydrogenases with preferential activity toward very long chain fatty acids. Interestingly, recent studies have uncovered an additional role for ACAD9 in supporting complex I activity, where mutations in this gene cause complex I deficiency in humans (Nouws et al., 2014). This raised the possibility that *CG7461* might also be required for maximal complex I activity in *Drosophila.*

dHNF4 directly associates with the *CG7461* promoter region and is required for its expression (Figure 4.4 A) (Barry and Thummel, 2016), and thus could represent an import target for dHNF4 to maintain complex I function. Similar to *dHNF4*, *CG7461* expression is enriched in the adult fat body (Figure 4.4 B). Tissue-specific RNAi against

CG7461 in the fat body significantly impairs complex I activity in adult flies to a similar level as disruption of a known complex I assembly factor, *CIA30* (Figure 4.4 C). These findings suggest that *CG7461* is an important transcriptional target of dHNF4 to support ETC complex I activity in *Drosophila*.

Conserved functions for HNF4 in regulating mitochondrial gene expression

To determine whether HNF4 has an evolutionarily conserved role in supporting mitochondrial function, we sought to examine the consequences of *HNF4A* loss-of-function in the adult mouse liver. To this end, adenovirus-mediated delivery of Cre recombinase was used for excision of a floxed *HNF4A* locus in adult mice. Three month-old *HNF4A*$^{flox/flox}$ mice received tail-vein injection of *AAV8-TBG-iCre* or *AAV8-TBG-eGFP* virus to provide hepatocyte-specific Cre expression compared to eGFP controls. One week after viral injection, *HNF4A* transcript was undetectable in the liver along with expected changes in known target genes, confirming a high efficiency of Cre-mediated recombination (Figure 4.5 A). Transcriptional profiling of mtDNA-encoded transcripts in *HNF4A* mutant livers revealed significant reduction in the expression of all mitochondrial genes examined, suggesting that HNF4A is important for mitochondrial activity in the adult liver (Figure 4.5 B). Furthermore, these findings provide evidence of a conserved function for HNF4 to maintain mitochondrial gene expression in both flies and mice.

My previous studies of *Drosophila* HNF4 uncovered evidence for a direct role in both nuclear and mtDNA-encoded gene expression (Barry and Thummel, 2016). To investigate whether mammalian HNF4A functions in a similar manner, HNF4A subcellular localization was examined in adult hepatocytes. Immunostaining showed

abundant nuclear localization, as expected, in addition to a substantial cytoplasmic signal (Figure 4.5 C). In contrast to *Drosophila*, however, there is not an appreciable amount of overlap with the mitochondrial marker ATP5A. This suggests that the effect of HNF4A loss-of-function on mtDNA gene expression is likely due to an indirect role in regulating mitochondrial gene expression through nuclear encoded target genes, or impacts mitochondrial copy number.

To investigate possible direct regulation of nuclear-encoded mitochondrial genes, publically available ChIP-seq data was examined for HNF4A genomic localization in the adult mouse liver (Alpern et al., 2014). Analysis of several candidate regions revealed HNF4A enrichment at loci encoding important regulators of mitochondrial gene expression and function. Amongst these include genes for the mitochondrial transcription factor Tfam, the mitochondrial RNA polymerase, Polrmt, a critical factor for mitochondrial quality control and complex I activity, PINK1, and ACAD9, an acyl-CoA dehydrogenase involved in both β-oxidation and ETC complex I activity (Figure 4.6 A and data not shown). These findings raised the possibility that HNF4A may regulate mitochondrial gene expression and function through nuclear-encoded genes. Furthermore, targeting of *ACAD9* in mammals, and *CG7461* in flies, represents a possible conserved role for HNF4 to support complex I activity.

Recent studies have uncovered a critical role for HNF4A in the liver to support thermoregulation under the metabolic stress condition of cold exposure (Judith Simcox et al., manuscript in preparation). To examine the requirement of hepatic HNF4A for expression of nuclear encoded mitochondrial genes, transcript abundance was assessed in *HNF4A* mutant livers under both room temperature and cold stress (Figure 4.6 B). *PINK1*

expression was significantly reduced under both conditions in *HNF4A* mutant livers, while *ACAD9* and *Polrmt* expression was significantly reduced only upon cold exposure. The paralog of *ACAD9*, *ACADVL*, which does not function in complex I activity, shows only minor ChIP-seq enrichment for HNF4A (Figure 4.6 A). *ACADVL* expression, however, was significantly reduced in *HNF4A* mutant liver under both conditions. Analysis of *Tfam* expression was unsuccessful due to poor detection. While these data further implicate HNF4A in regulating mitochondrial function, they do not fully explain the reduced mtDNA gene expression in *HNF4A* mutant livers at room temperature. Furthermore, these findings highlight the need to validate HNF4A ChIP-seq enrichment peaks for relevant changes in gene expression, as the putative targets *ACAD9* and *Polrmt* were unaffected by HNF4A loss-of-function under normal conditions. Nonetheless, our findings are consistent with a conserved role for HNF4A in supporting mitochondrial activity and suggest an increased need for this function upon cold exposure in mammals. The reason for this, however, remains unclear and further experiments are necessary to determine the extent to which hepatic mitochondria rely on HNF4A. Moreover, additional putative mitochondrial-localized HNF4A target genes have been identified through more systematic searches (Figure 4.7). Further studies are therefore needed to examine the full extent to which HNF4A directly regulates these loci to impact mitochondrial function.

Mitochondrial metabolism is critical for maximal GSIS from pancreatic β-cells (Aleyassine, 1970; Silva et al., 2000; Sivitz and Yorek, 2010; Soejima et al., 1996). Mutations in HNF4A result in impaired GSIS in both mice and humans, yet the molecular basis for this remains unknown. Although HNF4A was not localized to

mitochondria in hepatocytes, we sought to investigate this possibility in β-cells. Consistent with the important role for HNF4 in insulin secretion, immunostaining in the human pancreas showed enriched expression of HNF4A in islets of Langerhans (Figure 4.8 A). Similarly, the mitochondrial marker ATP5A is enriched in islets, consistent with previous reports (Figure 4.8 A). Unexpectedly, HNF4A showed no detectable nuclear signal, however substantial overlap with ATP5A was observed, suggesting mitochondrial localization (Figure 4.8 A-B). Although preliminary, these findings raise the possibility that HNF4A plays a direct role within mitochondria of the endocrine pancreas.

Discussion

By investigating the function of HNF4 across multiple animal systems, we have uncovered a conserved role for this transcription factor to support mitochondrial function. In *Drosophila*, HNF4 promotes a developmental switch towards OXPHOS at the transition to adulthood to promote glucose tolerance and GSIS in the mature animal (Barry and Thummel, 2016). Here we have provided additional evidence of an adult-specific role for dHNF4 to maintain mitochondrial integrity and increased activity of the ETC. Similar to *Drosophila*, mammalian HNF4A is also required for maximal expression of mtDNA-encoded transcripts in the mouse liver. Although HNF4A is not localized to mitochondria in hepatocytes, we uncovered evidence for direct regulation of several important nuclear-encoded mitochondrial genes by HNF4A. The specific mechanism affecting mtDNA gene expression remains unclear, but nonetheless, these findings demonstrate an important role for HNF4A to support mitochondrial activity. Furthermore, the observation that HNF4A colocalizes with mitochondria in the human endocrine pancreas raises the interesting possibility that HNF4A may directly promote

mtDNA gene expression in a tissue-specific manner. Although these findings are still preliminary, they set the framework for future studies of the potential role for mammalian HNF4A to maintain mitochondrial function in both the liver and β-cells to support glycemic control.

dHNF4 promotes increased mitochondrial function in adulthood

In *Drosophila*, dHNF4 contributes to a transcriptional switch that promotes increased OXPHOS in the mature fly, and defects in this process are linked to the onset of diabetes in mutant adults (Barry and Thummel, 2016). Further analysis of this activity has illustrated a specific role for HNF4 to support mitochondrial integrity and the activities of complexes I and IV of the ETC in the mature animal. The differential expression of OXPHOS genes during development, along with increased complex I activity in wild-type adults, likely relates to the known role of mitochondrial metabolism in supporting cellular differentiation versus growth. During early development, rapidly dividing and growing cells have large biosynthetic demands and predominantly employ a metabolic program of aerobic glycolysis (Shyh-Chang et al., 2013; Vander Heiden et al., 2009). Differentiated cells, in contrast, display a general increased reliance on mitochondrial respiration for ATP production. Thus, the role for dHNF4 to direct increased OXPHOS in fully differentiated adults can contribute to establishing the metabolic state that supports the energetic demands of this final stage in the life cycle (Barry and Thummel, 2016).

In mammals, HNF4A is a master regulator of hepatocyte differentiation. Therefore, a role for HNF4A to support hepatic mitochondrial function in the adult liver is consistent with the increased use of mitochondrial respiration in differentiated

hepatocytes (Wanet et al., 2014). The expression of mtDNA-encoded genes is broadly reduced in HNF4A-deficient livers, along with *PINK1*, a critical factor for mitochondrial quality control. PINK1 supports ETC activity and mtDNA abundance in addition to regulating micro-autophagy of damaged mitochondria (Gegg et al., 2009; Liu et al., 2011; Morais et al., 2014; Pogson et al., 2014). This raises the possibility that decreased *PINK1* expression may impact mitochondrial function in the *HNF4A* mutant liver. A previous study also demonstrated that liver-specific deletion of HNF4A exacerbates hyperglycemia in a mouse model of type-2 diabetes (*db/db* background) (Yin et al., 2011). These findings, along with my previous studies in *Drosophila*, suggest that HNF4A dysfunction in the liver may contribute to poor glucose control in MODY1 patients. Whether mitochondria dysfunction plays an important role in this process, however, warrants further investigation.

Defects in mitochondrial gene expression, polarization, or morphology are all known to impair insulin secretion and systemic glucose homeostasis in mammals (Gerbitz et al., 1996; Koeck et al., 2011; Silva et al., 2000; Sivitz and Yorek, 2010; Soejima et al., 1996; Wiederkehr and Wollheim, 2006; Zhang et al., 2011). Previous studies of HNF4 function in both *Drosophila* and rat insulinoma cells (INS-1) have implicated defects in mitochondrial metabolism as a potential cause of reduced insulin secretion due to HNF4 dysfunction (Barry and Thummel, 2016; Wang et al., 2000). It is therefore interesting to consider our observation of a potential direct role for HNF4 within mitochondria of human β-cells. Although surprising, the localization of nuclear transcription factors to the mitochondrial compartment is not unprecedented. Similar roles have been proposed for other nuclear transcriptional regulators, including members

of the nuclear receptor family (Casas et al., 2003; Leigh-Brown et al., 2010; Nargund et al., 2015; Szczepanek et al., 2012). In at least some cases, accounts of this phenomenon have also been reported to be tissue specific (Leigh-Brown et al., 2010). Nonetheless, whether HNF4A truly localizes to β-cell mitochondria, and the potential physiological significance of this, requires further examination.

Acknowledgments

We thank Dr. Mary Bronner for generously providing human pancreas specimens and Dr. Udayan Apte for providing mouse liver samples for analysis of HNF4A-dependent gene expression. We also thank Jon VanVranken for assistance with BN-PAGE, Dennis Winge for providing anti-SDHB antibodies, FlyBase for informatics support, and the Bloomington Stock Center for supply of fly stocks. *Drosophila* experiments were performed by W.B., immunostaining of mammalian tissues was performed by N.K. with confocal imaging by W.B., and gene expression analysis of liver tissue was performed by J.S. and W.B..

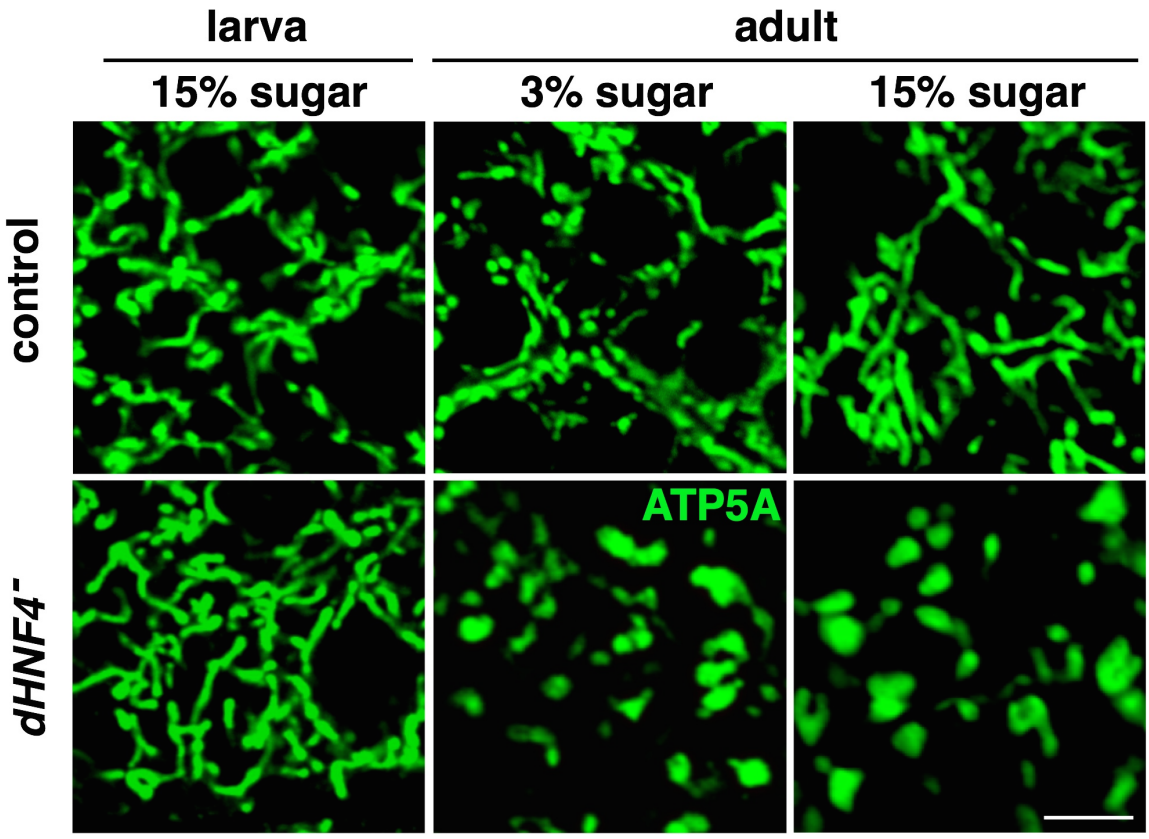

Figure 4.1. dHNF4 supports mitochondrial integrity in adulthood independent of dietary sugar

Whole mount staining of fat body dissected from feeding third-instar larvae or 8 day-old adult males. Immunostaining for ATP5A was used to mark mitochondria. *dHNF4* mutant larvae show normal mitochondrial morphology even on a high sugar diet. In contrast, mutant adults display fragmented and rounded mitochondrial morphology regardless of dietary sugar levels. Scale bar is equivalent to five microns.

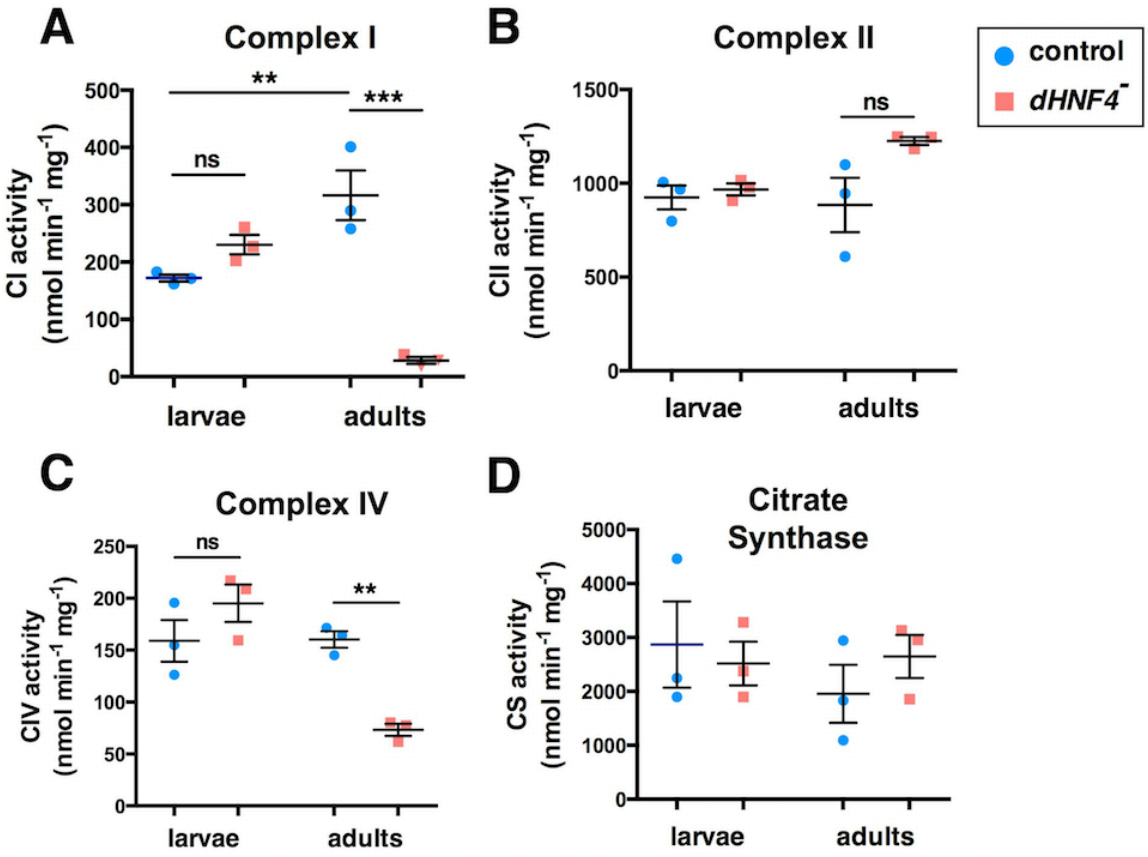

Figure 4.2. dHNF4 is required for activity of ETC complex I and IV in adults
Mitochondria were isolated from feeding third-instar larvae or 8 day-old adult males to assess enzymatic activity of specific ETC complexes. (A) Complex I activity increases during development, from larvae to adults, and is significantly impaired in *dHNF4* mutant adults, but not larvae. (B) Complex II activity is unaffected by a loss of *dHNF4* function in either the adult or larval stage. (C) Similar to complex I, complex IV activity is reduced specifically in *dHNF4* mutant adults. (D) Citrate synthase activity is unaffected in *dHNF4* mutants regardless of the developmental stage. The same mitochondrial extracts were used for all assays shown above. This, combined with the normal activities of citrate synthase and complex II in *dHNF4* mutants, indicates that the effect on I and IV are specific, and not a result of gross mitochondrial damage. *P* values represent one-way ANOVA with Šídák multiple test correction, * ≤ 0.05, ** ≤ 0.01. Mitochondrial isolates were obtained from 60-100 animals per sample, with each experiment including three separate biological samples per condition.

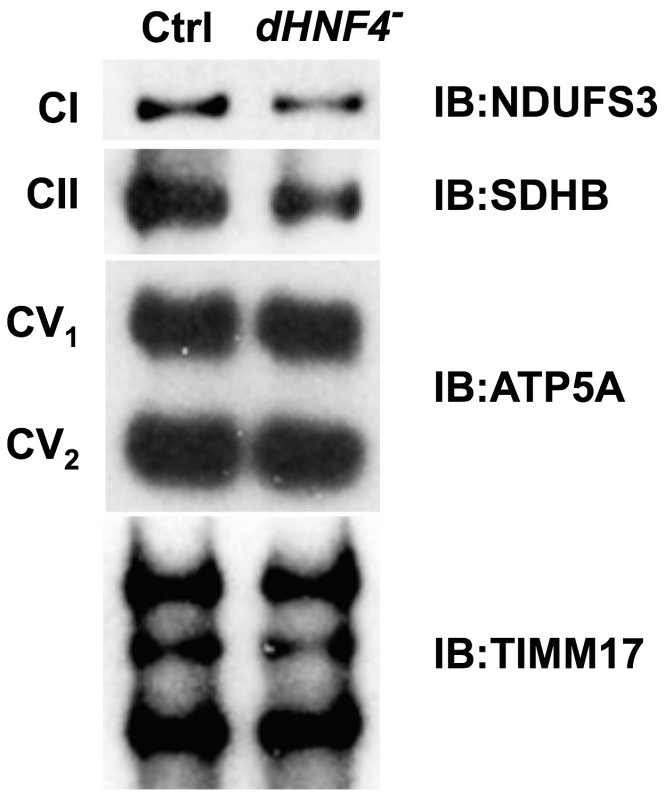

Figure 4.3. BN-PAGE analysis of ETC complex stability/assembly in *dHNF4* mutant adults
Mitochondria extracted from 8 day-old control or *dHNF4* mutant adults fed a 15% sugar diet were subjected to blue-native PAGE followed by immunoblotting for ETC complexes I (NDUFS3), II (SDHB), V (ATP5A), and mitochondrial import inner membrane translocase 17 (TIMM17) to control for loading and transfer.

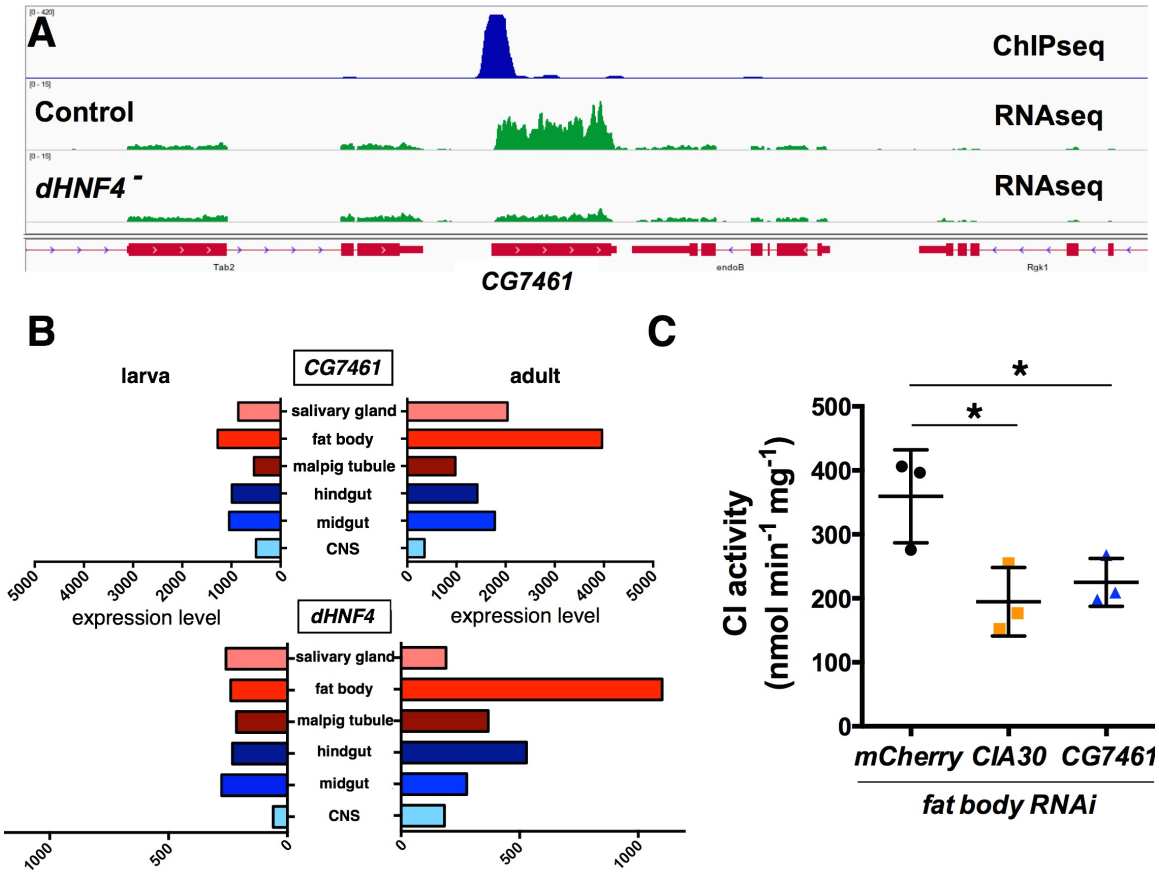

Figure 4.4. *CG7461* is a direct target of dHNF4 and is required for ETC complex I activity

(A) *CG7461* is a direct target of dHNF4. ChIP-seq enrichment for dHNF4 (blue) at the *CG7461* locus in chromatin isolated from wild-type adult flies. Poly(A)-selected RNA extracted from control or *dHNF4* mutant adult males was subjected to high throughput sequencing (green) and shows reduced expression in *dHNF4* mutants. Raw data from (Barry and Thummel, 2016) was used to generate panel A by a screen shot of data tracks viewed with the IGV browser (Broad Institute, MIT). (B) FlyAtlas mRNA expression levels show enrichment of *CG7461* in the adult fat body, similar to *dHNF4*. (C) Quantitation of complex I specific-activity in mitochondria isolated from adult flies expressing fat body-specific RNAi against a known complex I assembly factor, *CIA30*, *CG7461,* or *mCherry* as a negative control. *P* values were calculated by one-way ANOVA with Dunnett's correction, * ≤ 0.05. Mitochondrial isolates were obtained from 60 animals per sample, with each experiment including three separate biological samples per condition.

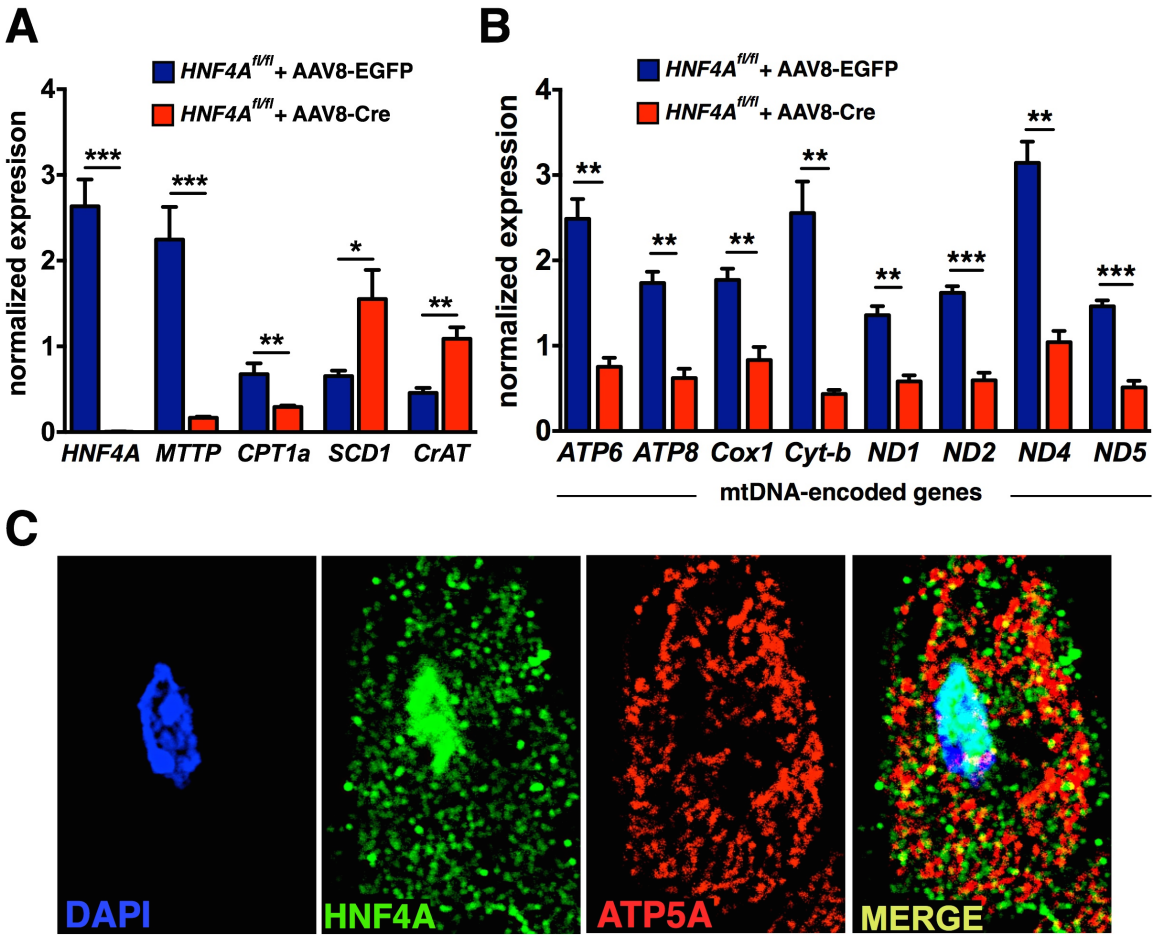

Figure 4.5. HNF4A is required in the liver for maximal expression of mtDNA-encoded transcripts

(A) Quantitative RT-PCR analysis of transcript abundance in control and *HNF4A* deficient adult liver. Mice were injected with virus for hepatic expression of either Cre recombinase or EGFP under the control of the liver-specific *TBG* promoter element. *HNF4A* is undetectable one week after viral injection, indicating a high efficiency of recombination. *MTTP* and *CPT1a* are known HNF4A target genes showing expected effects on gene expression upon *HNF4A* deletion. *SCD1* and *CrAT* expression levels are provided as supporting evidence that the reduced gene expression levels in *HNF4A* mutant liver are not due to a global decrease in transcription or mRNA stability. Transcripts were normalized to *Rpl13* mRNA. (B) Quantitative RT-PCR for mRNA levels of mtDNA-encoded transcripts show reduced expression of all genes analyzed in *HNF4A*-deficient livers. (C) Immunostaining of wild-type adult liver for HNF4A (green) and ATP5A (red) to mark mitochondria, and DAPI stain for nuclei (blue). A single hepatocyte is displayed at high magnification showing nuclear and cytoplasmic HNF4A staining with little appreciable overlap with mitochondria. (A-B) Data represents the mean +/- 1x SEM. *P* values * ≤ 0.05, ** ≤ 0.01, *** ≤ 0.001.

Figure 4.6. Putative nuclear-encoded HNF4A targets involved in mitochondrial gene expression and ETC function
(A) ChIP-seq enrichment peaks for hepatic HNF4A in the mouse liver (postnatal day 12). Data tracks were viewed in the IGV browser (Broad Institute, MIT) using publically available processed HNF4A ChIP-seq reads (Alpern et al., 2014). (B) Quantitative RT-PCR analysis of transcript abundance of putative HNF4A target genes. RNA was extracted from control (*HNF4A*$^{flox/flox}$ + AAV8-EGFP) or *HNF4A* deficient (*HNF4A*$^{flox/flox}$ + AAV8-Cre) adult liver one week after viral injection. Mice were either maintained at room temperature (RT) or placed at 4˚C for 5 hr prior to analysis. Data represents the mean +/- 1x SEM. *P* values ** ≤ 0.01, *** ≤ 0.001.

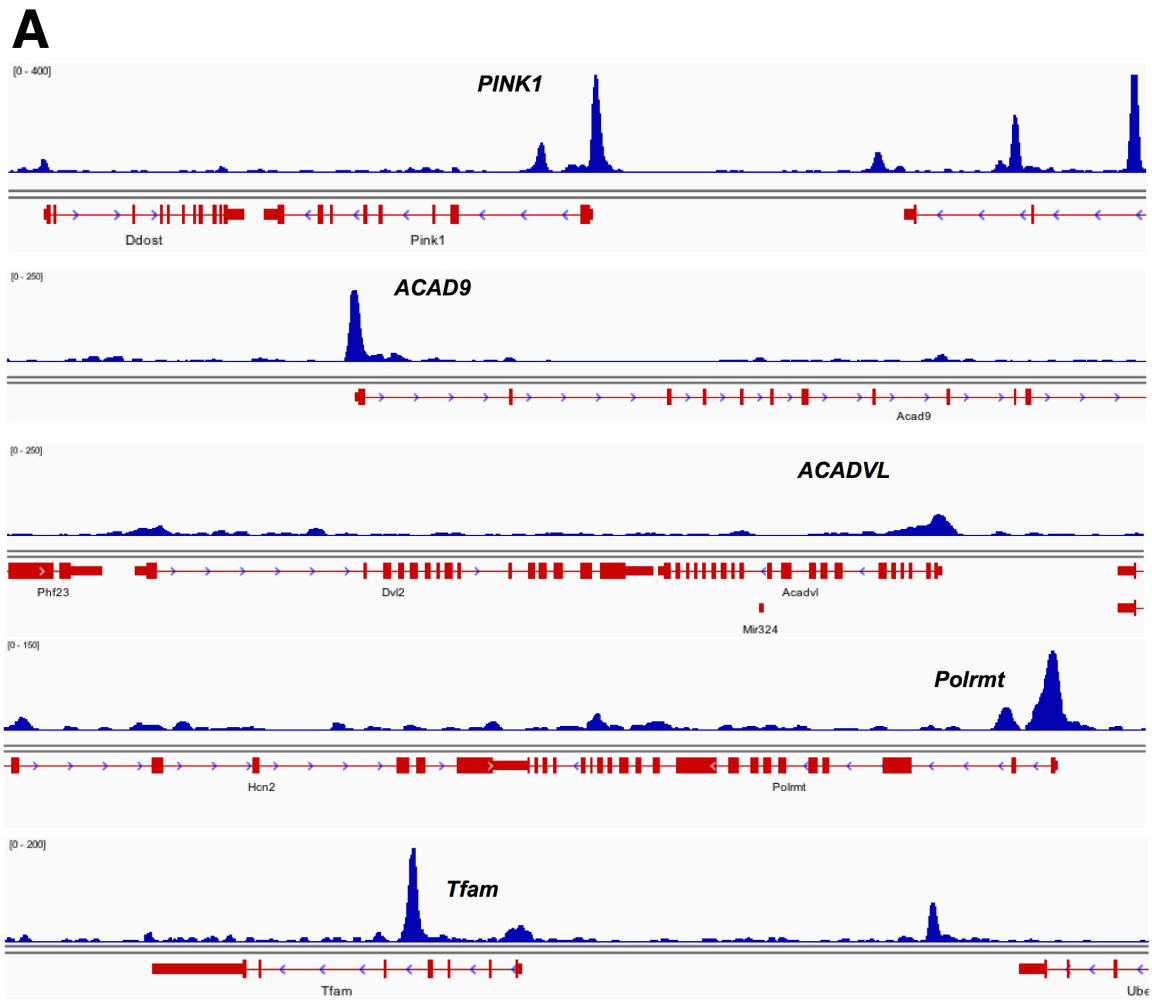
A
PINK1
Ddost
Pink1
ACAD9
Acad9
ACADVL
Phf23
Dvl2
Acadvl
Mir324
Polrmt
Hcn2
Polrmt
Tfam
Tfam

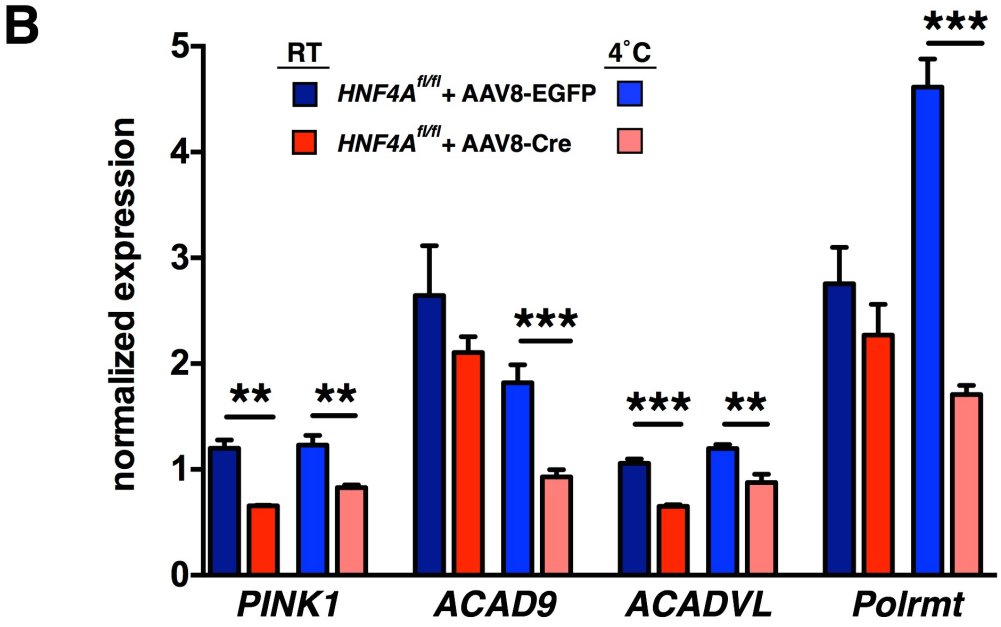
B
RT
4˚C
HNF4A fl/fl + AAV8-EGFP
HNF4A fl/fl + AAV8-Cre
normalized expression
0
1
2
3
4
5
**
**
***
***
**
***
PINK1
ACAD9
ACADVL
Polrmt

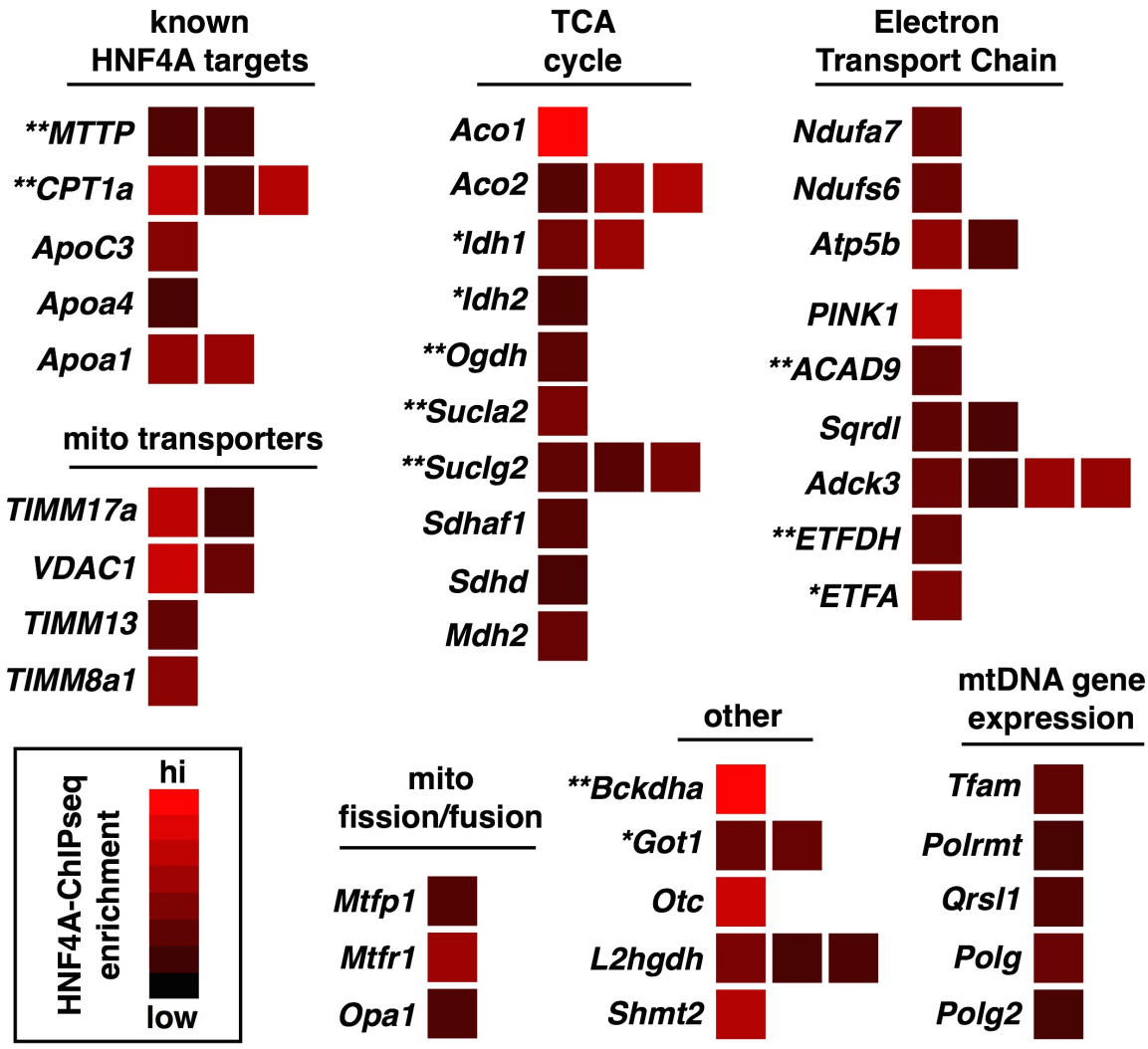

Figure 4.7. Candidate HNF4A target genes involved in mitochondrial function
Publically available data of chromatin-immunoprecipitation for HNF4A protein followed by high-throughput sequencing (ChIP-seq) from adult mouse liver was manually scanned for association with important regulators of mitochondrial function (Alpern et al., 2014). Boxes represent individual enrichment peaks at the indicated locus. Genes homologous to those downregulated in *Drosophila HNF4* mutants are marked with a single asterisk. Genes with homologs directly targeted by *Drosophila* HNF4 are indicated with a double asterisk.

Figure 4.8. HNF4A colocalizes with mitochondria in pancreatic islets of Langerhans in humans

De-identified specimens of human pancreas were fixed in paraffin and immunostained for HNF4A (green), ATP5A (to mark mitochondria, red), INS (to mark β-cells, white), and DAPI stain to mark nuclei (blue). (A) HNF4A is enriched in the human endocrine pancreas and shows a high degree of overlap with ATP5A. (B) High magnification image of a separate human islet showing partial overlap of HNF4A signal with mitochondria and a lack of HNF4A nuclear stain. Arrowheads point to several regions of overlap between HNFA and ATP5A.

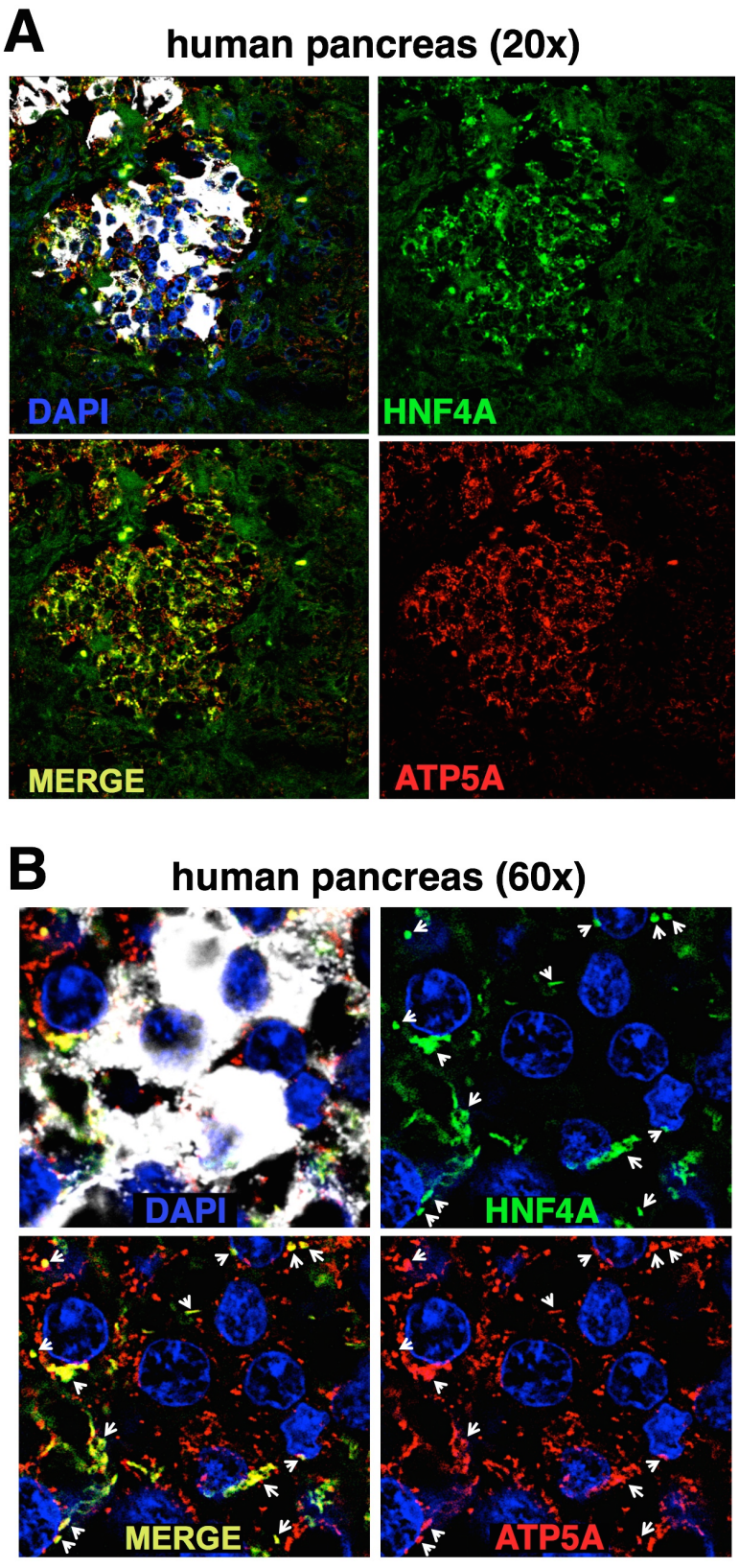
A
human pancreas (20x)
DAPI
HNF4A
MERGE
ATP5A
B
human pancreas (60x)
DAPI
HNF4A
MERGE
ATP5A

References

Aleyassine, H. (1970). Energy requirements for insulin release from rat pancreas in vitro. Endocrinology *87*, 84-89.

Alpern, D., Langer, D., Ballester, B., Le Gras, S., Romier, C., Mengus, G., and Davidson, I. (2014). TAF4, a subunit of transcription factor II D, directs promoter occupancy of nuclear receptor HNF4A during post-natal hepatocyte differentiation. eLife *3*, e03613.

Barry, W.E., and Thummel, C.S. (2016). The *Drosophila* HNF4 nuclear receptor promotes glucose-stimulated insulin secretion and mitochondrial function in adults. eLife *5*.

Bonzo, J.A., Ferry, C.H., Matsubara, T., Kim, J.H., and Gonzalez, F.J. (2012). Suppression of hepatocyte proliferation by hepatocyte nuclear factor 4alpha in adult mice. J. Biol. Chem. *287*, 7345-7356.

Casas, F., Daury, L., Grandemange, S., Busson, M., Seyer, P., Hatier, R., Carazo, A., Cabello, G., and Wrutniak-Cabello, C. (2003). Endocrine regulation of mitochondrial activity: involvement of truncated RXRalpha and c-Erb Aalpha1 proteins. FASEB J. *17*, 426-436.

Chen, W.S., Manova, K., Weinstein, D.C., Duncan, S.A., Plump, A.S., Prezioso, V.R., Bachvarova, R.F., and Darnell, J.E., Jr. (1994). Disruption of the HNF-4 gene, expressed in visceral endoderm, leads to cell death in embryonic ectoderm and impaired gastrulation of mouse embryos. Genes Dev. *8*, 2466-2477.

Erecinska, M., Bryla, J., Michalik, M., Meglasson, M.D., and Nelson, D. (1992). Energy metabolism in islets of Langerhans. Biochim. Biophys. Acta. *1101*, 273-295.

Fajans, S.S., and Bell, G.I. (2011). MODY: history, genetics, pathophysiology, and clinical decision making. Diabetes Care *34*, 1878-1884.

Gegg, M.E., Cooper, J.M., Schapira, A.H., and Taanman, J.W. (2009). Silencing of PINK1 expression affects mitochondrial DNA and oxidative phosphorylation in dopaminergic cells. PloS One *4*, e4756.

Gerbitz, K.D., Gempel, K., and Brdiczka, D. (1996). Mitochondria and diabetes. Genetic, biochemical, and clinical implications of the cellular energy circuit. Diabetes *45*, 113-126.

Gupta, R.K., Vatamaniuk, M.Z., Lee, C.S., Flaschen, R.C., Fulmer, J.T., Matschinsky, F.M., Duncan, S.A., and Kaestner, K.H. (2005). The MODY1 gene HNF-4alpha regulates selected genes involved in insulin secretion. J. Clin. Invest. *115*, 1006-1015.

Hayhurst, G.P., Lee, Y.H., Lambert, G., Ward, J.M., and Gonzalez, F.J. (2001). Hepatocyte nuclear factor 4alpha (nuclear receptor 2A1) is essential for maintenance of hepatic gene expression and lipid homeostasis. Mol. Cell Biol. *21*, 1393-1403.

Koeck, T., Olsson, A.H., Nitert, M.D., Sharoyko, V.V., Ladenvall, C., Kotova, O., Reiling, E., Ronn, T., Parikh, H., Taneera, J., et al. (2011). A common variant in TFB1M is associated with reduced insulin secretion and increased future risk of type 2 diabetes. Cell Metab. *13*, 80-91.

Krah, N.M., De La, O.J., Swift, G.H., Hoang, C.Q., Willet, S.G., Chen Pan, F., Cash, G.M., Bronner, M.P., Wright, C.V., MacDonald, R.J., et al. (2015). The acinar differentiation determinant PTF1A inhibits initiation of pancreatic ductal adenocarcinoma. eLife *4*.

Lee, G., and Park, J.H. (2004). Hemolymph sugar homeostasis and starvation-induced hyperactivity affected by genetic manipulations of the adipokinetic hormone-encoding gene in *Drosophila melanogaster*. Genetics *167*, 311-323.

Leigh-Brown, S., Enriquez, J.A., and Odom, D.T. (2010). Nuclear transcription factors in mammalian mitochondria. Genome Biol. *11*, 215.

Liu, W., Acin-Perez, R., Geghman, K.D., Manfredi, G., Lu, B., and Li, C. (2011). Pink1 regulates the oxidative phosphorylation machinery via mitochondrial fission. Proc. Natl. Acad. of Sci. U.S.A. *108*, 12920-12924.

Miura, A., Yamagata, K., Kakei, M., Hatakeyama, H., Takahashi, N., Fukui, K., Nammo, T., Yoneda, K., Inoue, Y., Sladek, F.M., et al. (2006). Hepatocyte nuclear factor-4alpha is essential for glucose-stimulated insulin secretion by pancreatic beta-cells. J. Biol. Chem. *281*, 5246-5257.

Morais, V.A., Haddad, D., Craessaerts, K., De Bock, P.J., Swerts, J., Vilain, S., Aerts, L., Overbergh, L., Grunewald, A., Seibler, P., et al. (2014). PINK1 loss-of-function mutations affect mitochondrial complex I activity via NdufA10 ubiquinone uncoupling. Science *344*, 203-207.

Nargund, A.M., Fiorese, C.J., Pellegrino, M.W., Deng, P., and Haynes, C.M. (2015). Mitochondrial and nuclear accumulation of the transcription factor ATFS-1 promotes OXPHOS recovery during the UPRmt. Mol. Cell *58*, 123-133.

Nouws, J., Te Brinke, H., Nijtmans, L.G., and Houten, S.M. (2014). ACAD9, a complex I assembly factor with a moonlighting function in fatty acid oxidation deficiencies. Hum. Mol. Genet. *23*, 1311-1319.

Palanker, L., Tennessen, J.M., Lam, G., and Thummel, C.S. (2009). *Drosophila* HNF4 regulates lipid mobilization and beta-oxidation. Cell Metab. *9*, 228-239.

Pogson, J.H., Ivatt, R.M., Sanchez-Martinez, A., Tufi, R., Wilson, E., Mortiboys, H., and Whitworth, A.J. (2014). The complex I subunit NDUFA10 selectively rescues *Drosophila* pink1 mutants through a mechanism independent of mitophagy. PLoS Genet. *10*, e1004815.

Shyh-Chang, N., Daley, G.Q., and Cantley, L.C. (2013). Stem cell metabolism in tissue development and aging. Development *140*, 2535-2547.

Silva, J.P., Kohler, M., Graff, C., Oldfors, A., Magnuson, M.A., Berggren, P.O., and Larsson, N.G. (2000). Impaired insulin secretion and beta-cell loss in tissue-specific knockout mice with mitochondrial diabetes. Nat. Genet. *26*, 336-340.

Sivitz, W.I., and Yorek, M.A. (2010). Mitochondrial dysfunction in diabetes: from molecular mechanisms to functional significance and therapeutic opportunities. Antioxid. Redox Signal. *12*, 537-577.

Soejima, A., Inoue, K., Takai, D., Kaneko, M., Ishihara, H., Oka, Y., and Hayashi, J.I. (1996). Mitochondrial DNA is required for regulation of glucose-stimulated insulin secretion in a mouse pancreatic beta cell line, MIN6. J. Biol. Chem. *271*, 26194-26199.

Spinazzi, M., Casarin, A., Pertegato, V., Salviati, L., and Angelini, C. (2012). Assessment of mitochondrial respiratory chain enzymatic activities on tissues and cultured cells. Nat. Protoc. *7*, 1235-1246.

Szczepanek, K., Lesnefsky, E.J., and Larner, A.C. (2012). Multi-tasking: nuclear transcription factors with novel roles in the mitochondria. Trends Cell Biol. *22*, 429-437.

Van Vranken, J.G., Bricker, D.K., Dephoure, N., Gygi, S.P., Cox, J.E., Thummel, C.S., and Rutter, J. (2014). SDHAF4 promotes mitochondrial succinate dehydrogenase activity and prevents neurodegeneration. Cell Metab. *20*, 241-252.

Vander Heiden, M.G., Cantley, L.C., and Thompson, C.B. (2009). Understanding the Warburg effect: the metabolic requirements of cell proliferation. Science *324*, 1029-1033.

Walesky, C., Edwards, G., Borude, P., Gunewardena, S., O'Neil, M., Yoo, B., and Apte, U. (2013a). Hepatocyte nuclear factor 4 alpha deletion promotes diethylnitrosamine-induced hepatocellular carcinoma in rodents. Hepatology *57*, 2480-2490.

Walesky, C., Gunewardena, S., Terwilliger, E.F., Edwards, G., Borude, P., and Apte, U. (2013b). Hepatocyte-specific deletion of hepatocyte nuclear factor-4alpha in adult mice results in increased hepatocyte proliferation. Am. J. Physiol. Gastrointest. Liver Physiol. *304*, G26-37.

Wanet, A., Remacle, N., Najar, M., Sokal, E., Arnould, T., Najimi, M., and Renard, P. (2014). Mitochondrial remodeling in hepatic differentiation and dedifferentiation. Int. J. Biochem. Cell Biol. *54*, 174-185.

Wang, H., Maechler, P., Antinozzi, P.A., Hagenfeldt, K.A., and Wollheim, C.B. (2000). Hepatocyte nuclear factor 4alpha regulates the expression of pancreatic beta-cell genes implicated in glucose metabolism and nutrient-induced insulin secretion. J. Biol. Chem. *275*, 35953-35959.

Wiederkehr, A., and Wollheim, C.B. (2006). Minireview: implication of mitochondria in insulin secretion and action. Endocrinology *147*, 2643-2649.

Yamagata, K., Furuta, H., Oda, N., Kaisaki, P.J., Menzel, S., Cox, N.J., Fajans, S.S., Signorini, S., Stoffel, M., and Bell, G.I. (1996). Mutations in the hepatocyte nuclear factor-4alpha gene in maturity-onset diabetes of the young (MODY1). Nature *384*, 458-460.

Yin, L., Ma, H., Ge, X., Edwards, P.A., and Zhang, Y. (2011). Hepatic hepatocyte nuclear factor 4alpha is essential for maintaining triglyceride and cholesterol homeostasis. Arterioscler. Thromb. Vasc. Biol. *31*, 328-336.

Yoon, J.C., Puigserver, P., Chen, G., Donovan, J., Wu, Z., Rhee, J., Adelmant, G., Stafford, J., Kahn, C.R., Granner, D.K., et al. (2001). Control of hepatic gluconeogenesis through the transcriptional coactivator PGC-1. Nature *413*, 131-138.

Zhang, Z., Wakabayashi, N., Wakabayashi, J., Tamura, Y., Song, W.J., Sereda, S., Clerc, P., Polster, B.M., Aja, S.M., Pletnikov, M.V., et al. (2011). The dynamin-related GTPase Opa1 is required for glucose-stimulated ATP production in pancreatic beta cells. Mol. Biol. Cell *22*, 2235-2245.

CHAPTER 5

CONCLUSIONS

Studies of nuclear receptors have provided important insights into the transcriptional regulation of animal physiology, development, and disease. The fruit fly, *Drosophila melanogaster,* has proved to be a valuable model system to expand our understanding of how nuclear receptors contribute to these processes (King-Jones and Thummel, 2005). My studies of *Drosophila HNF4* (*dHNF4*) have contributed to this effort by identifying novel functions that are conserved through evolution. *dHNF4* mutants recapitulate the hallmark features of Maturity-Onset Diabetes of the Young 1 (MODY1), a monogenic form of diabetes caused by *HNF4A* dysfunction in humans. Diabetic phenotypes first manifest in *dHNF4* mutants during the transition to adulthood, revealing a coordination of metabolic dysfunction with developmental progression. These defects are linked to an important role for dHNF4 in supporting a developmental switch in glucose homeostasis, in part by promoting increased oxidative phosphorylation (OXPHOS) during adulthood. dHNF4 acts in both the fat body and adult insulin-producing cells (IPCs) to support peripheral glucose uptake and glucose-stimulated insulin secretion (GSIS). My studies have uncovered valuable insights into the potential etiology of MODY1 and identified the mitochondrion as a central target of dHNF4 activity to maintain cellular and organismal metabolic homeostasis.

By extending our analysis to mice, we identified a conserved role for HNF4A in

maintaining mtDNA gene expression in the adult liver. Several important nuclear-encoded regulators of mitochondrial function were also identified as putative targets of HNF4A. Finally, we uncovered evidence for a potential direct role for HNF4A within the mitochondria of human β-cells. Although our studies in mammals are still preliminary, they strongly support the hypothesis that HNF4 is a critical regulator of mitochondrial function in flies, mice, and humans.

Drosophila as a model system for studies of metabolism and physiology

The global rise in the prevalence of diabetes and obesity has sparked a resurgence of studies focused on understanding the mechanisms regulating metabolic homeostasis. The high conservation of pathways for intermediary metabolism makes simple genetic systems a useful context to gain insight into how these pathways are regulated. This is especially true for *Drosophila*, which employ conserved signaling pathways to regulate systemic metabolism, along with functionally analogous tissues to many important metabolic organs in mammals (Alfa and Kim, 2016; Owusu-Ansah and Perrimon, 2014; Padmanabha and Baker, 2014; Reyes-DelaTorre, 2012; Teleman et al., 2012). In Chapter 2, I present methods that we developed to help advance studies of metabolism in the fruit fly. These include assays to examine carbohydrate, lipid, protein, and energy metabolism, along with a discussion of important considerations for determining appropriate methodologies and the effects of developmental progression on organismal metabolism. Our work, along with that of a growing number of investigators in the field, has helped to establish *Drosophila* as a powerful genetic system for understanding the mechanisms by which metabolic homeostasis is maintained.

Drosophila HNF4 mutants recapitulate the major symptoms of MODY1

Mutations in the HNF4A locus were identified as the underlying cause of MODY1 inheritance twenty years ago (Yamagata et al., 1996). Although the molecular link between HNF4A dysfunction and diabetes-onset has remained elusive, my studies in *Drosophila* have provided new insights into the mechanistic functions of HNF4 in supporting systemic glucose homeostasis. Through this work, I identified a dramatic effect of dietary sugar on the viability of *dHNF4* null mutants. Although these animals normally die at the transition to adulthood, rearing them on a low sugar diet can almost completely suppress this lethality and supports adult survival for several weeks (Figure 3.1 A-B). This demonstrated a severe intolerance of *dHNF4* mutants to dietary sugar, suggesting a critical function for maintaining carbohydrate homeostasis in *Drosophila*. Consistent with this, *dHNF4* mutant adults are hyperglycemic when fed a normal sugar diet and display adult-specific defects in insulin secretion. The developmental-onset of these phenotypes corresponds to a metabolic switch in systemic glucose homeostasis that occurs during the transition to adulthood.

In contrast to humans, glucose has long been considered as a minor circulating sugar in *Drosophila*. Rather, the predominant circulating carbohydrate is trehalose, a glucose disaccharide (Reyes-DelaTorre, 2012). Analysis of glycemia throughout development, however, revealed that free glucose is an abundant circulating sugar during the final stages of pupal development and that this is maintained throughout adulthood (Figure 3.6 E). Furthermore, previous studies had demonstrated that *Drosophila* larvae do not respond to glucose for secretion of insulin-like peptides, again in contrast to humans

(Geminard et al., 2009). Adult flies, however, display a robust response to glucose for insulin secretion, and dHNF4 is critical for this process (Figures 3.5 A-E, 3.6 A-D) (Park et al., 2014). Taken together, these studies uncovered a previously unrecognized developmental switch in systemic glucose homeostasis in *Drosophila* that requires dHNF4. Furthermore, my work has helped to establish the adult stage of *Drosophila* as an accurate context for studies relating to diabetes and GSIS in humans.

Drosophila undergo a developmental switch in glucose homeostasis

In light of these findings, it is interesting to consider the physiological basis for the developmental switch in glucose homeostasis that occurs during *Drosophila* development. Unlike mammals, fruit flies employ a single insulin receptor through which insulin-like peptides signal to mediate functions in both metabolic homeostasis and growth promotion (Teleman et al., 2012). During larval development, the animal undergoes an extended phase of exponential growth, with amino acids acting as the primary stimulus for secretion of insulin-like peptides to support this growth (Geminard et al., 2009; Géminard, 2006). As glucose alone does not provide the nitrogen required for biosynthetic processes, a lack of response to glucose for insulin secretion is biologically rational. Rearing larvae on a sugar-only diet, for example, is not sufficient to support developmental progression and results in eventual lethality (data not shown). The adult stage, in contrast, does not have these same growth requirements, as the animal has reached final body size and mostly consists of differentiated tissues. The IPCs therefore have a less prominent role in promoting growth during this stage, while the need for insulin signaling to maintain metabolic homeostasis persists.

Although the reason for the developmental difference in circulating glucose abundance is unknown, this may be at least be partially influenced by the general change in glycolytic and oxidative metabolism between larvae and adults. While larvae are programmed toward aerobic glycolysis, characterized by high glycolytic flux, the adult fly shifts toward a general increase in OXPHOS, likely accompanied by reduced glycolytic flux (Barry and Thummel, 2016; Tennessen et al., 2011). This could allow for greater glucose retention in the circulatory fluid resulting from slower glucose utilization by adult peripheral tissues. Although seemingly logical, these physiological considerations are only speculative. It will therefore be interesting to further examine the molecular basis of this physiological switch. While additional factors certainly contribute to this coordination between development and systemic metabolism, my studies indicate that HNF4 and mitochondrial function are central to this process.

A direct role for *Drosophila HNF4* in mtDNA gene expression

The mitochondrion is unique amongst cellular organelles in that it carriers its own genome (mtDNA), encoding rRNAs and tRNAs important for mitochondrial translation, along with 13 protein coding genes, all of which function in the ETC. dHNF4 supports expression of mtDNA-encoded transcripts in adulthood, likely through a direct role in this process (Figures 3.3 A, 3.6 E). Evidence for this includes ChIP-seq enrichment for dHNF4 at a predicted promoter region for mtDNA gene expression, along with immunostaining showing both nuclear and mitochondrial localization (Figures 3.3 C, 3.3 S2B). Furthermore, although most mtDNA transcripts are reduced in *dHNF4* mutants, *mt:Cyt-b* is unaffected, consistent with a specific regulatory defect in mitochondrial transcription, rather than a general reduction in mtDNA abundance. The expression of

mt:Cyt-b is also predicted to contain a separate promoter region, and dHNF4 does not associate with this locus (Berthier et al., 1986; Roberti et al., 2006). Moreover, mtDNA copy number is unchanged in mutant animals as assayed by determining the ratio of mtDNA to nuclear DNA (Figure 3.3 S2A). Due to technical limitations, however, I was unable to confirm the mitochondrial localization for dHNF4 through additional biochemical approaches. Taken together, these data nonetheless support the possibility that dHNF4 directly functions within mitochondria.

CG7461 is an important nuclear-encoded target of dHNF4 to support complex I activity

In addition to regulating mtDNA genes, dHNF4 is required for the expression of several nuclear-encoded transcripts involved in mitochondrial metabolism. Although some of these have predicted functions in OXPHOS, the majority represent genes involved in mitochondrial β-oxidation. One of these, *CG7461*, is homologous to two genes in mammals, *ACAD9* and *ACADVL*. In addition to its function as an acyl-CoA dehydrogenase, ACAD9 was recently shown to be required for complex I activity in mammals (Haack et al., 2010; Nouws et al., 2014). This led me to assess the role of *CG7461* in supporting complex I activity in *Drosophila,* revealing that this gene is an important target of dHNF4 to support complex I function. Complex I subunits are also encoded by the mitochondrial genome, suggesting that the defect in complex I activity in *dHNF4* mutants results from the reduced expression of both mtDNA genes and *CG7461*. Although the mechanistic link between CG7461 and complex I activity was not examined, ACAD9 has been identified as an important assembly factor for the complex (Nouws et al., 2010). It will therefore be interesting to determine if this is also the case in

Drosophila.

Evidence for mitochondrial regulation by HNF4A in mammals

As an initial approach to determine whether the role for dHNF4 in supporting mitochondrial function is conserved in mammals, we examined the effects on mtDNA gene expression upon acute deletion of HNF4A in the adult mouse liver. Similar to my findings in *Drosophila*, hepatic *HNF4A* is required to promote mitochondrial-encoded gene expression (Figure 4.5). Although we did not observe evidence for mitochondrial localization in hepatocytes, analysis of publically available HNF4A ChIP-seq data showed association with several loci encoding important genes involved in mitochondrial metabolism, gene expression, and other aspects of mitochondrial structure and function (Figure 4.5 C, 4.6, and 4.7). These findings suggest that HNF4A may indirectly promote expression of mtDNA genes through nuclear-encoded factors. Indeed, a critical regulator of mitochondrial quality control and ETC function, *PINK1*, was identified as a potential target of HNF4A and showed reduced expression upon HNF4A deletion in the liver (Figure 4.6 B). It will be interesting to examine the role for HNF4A in the expression of other putative target genes involved in mitochondrial function and the extent to which hepatic mitochondrial activity relies on HNF4A.

Although β-cell dysfunction is considered to be the primary cause of MODY1, the molecular function of HNF4A in this cell type is still unclear (Fajans and Bell, 2011). This is due, in part, to the paucity of *HNF4A* metabolic studies over the past decade. As a result, mice with pancreas-specific deletion of *HNF4A* were not readily available for analysis at the time we initiated our work in mammals. We therefore sought to examine the subcellular localization of HNF4A in human β-cells as a preliminary approach to

address a possible tissue-restricted role for HNF4A within mitochondria. In contrast to hepatocytes, we observed an unexpected lack of nuclear localization in human islets, but substantial colocalization with a subset of mitochondria. Future efforts will address the functional significance of this observation through genetic studies of *HNF4A* loss-of-function in the mouse pancreas and the resulting consequences on mitochondrial function.

References

Alfa, R.W., and Kim, S.K. (2016). Using *Drosophila* to discover mechanisms underlying type 2 diabetes. Dis. Model Mech. *9*, 365-376.

Barry, W.E., and Thummel, C.S. (2016). The *Drosophila* HNF4 nuclear receptor promotes glucose-stimulated insulin secretion and mitochondrial function in adults. eLife *5*.

Berthier, F., Renaud, M., Alziari, S., and Durand, R. (1986). RNA mapping on *Drosophila* mitochondrial DNA: precursors and template strands. Nucleic Acids Res. *14*, 4519-4533.

Fajans, S.S., and Bell, G.I. (2011). MODY: history, genetics, pathophysiology, and clinical decision making. Diabetes Care *34*, 1878-1884.

Geminard, C., Rulifson, E.J., and Leopold, P. (2009). Remote control of insulin secretion by fat cells in *Drosophila*. Cell Metab. *10*, 199-207.

Géminard, C., Arquier, N., Layalle, S., Bourouis, M., Slaidina, M., Delanoue, R., Bjordal, M., Ohanna, M., Ma, M., Colombani, J., at al. (2006). Control of Metabolism and Growth Through Insulin-Like Peptides in *Drosophila*. Diabetes *55*, S5-S8.

Haack, T.B., Danhauser, K., Haberberger, B., Hoser, J., Strecker, V., Boehm, D., Uziel, G., Lamantea, E., Invernizzi, F., Poulton, J., et al. (2010). Exome sequencing identifies ACAD9 mutations as a cause of complex I deficiency. Nat. Genet. *42*, 1131-1134.

King-Jones, K., and Thummel, C.S. (2005). Nuclear receptors - a perspective from *Drosophila*. Nature Rev. Genet. *6*, 311-323.

Nouws, J., Nijtmans, L., Houten, S.M., van den Brand, M., Huynen, M., Venselaar, H., Hoefs, S., Gloerich, J., Kronick, J., Hutchin, T., et al. (2010). Acyl-CoA dehydrogenase 9

is required for the biogenesis of oxidative phosphorylation complex I. Cell Metab. *12*, 283-294.

Nouws, J., Te Brinke, H., Nijtmans, L.G., and Houten, S.M. (2014). ACAD9, a complex I assembly factor with a moonlighting function in fatty acid oxidation deficiencies. Hum. Mol. Genet. *23*, 1311-1319.

Owusu-Ansah, E., and Perrimon, N. (2014). Modeling metabolic homeostasis and nutrient sensing in *Drosophila*: implications for aging and metabolic diseases. Dis. Model. Mech. *7*, 343-350.

Padmanabha, D., and Baker, K.D. (2014). *Drosophila* gains traction as a repurposed tool to investigate metabolism. Trends Endocrin. Met. *25*, 518-527.

Park, S., Alfa, R.W., Topper, S.M., Kim, G.E., Kockel, L., and Kim, S.K. (2014). A genetic strategy to measure circulating *Drosophila* insulin reveals genes regulating insulin production and secretion. PLoS Genet. *10*, e1004555.

Reyes-DelaTorre, A.P.-R., M.T; Riesgo-Escovar, J.R. (2012). Carbohydrate metabolism in D*rosophila*: reliance on the disaccharide trehalose. In Carbohydrates - Comprehensive Studies on Glycobiology and Glycotechnology, C.-F. Chang, ed. (InTech), pp. 317-338.

Roberti, M., Bruni, F., Polosa, P.L., Gadaleta, M.N., and Cantatore, P. (2006). The *Drosophila* termination factor DmTTF regulates in vivo mitochondrial transcription. Nucleic Acids Res. *34*, 2109-2116.

Teleman, A.A., Ratzenbock, I., and Oldham, S. (2012). *Drosophila*: a model for understanding obesity and diabetic complications. Exp. Clin. Endocrinol. Diabetes *120*, 184-185.

Tennessen, J.M., Baker, K.D., Lam, G., Evans, J., and Thummel, C.S. (2011). The Drosophila estrogen-related receptor directs a metabolic switch that supports developmental growth. Cell Metab. *13*, 139-148.

Yamagata, K., Furuta, H., Oda, N., Kaisaki, P.J., Menzel, S., Cox, N.J., Fajans, S.S., Signorini, S., Stoffel, M., and Bell, G.I. (1996). Mutations in the hepatocyte nuclear factor-4alpha gene in maturity-onset diabetes of the young (MODY1). Nature *384*, 458-460.